

**Arginine metabolism in experimental and idiopathic pulmonary fibrosis**

Inaugural Dissertation  
submitted to the  
Faculty of Medicine  
in partial fulfillment of the requirements  
for the PhD-Degree  
of the Faculties of Veterinary Medicine and Medicine  
of the Justus Liebig University Giessen

by  
Kitowska, Kamila Ewa  
of  
Gdansk, Poland

Giessen 2007

From the Department of Medicine  
Director / Chairman: Prof. Dr. Werner Seeger  
of Medicine of the Justus Liebig University Giessen

First Supervisor and Committee Member:  
Second Supervisor and Committee Member:  
Committee Members:  
Date of Doctoral Defense:

# I. Table of contents

I.	Table of contents.....	I
II.	List of figures.....	V
III.	List of tables .....	VII
IV.	List of abbreviations.....	VIII
V.	Summary .....	XI
VI.	Zusammenfassung.....	XIII
1.	Introduction .....	1
1.1.	Idiopathic pulmonary fibrosis .....	1
1.1.1.	Characteristics of idiopathic pulmonary fibrosis.....	1
1.1.2.	Histopathology of idiopathic pulmonary fibrosis.....	2
1.1.3.	Pathogenesis of idiopathic pulmonary fibrosis .....	3
1.1.4.	Animal models of pulmonary fibrosis .....	4
1.1.5.	Fibroblasts: key effector cells in fibrogenesis.....	5
1.1.6.	Collagen – a key compound of the extracellular matrix.....	8
1.2.	L-arginine metabolism.....	9
1.2.1.	L-arginine physiology .....	9
1.2.2.	L-arginine synthesis and transport.....	9
1.2.3.	L-arginine catabolism .....	12
1.2.4.	Arginase and nitric oxide synthase balance .....	15
1.2.4.1.	Functional consequences of arginase and nitric oxide synthase regulation.....	16
1.2.4.2.	Arginase and nitric oxide synthase regulation in lung disorders.....	17
1.2.4.3.	L-Arginine metabolism in idiopathic pulmonary fibrosis.....	18
2.	Aim of the study .....	20
3.	Materials and Methods .....	21
3.1.	Materials .....	21
3.1.1.	Equipment .....	21
3.1.2.	Reagents.....	23

---

3.1.3.	Mammalian cells .....	26
3.1.3.1.	Cell lines.....	26
3.1.3.2.	Primary cells.....	26
3.1.4.	Animal model of pulmonary fibrosis.....	26
3.1.4.1.	Bleomycin-induced lung fibrosis in mice .....	26
3.2.	Methods .....	27
3.2.1.	RNA isolation.....	27
3.2.2.	Reverse transcription reaction.....	27
3.2.3.	Polymerase chain reaction .....	28
3.2.3.1.	Semi-quantitative polymerase chain reaction.....	28
3.2.3.2.	Real-time polymerase chain reaction.....	29
3.2.4.	DNA agarose gel electrophoresis .....	30
3.2.5.	Protein isolation.....	31
3.2.5.1.	Protein isolation from tissues .....	31
3.2.5.2.	Protein isolation from cells .....	32
3.2.5.3.	Protein quantification.....	32
3.2.6.	SDS polyacrylamide gel electrophoresis .....	33
3.2.7.	Immunoblotting .....	34
3.2.7.1.	Protein blotting .....	34
3.2.7.2.	Protein detection .....	34
3.2.8.	Densitometry .....	35
3.2.9.	Immunohistochemistry .....	36
3.2.10.	Immunocytochemistry .....	36
3.2.11.	Amino acid analysis.....	37
3.2.11.1.	Isolation of basic amino acids .....	37
3.2.11.2.	Derivatization and chromatographic separation.....	38
3.2.12.	Culture of mammalian cells .....	38
3.2.12.1.	Cell culture condition.....	38
3.2.12.2.	Isolation of primary lung fibroblasts .....	39
3.2.12.3.	Transient transfection using lipofectamine .....	40
3.2.13.	Luciferase assay.....	40



---

3.2.14.	Sircol collagen assay.....	41
3.2.15.	Arginase activity assay .....	41
4.	Results .....	42
4.1.	Analysis of L-arginine metabolism during bleomycin-induced lung fibrosis .....	42
4.1.1.	Expression analysis of L-arginine transporters .....	42
4.1.2.	Analysis of protein arginine methyltransferase expression .....	43
4.1.3.	Analysis of L-arginine catabolic enzymes expression.....	45
4.1.4.	Expression of arginase-1, -2 during development of lung fibrosis .....	46
4.1.5.	Levels of free L-arginine during lung fibrosis .....	48
4.1.6.	Localization of arginase-1, -2 in the lung during lung fibrosis.....	50
4.2.	Expression of arginase-1, -2 in fibroblasts .....	51
4.2.1.	Arginase-1, -2 expression in primary mouse fibroblasts .....	51
4.2.2.	Arginase-1, -2 immunolocalization in primary mouse fibroblasts.....	53
4.2.3.	Induction of arginase-1, -2 expression by profibrotic agents.....	55
4.3.	Effect of arginase inhibitor on TGF- $\beta$ 1 signaling and extracellular matrix formation.....	57
4.3.1.	Arginase inhibition in NIH-3T3 fibroblasts.....	57
4.3.1.1.	Effect of arginase inhibition on TGF- $\beta$ 1-induced collagen deposition ...	57
4.3.1.2.	Effect of arginase inhibition on TGF- $\beta$ 1 signaling.....	58
4.3.1.3.	Effect of arginase inhibition on extracellular matrix components expression.....	59
4.3.2.	Arginase inhibition in human primary fibroblasts.....	61
4.3.2.1.	Effect of arginase inhibition on TGF- $\beta$ 1-induced collagen deposition ...	61
4.3.2.2.	Arginase inhibitor effect on expression of extracellular matrix components.....	62
4.4.	Arginase-1, -2 in idiopathic pulmonary fibrosis .....	63
4.4.1.	Arginase-1, -2 localization in human lungs .....	63
4.4.2.	Arginase-1, -2 expression in human lungs.....	65
4.4.3.	Arginase-1,-2 activity in human lungs.....	66
5.	Discussion.....	67

---

5.1.	Involvement of arginase-1, -2 in lung diseases.....	67
5.2.	Arginase isoenzymes in an animal model of lung fibrosis.....	67
5.2.1.	Arginase-1, -2 expression pattern.....	67
5.2.2.	Cellular localization of arginase-1, -2.....	68
5.2.3.	Regulation of arginase-1, -2 by profibrotic factors .....	69
5.2.3.1.	TGF- $\beta$ 1-mediated arginase expression .....	69
5.2.3.2.	Arginase-dependent collagen synthesis .....	70
5.2.3.3.	Influence of arginase on TGF- $\beta$ 1 signaling .....	71
5.3.	Limitations of the bleomycin model of lung fibrosis.....	72
5.4.	Arginase-1, -2 in idiopathic pulmonary fibrosis.....	74
5.4.1.	Arginase-1, 2 localization in human lung tissues.....	74
5.4.2.	Expression of arginase-1, -2 in human lung tissues .....	74
5.5.	Conclusions and future perspectives .....	75
6.	Appendix .....	77
6.1.	List of primers used for PCR amplification.....	77
6.1.1.	Quantitative RT-PCR.....	77
6.1.2.	Semi-quantitative RT-PCR .....	78
6.2.	List of antibodies.....	79
6.2.1.	Primary antibodies.....	79
6.2.2.	Secondary antibodies .....	80
7.	References .....	81
8.	Declaration.....	89
9.	Curriculum vitae .....	90
10.	Acknowledgements.....	95

## II. List of figures

- Figure 1.1.** Histopathological changes in the lung in IPF.
- Figure 1.2.** Representation of the two hypotheses of IPF pathogenesis.
- Figure 1.3.** The primary pathogenic events in IPF.
- Figure 1.4.** Fibroblast foci in IPF lung.
- Figure 1.5.** Pathways of arginine synthesis.
- Figure 1.6.** The citrulline/NO cycle.
- Figure 1.7.** Arginine metabolic pathways.
- Figure 4.1.** Expression analysis of SLC during bleomycin-induced lung fibrosis.
- Figure 4.2.** Analysis of PRMT mRNA expression during bleomycin-induced lung fibrosis.
- Figure 4.3.** Analysis of PRMT protein expression during bleomycin-induced lung fibrosis.
- A.** Protein levels analysis by immunoblotting.
  - B.** Densitometric analysis of PRMT protein expression.
- Figure 4.4.** Expression of L-arginine catabolic enzymes during bleomycin-induced lung fibrosis.
- Figure 4.5.** ARG mRNA expression during bleomycin-induced lung fibrosis.
- Figure 4.6.** ARG protein expression during bleomycin-induced lung fibrosis.
- A.** Protein levels analysis by immunoblotting.
  - B.** Densitometric analysis of ARG protein expression.
- Figure 4.7.** Levels of free cellular L-arginine during bleomycin-induced lung fibrosis.
- A.** HPLC chromatograms of free L-arginine levels.
  - B.** Concentration of free L-arginine.
- Figure 4.8.** Localization of ARG1 and ARG2 in mouse lung sections.
- Figure 4.9.** ARG mRNA expression in primary mouse lung fibroblasts.
- A.** mRNA levels analysis by semi-quantitative RT-PCR.
  - B.** mRNA levels analysis by quantitative RT-PCR.

- 
- Figure 4.10.** ARG protein expression in primary mouse lung fibroblasts.
- A. Protein levels analysis by immunoblotting.
  - B. Densitometric analysis of ARG protein expression.
- Figure 4.11.** ARG localization in primary mouse lung fibroblasts.
- A. ARG localization in mice primary lung fibroblasts.
  - B. ARG localization in NIH-3T3 cell line.
- Figure 4.12.** TGF- $\beta$ 1-induced ARG expression in fibroblasts.
- A. mRNA levels analysis in mice primary lung fibroblasts by semi-quantitative RT-PCR.
  - B. mRNA levels analysis in mice primary lung fibroblasts by quantitative RT-PCR.
  - C. mRNA levels analysis in NIH-3T3 fibroblasts by quantitative RT-PCR.
- Figure 4.13.** Regulation of collagen deposition by NOHA in NIH-3T3 fibroblasts.
- Figure 4.14.** TGF- $\beta$ 1 signaling in the presence of NOHA in NIH-3T3 fibroblasts.
- A. Cells transfected with luciferase reporter control plasmid pGL3.
  - B. Cells transfected with luciferase reporter plasmid pCAGA<sub>12</sub>-luc.
- Figure 4.15.** Influence of NOHA on expression of ECM components by NIH-3T3 fibroblasts.
- A. COL1A1 mRNA levels analysis by quantitative RT-PCR.
  - B.  $\alpha$ -SMA mRNA levels analysis by quantitative RT-PCR.
- Figure 4.16.** Effect of NOHA on collagen deposition by human primary fibroblasts.
- Figure 4.17.** Effect of NOHA on expression of ECM components by human primary fibroblasts.
- A. COL1A1 mRNA levels analysis by quantitative RT-PCR.
  - B.  $\alpha$ -SMA mRNA levels analysis by quantitative RT-PCR.
- Figure 4.18.** Localization of ARG1 and ARG2 in human lung sections.
- A.  $\alpha$ -SMA staining.
  - B. ARG1 and ARG2 staining.
- Figure 4.19.** ARG mRNA expression in human lung homogenates.
- Figure 4.20.** ARG activity in human lung homogenates.

### **III. List of tables**

**Table 1.1.** Approaches for inducing pulmonary fibrosis in animal models.

**Table 6.1.1.** List of primers used for quantitative RT-PCR.

**Table 6.1.2.** List of primers used for semi-quantitative RT-PCR.

**Table 6.2.1.** List of primary antibodies.

**Table 6.2.1.** List of secondary antibodies.

## IV. List of abbreviations

AA	Amino acid
ADC	Arginine decarboxylase
ADMA	Asymmetric dimethylarginine
ALK	Activin-like kinase
ARG	Arginase
APS	Ammonium persulfate
BSA	Bovine serum albumin
cAMP	Cyclic adenosine monophosphate
cDNA	Complementary deoxyribonucleic acid
CF	Cystic fibrosis
CHAPS	3-[3-chloramidopropyl]dimethylammonio]-1-propanesulfonate
COL1A1	Collagen 1A1
DAPI	4',6-diamidino-2-phenylindole
DDAH	N <sup>G</sup> ,N <sup>G</sup> -dimethylarginine dimethylaminohydrolase
DMSO	Dimethyl sulfoxide
DTT	Dithiothreitol
ECM	Extracellular matrix
EDTA	Ethylendinitrilo-N,N,N',N',-tetra-acetate
EGTA	Ethylene glycol-bis (2-amino-ethylether)-N,N,N',N', -tetraacetic-acid
FITC	Fluorescein-5-isothiocyanate
FCS	Fetal calf serum
GAPDH	Glyceraldehyde 3-phosphate dehydrogenase
HEPES	2-(-4-2-hydroxyethyl)-piperazinyl-1-ethansulfonate
HPLC	High Performance Liquid Chromatography
HRP	Horseradish peroxidase
IB	Immunoblotting
ICCH	Immunocytochemistry

---

IHCH	Immunohistochemistry
IL	Interleukin
INF	Interferon
IPF	Idiopathic pulmonary fibrosis
NO	Nitric oxide
NOHA	N <sup>G</sup> -hydroxy-L-arginine, monoacetate salt
NOS	Nitric oxide synthase
OAT	Ornithine aminotransferase
OD	Optical density
ODC	Ornithine decarboxylase
OPA	<i>Ortho</i> -phthaldialdehyde
PAH	Pulmonary arterial hypertension
PBGD	Porphobilinogen deaminase
PBS	Phosphate-buffered saline
PBST	Phosphate-buffered saline + 0,1 % Tween 20
PCR	Polymerase chain reaction
PRMT	Protein arginine methyltransferase
PVDF	Ployvinylidene difluoride
qRT-PCR	Quantitative real time PCR
Rel.	Relative
RT-PCR	Reverse transcription PCR
SDS	Sodium dodecyl sulfate
SDS-PAGE	SDS polyacrylamide gel electrophoresis
SLC	Solute carrier
SMA	Smooth muscle actin
SPE	Solid-phase extraction
TAE	Tris-acetate-EDTA
TE	Tris/ EDTA
TEMED	<i>N,N,N',N'</i> -tetramethyl-ethane-1,2-diamine
TGF	Transforming growth factor
TGF-βRI	TGF-β receptor type I

TGF- $\beta$ RII	TGF- $\beta$ receptor type II
Th	T helper
TNF	Tumor necrosis factor
UIP	Usual interstitial pneumonia



## V. Summary

Idiopathic pulmonary fibrosis (IPF) is a progressive and fatal lung disease of unknown origin, characterized by alveolar epithelial cell damage, increased deposition of extracellular matrix (ECM) in the lung interstitium, enhanced fibroblast/myofibroblast proliferation and activation, which ultimately lead to distortion of normal lung architecture and loss of respiratory function. While the initial trigger of this disease is most likely an epithelial injury, the interstitial fibroblast/myofibroblast represents the key effector cell responsible for the increased ECM deposition characteristic of IPF. Fibroblasts secrete large amounts of fibrillar collagens, which are the key ECM proteins that are significantly increased in this disease. L-arginine is a precursor of many active compounds including: nitric oxide, asymmetrical dimethylarginine, and praline, an amino acid that is enriched in collagen. Thus, it was hypothesized that L-arginine metabolism is altered in pulmonary fibrosis, ultimately affecting collagen synthesis.

In this study, the expression of key enzymes of the L-arginine pathway was characterized in bleomycin-induced pulmonary fibrosis in mice. Expression of arginase-1 and arginase-2 was significantly upregulated during bleomycin-induced lung fibrosis, which correlated with a decrease in lung L-arginine levels, as measured by high performance liquid chromatography. Furthermore, arginase-1 and arginase-2 mRNA and protein expression localized to fibroblasts, and their expression was increased in primary fibroblasts isolated from bleomycin-treated mice, compared to controls, as assessed by semi-quantitative and quantitative RT-PCR, and immunoblotting. Moreover, TGF- $\beta$ 1, a key profibrotic mediator, induced arginase-1 mRNA expression in primary and NIH-3T3 fibroblasts. Finally, treatment of NIH-3T3 fibroblasts and primary human lung fibroblasts with the arginase inhibitor, N<sup>G</sup>-hydroxy-L-arginine, attenuated TGF- $\beta$ 1-stimulated collagen deposition, but not Smad signaling. Arginase-1 and arginase-2 mRNA expression, as well as their activity, however, was unchanged in total human lung homogenates from IPF patients compared to controls.

These results demonstrated that arginase isoforms, key enzymes in nitric oxide and collagen metabolism, were expressed and functional in lung fibroblasts and

upregulated in the early stages of bleomycin-induced pulmonary fibrosis. These changes were limited to the animal model of pulmonary fibrosis, as no changes in expression were observed in lungs from IPF patients. The TGF- $\beta$ 1-induced upregulation of arginase-1 suggested an interplay between profibrotic agents and L-arginine metabolism during the course of experimental lung fibrosis, therapeutic manipulation of which may foster novel treatment options.

## VI. Zusammenfassung

Die Idiopathische Lungenfibrose (Idiopathic pulmonary fibrosis – IPF) ist eine progrediente und fatale Lungenerkrankung unbekanntes Ursprungs. Sie ist gekennzeichnet durch eine Schädigung der alveolären Epithelzellen, vermehrter Ablagerung von extrazellulärer Matrix im Interstitium der Lunge, verstärkter Proliferation und Aktivierung von Fibroblasten bzw. Myofibroblasten, was schließlich zu einer Zerstörung des normalen Gewebes führt, sowie zum Verlust der Lungenfunktion. Während die Krankheit initial höchstwahrscheinlich durch eine Verletzung des Lungenepithels ausgelöst wird, gelten die Fibroblasten bzw. die Myofibroblasten als Schlüsselzellen, da sie für die charakteristische Ablagerung extrazellulärer Matrix während des Krankheitsverlaufes der IPF verantwortlich sind. Fibroblasten produzieren große Mengen an fibrillärem Kollagen, welches die Hauptkomponenten der Extrazellulären Matrix darstellen, die bei der Lungenfibrose signifikant erhöht vorkommen. L-Arginin ist eine wichtige biologische Vorstufe vieler aktiver Verbindungen, wie zum Beispiel Stickoxid, asymmetrisches Dimethylarginin, und Prolin – einer Aminosäure, die besonders häufig in Kollagen vorkommt. Daher stellten wir die Hypothese auf, dass der L-Arginin-Metabolismus in der Lungenfibrose verändert ist, was schließlich die Kollagensynthese in Fibroblasten beeinflusst.

In dieser Studie wurde die Expression der Schlüsselenzyme des L-Arginin-Stoffwechselwegs während der Bleomycin-induzierten Lungenfibrose in Mäusen untersucht. Arginase-1 und Arginase-2 waren während der Bleomycin-induzierten Lungenfibrose signifikant hochreguliert, was mit einer gleichzeitigen Verringerung der L-Arginin-Level in der Lunge, gemessen mit high performance liquid chromatography (HPLC), einherging. Weiterhin war die Arginase-1 und Arginase-2 in den Fibroblasten exprimiert und war in primären Fibroblasten, isoliert aus Bleomycin-behandelten Mäusen im Vergleich zu unbehandelten Kontrollen, erhöht. Interessanterweise induzierte TGF- $\beta$ 1, ein profibrotischer Schlüsselmediator, die Arginase-1 mRNA-Expression in primären Fibroblasten und in NIH3T3-Zellen. Schließlich verringerte eine Behandlung

von NIH3T3-Fibroblasten sowie humaner Lungenfibroblasten mit dem Arginase-Inhibitor N<sup>G</sup>-hydroxy-L-arginin die TGF- $\beta$ 1-induzierte Kollagenablagerung, jedoch nicht die Signaltransduktion durch Smads. Die mRNA-Expression von Arginase-1 und Arginase-2, sowie deren Aktivitäten zeigten jedoch in Lungenhomogenaten von Fibrosepatienten im Vergleich zu gesunden Kontrolllungen keine Veränderung.

Diese Ergebnisse zeigen, dass Isoformen der Arginase, die Schlüsselenzyme im Stickoxid- und im Kollagenstoffwechsel sind, in Lungenfibroblasten exprimiert werden und funktional von Bedeutung sind. Dies konnte im Tiermodell gezeigt werden, während keine Veränderungen der Expression in Lungen von Fibrosepatienten festgestellt wurden. Die TGF- $\beta$ 1-induzierte Hochregulierung von Arginase-1 deutet auf eine Wechselwirkung zwischen profibrotischen Molekülen und dem L-Arginin-Metabolismus während des Verlaufs der experimentellen Lungenfibrose hin, welche ein Ansatzpunkt für eine Entwicklung neuer medizinischer Behandlungsmethoden darstellen könnte.

# 1. Introduction

## 1.1. Idiopathic pulmonary fibrosis

### 1.1.1. Characteristics of idiopathic pulmonary fibrosis

Idiopathic pulmonary fibrosis (IPF), also referred to as cryptogenic fibrosing alveolitis, is a progressive and fatal lung disease of unknown etiology <sup>1</sup>. In principal, IPF is characterized by alveolar epithelial cell damage, increased deposition of extracellular matrix (ECM) in the lung interstitium, and enhanced fibroblast/myofibroblast proliferation and activation. These processes ultimately lead to distortion of normal lung architecture and loss of respiratory function <sup>2</sup>.

Idiopathic pulmonary fibrosis is a relatively rare lung disorder with prevalence rate of three to six cases per 100 000 individuals with, mean survival ranging from two to four years after diagnosis <sup>3</sup>. It is also reported that IPF is more common amongst men than women <sup>4</sup>. The disease occurs predominantly from middle age onwards, with patients usually between 50 to 70 years of age at presentation. Two thirds of the patients are older than 60 years, which makes prognosis poor, since both incidence and death rate increase with age <sup>5</sup>. Although IPF affects millions of individuals worldwide, there is still no effective therapeutic approach, and so far, lung transplantation is the only viable option for patients that are refractory to medical therapy.

Since the pathogenesis of IPF is complex and poorly understood, identification of risk factors that may contribute to the development of the disease is essential. Although cigarette smoking <sup>6</sup>, the presence of several viruses <sup>7-9</sup>, and environmental factors <sup>10,11</sup> have been suggested to increase the risk of developing IPF, their impact remains to be fully elucidated. Some reports have speculated that genetic factors may contribute to the familial cases of pulmonary fibrosis, nevertheless, no specific genetic abnormalities have been identified to date <sup>12,13</sup>. While the cause of IPF remains unknown, advances in cellular and molecular biology have extended our understanding of the biological processes involved in the initiation and progression of this disease.

### 1.1.2. Histopathology of idiopathic pulmonary fibrosis

Idiopathic pulmonary fibrosis is characterized histologically by features of usual interstitial pneumonia (UIP) that include alveolitis, disruption of the pulmonary vascular bed, and fibrosis of the pulmonary parenchyma. The histological hallmark of this disorder is a heterogeneous appearance of the normal lung alternating with areas of interstitial inflammation, peripheral fibrosis and honeycomb changes<sup>4,14</sup>. Usually the peripheral subpleural parenchyma is most severely affected by these histopathologic changes. Inflammatory components observed in the lungs of patients with IPF typically consist of lymphocytes and plasma cells, and to some extent eosinophiles and neutrophils. Clusters of fibroblasts/myofibroblasts can be observed at the borders between fibrotic and normal lung, they create so called fibrotic foci. Moreover, alveolar epithelial injury with hyperplasia of type II pneumocytes is often seen in areas of active fibrosis<sup>14</sup>. Dense fibrosis leads to scarring and lesions followed by architectural destruction of the lung and the resultant loss of its respiratory function (Figure 1.1.).

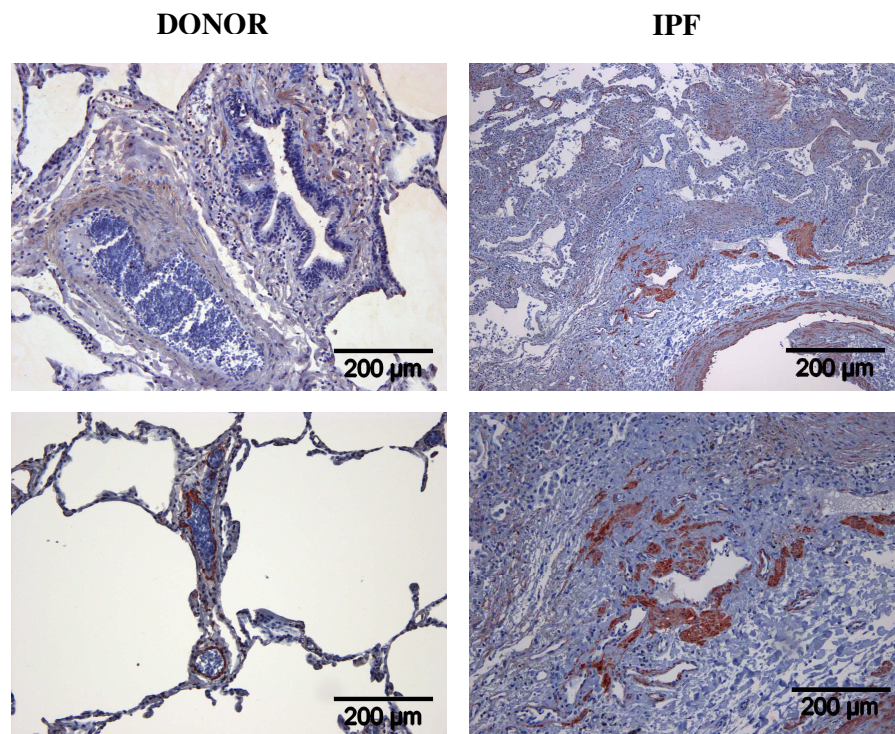


**Figure 1.1. Histopathological changes in the lung in IPF.**

Structure of the lung in a healthy donor (left) and in a patient with IPF (right). Paraffin embedded sections stained for  $\alpha$ -smooth muscle actin, and with hematoxylin and eosin.

### 1.1.3. Pathogenesis of idiopathic pulmonary fibrosis

The pathogenesis of IPF is complex and poorly understood. Several studies have been performed to elucidate pathogenic mechanisms that are involved in this disease. From these attempts, two hypotheses of IPF pathogenesis have arisen. The original so-called “old” hypothesis asserts that unknown stimuli injure the lung resulting in chronic inflammation which triggers fibrogenesis followed by the end-stage fibrotic scar <sup>15</sup> (Figure 1.2.A.). Idiopathic pulmonary fibrosis was believed to be a process of chronic repair that resulted from persistent inflammation accompanied by activation of inflammatory cells and the presence of cytokine and growth factors, which lead to activation of mesenchymal cells, with enhanced matrix deposition <sup>16</sup>.

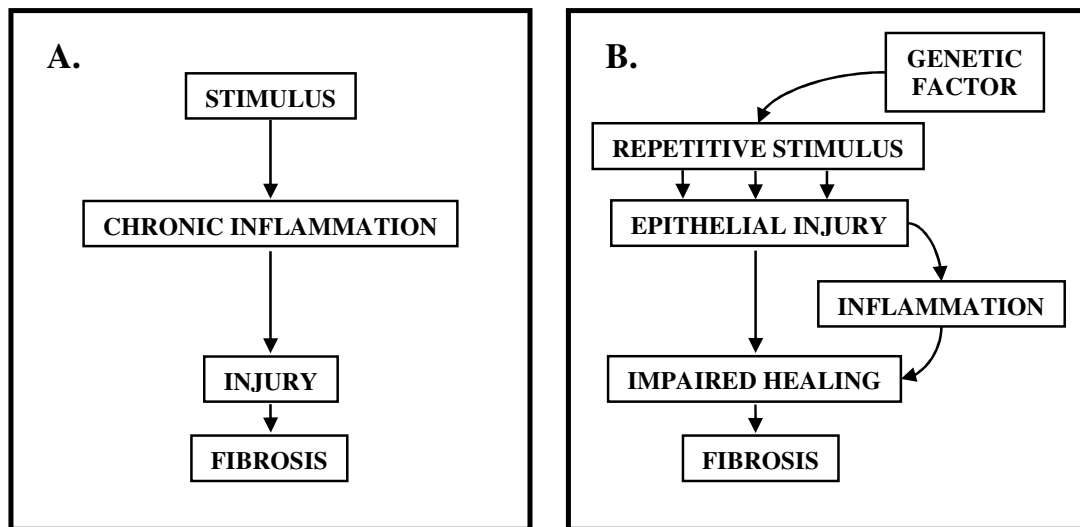


**Figure 1.2. Representation of the two hypotheses of IPF pathogenesis.**

The (A) old, and (B) new hypothesis of the pathogenesis of idiopathic pulmonary fibrosis.

However, this hypothesis had to be revised as more detailed subsequent studies revealed that inflammatory processes were mild in lung biopsies from patients with IPF, and occurred mainly in areas of collagen deposition and honeycombing <sup>17</sup>. Moreover, the role of inflammation at early stages of IPF is not clear, since little evidence supported the concept that inflammation is more prominent during the onset of the disease. Additionally, there are no data describing the early phase of IPF, since the histology of patients presenting with IPF, both at six months and at two years after recognition of

symptoms, exhibits variable degrees of fibrosis and honeycombing with mild to moderate inflammation<sup>2</sup>. Furthermore, the lack of effect of anti-inflammatory drugs in patients with IPF also suggested that inflammation may not be the driving force in IPF<sup>3,18</sup>.

On the basis of this evidence, it has been proposed that IPF results from sequential alveolar epithelial injury and abnormal wound repair<sup>15,17</sup>. According to this “new” hypothesis, epithelial injury and activation rather than alveolitis is the key factor in this disease<sup>19</sup> (Figure 1.2.B.). Alveolar epithelial cell injury induces the proliferation of fibroblasts and their differentiation into myofibroblasts. The activated interstitial fibroblasts/myofibroblasts represent effector cells responsible for the increased ECM deposition characteristic of the disease<sup>5,20</sup>.

#### 1.1.4. Animal models of pulmonary fibrosis

Several animal models of pulmonary fibrosis have been developed in order to better understand the mechanism and pathogenesis of IPF. Despite a number of exogenously administered agents that can induce pulmonary fibrosis in a variety of animal species (Table 1.1.)<sup>21</sup>, data indicate discrepancies between animal models of pulmonary fibrosis and human IPF. Although an ideal experimental animal model of this disease remains elusive, over last three decades, the bleomycin model has been at the forefront of basic research into the regulation of pulmonary fibrosis.

**Table 1.1. Approaches for inducing pulmonary fibrosis in animal models<sup>21</sup>.**

Exogenous agent/ Approach	Nature of tissue damage	Animal species used
Bleomycin	Oxidant-mediated DNA scission leading to fibrogenic cytokine release	Mice, rats, hamsters, rabbits, dogs, primates, pheasants
Inorganic particles (silica)	Hypersensitivity reactions with or without granuloma formation	Mice, rats, hamsters, rabbits, sheep
Irradiation	Free radical-mediated DNA damage	Mice, rats, hamsters, rabbits, dogs, sheep, primates
Gene transfer (TGF- $\beta$ , IL-1 $\beta$ )	Downstream activation of specific cytokine pathways	Mice, rats
Fluorescein isothiocyanate	Incompletely understood. Presumed T-cell-independent	Mice
Vanadium pentoxide	Incompletely understood. An inorganic metal oxide.	Mice, rats
Haptenic antigens	Recall cell-mediated immune response	Mice, hamsters



Bleomycin is an antibiotic agent with antitumor activity, originally isolated from *Streptomyces verticillus*. It is used as a part of cytostatic treatment of several tumors such as germ-cell tumors, lymphomas, Kaposi's sarcoma, cervical cancer, and squamous cell carcinomas of head and neck<sup>22</sup>. It exerts a cytotoxic effect by induction of free radicals that cause DNA breaks leading ultimately to cell death<sup>23</sup>. Bleomycin is eliminated primarily by the kidneys, and further deactivation of this agent can be carried out by bleomycin hydrolyse, an enzyme expressed in the liver, spleen, bone marrow and intestine<sup>24</sup>. Due to the lack of this enzyme in the lungs and the skin, bleomycin-induced toxicity is predominantly observed in these organs.

Bleomycin-induced lung fibrosis was observed in mice, rats, hamsters, rabbits, dogs, primates and pheasants. The bleomycin model is characterized by biochemical and functional features that closely resemble those found in human pulmonary fibrosis. Among these features are: alveolar epithelial cell damage, recruitment of inflammatory cells releasing mediators of inflammation, abnormal fibroblast activation and proliferation, increased deposition of ECM in the interstitium and alveolar space, leading to a reduction of lung volume and poor compliance<sup>19</sup>.

Although the bleomycin model is the most frequently employed model to study the pathogenesis of lung fibrosis, it has several limitations. Multiple studies have pointed out the differences between this model and human IPF including the speed of onset – as the remodeling is accelerated in bleomycin induced pulmonary fibrosis, durability – as in the model of fibrosis in its chronic stage may develop focal emphysema-like changes<sup>16</sup>. Moreover, administration of bleomycin leads to pneumonitis/fibrosis, which is reversible with steroids, whereas progression of IPF is influenced by these agents only to a limited extent<sup>21</sup>. Despite its limitations, the bleomycin model represents a promising approach to examine the molecular players involved in the pathogenesis of IPF.

### **1.1.5. Fibroblasts: key effector cells in fibrogenesis**

Fibroblasts belong to the connective tissue cell family. They are able to undergo various phenotypic conversions. This phenotypic plasticity is an important feature of the response to many types of tissue injury<sup>25</sup>. The main role of fibroblasts is in the repair and

regenerative processes in every tissue and organ. This primary function is achieved by secretion of ECM proteins that provide a tissue scaffold for normal repair processes course such as epithelial cell migration. Importantly, final dissolution of this scaffold and apoptosis of fibroblasts/myofibroblasts seem to be pivotal for restoration of the normal tissue architecture <sup>26</sup>.

A number of studies have reported that alveolar epithelial cells may initiate the pathogenic processes in IPF by production of the active mediators affecting fibroblasts which induce phenotypic changes in these cells during the progression and end-stage of fibrosis <sup>17,27</sup> (Figure 1.3.) <sup>2</sup>. The presence of these activated fibroblasts with myofibroblast phenotype was described in fibroblastic foci which suggested a role in disease development (Figure 1.4.) <sup>15,17</sup>. In normal repair and regenerative processes, activated fibroblasts produce contractile proteins which are crucial in the re-epithalization events, since they bring the wound closer together <sup>26</sup>. In addition, these cells have the capacity to produce ECM proteins, growth factors, growth factor receptors, cytokines, integrins and oxidants <sup>28,29</sup>. It has been proposed that programmed cell death mediates the decrease in the number of mesenchymal cells finally, allowing differentiation of other cell types to reestablish tissue.

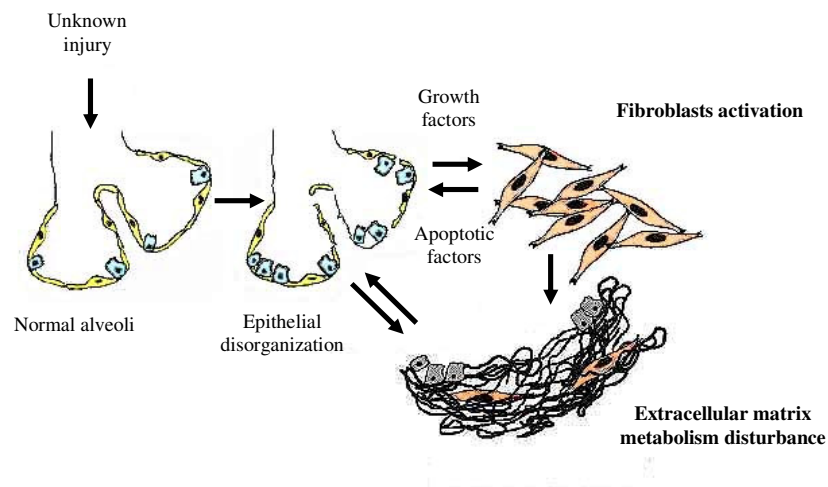


**Figure 1.3. The primary pathogenic events in IPF.**

Unknown injury causes activation of alveolar epithelial cells that release factors inducing migration and proliferation of fibroblasts and changes in their phenotype. In the lesion, myofibroblasts can induce epithelial cell apoptosis and disruption of basement membrane which leads to abnormal re-epithalization. Activated fibroblasts and myofibroblasts secrete excessive amounts of ECM <sup>2</sup>.

Several studies have attempted to characterize the phenotype of fibroblasts in IPF in a more detailed manner. However, these studies have generated conflicting results. According several studies, fibroblasts first assume a migratory phenotype, then a proliferative phenotype, and finally a profibrotic phenotype, during which they produce abundant ECM components. Moreover, there are reports suggesting that fibroblasts from IPF lungs induce alveolar epithelial cell death, which leads to the abnormal wound healing observed in this disease<sup>30</sup>. The repair failure of the damaged alveolar epithelium cells is not only directly caused by fibroblasts, but also indirectly by the degenerative effects of fibroblasts on the basement membrane. The basement membrane is a complex structure that includes type IV collagen, laminin, entactin, fibronectin, and heparin sulfate-chondroitin proteoglycans<sup>31</sup>. In IPF, fibroblasts/myofibroblasts contribute to the degeneration of this complex structure by production of gelatinases A and B, enzymes that degrade components of the membrane<sup>32</sup>. Disrupted basement membrane can no longer play a dynamic role in maintaining the integrity and differentiation of the alveolar epithelium. Moreover, under this condition, the migration of fibroblasts and myofibroblasts into the alveolar space is facilitated<sup>33</sup>.

Fibroblasts and myofibroblasts have key functions in the synthesis, deposition, and remodeling of the ECM. Increased ECM deposition, including fibrillar collagens, fibronectin, elastic fibers, and proteoglycans, is the hallmark of the abnormal tissue remodeling in IPF<sup>14,34</sup>.

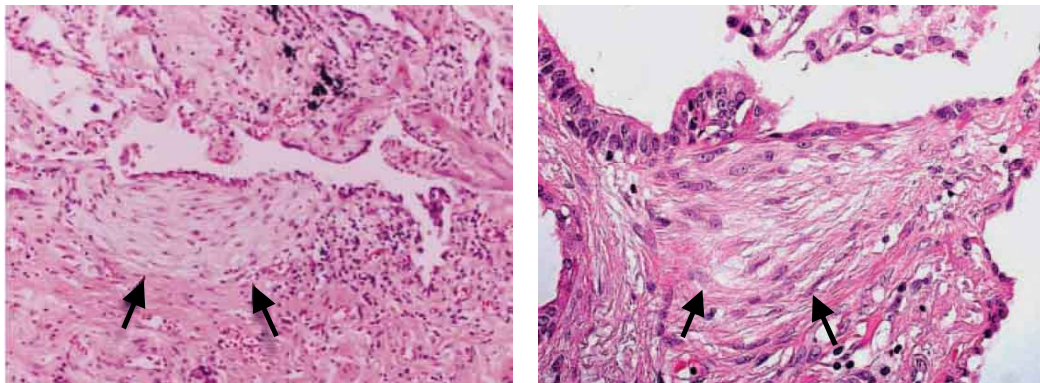


**Figure 1.4. Fibroblast foci in IPF lung.** Fibroblasts foci are indicated with arrows. Hematoxylin and eosin staining<sup>15,17</sup>.

### 1.1.6. Collagen – a key compound of the extracellular matrix

Collagen fibrils are the key ECM proteins that display significantly increased levels in IPF<sup>35</sup>. The fibrils are synthesized and secreted by fibroblasts but how this process is controlled during regeneration and tissue repair remains poorly understood. Collagens are trimeric molecules in which each chain consists of repeating Gly-X-Y triplets, where X and Y are usually proline and hydroxyproline, respectively<sup>36</sup>. This triplet motif results in a left-handed helix that, together with two other helices, can form a right-handed triple-helical structure that (dependent on collagen type) can be homotrimeric or heterotrimeric<sup>37</sup>. Until now, 27 different collagen types have been identified.

Biosynthesis of collagen is a complex process that requires the formation of procollagen, which undergoes extensive post-translational modification. These modifications occur prior to triple helix formation, and consist of hydroxylation of proline and lysine. Hydroxylation of L-proline occurs in an ascorbic acid-dependent manner and is essential for collagen stability<sup>36</sup>. L-proline is generated sequentially from L-ornithine and L-arginine by a set of highly regulated enzymes. Therefore, the abundance of L-arginine, as well as the expression of enzymes metabolizing this amino acid, represent essential determinants of L-proline supply<sup>38-40</sup> and may be a limiting factor in the process of fibrosis. It has been reported that L-arginine becomes essential for growth and development in post-traumatic situations<sup>41</sup>. L-arginine enhances wound healing which also suggests its involvement in collagen metabolism.

## 1.2. L-arginine metabolism

### 1.2.1. L-arginine physiology

L-arginine is a proteinogenous basic amino acid that carries guanidinium groups on its side chains, and has positive charge at neutral pH. In animals, L-arginine is classified as semi-essential amino acid that can be synthesized by several pathways<sup>39</sup>. However, in cases of immaturity, disease or injury, endogenous production of this amino acid may be insufficient to meet higher demand. L-arginine is one of the most metabolically versatile amino acids in animal cells. It serves as a precursor for the synthesis of a vast range of substances including urea, nitric oxide, polyamines, proline, glutamate, and creatine<sup>42</sup>.

Given its diverse roles, L-arginine is metabolized by a complex and highly regulated set of enzymes in several pathways that remain to be explored in more detailed manner. It is known that intracellular L-arginine concentrations may, to some extent, affect the expression of L-arginine metabolic enzymes. By its diversity of function, L-arginine can modulate immune function<sup>43</sup>, wound healing<sup>44</sup>, hormone secretion<sup>45</sup>, vascular tone<sup>46</sup>, insulin sensitivity<sup>47</sup>, and endothelial function<sup>48</sup>.

### 1.2.2. L-arginine synthesis and transport

The sources of L-arginine in the body are dietary proteins, endogenous synthesis, and protein turnover. The majority of plasma L-arginine is derived from protein metabolism and turnover, whereas *de novo* synthesis accounts for only 5–15 % of the endogenous supply. Three organs are involved in the synthesis of this amino acid: the small intestine, the kidneys, and the liver<sup>38,49</sup>.

Glutamine, and glutamate are the dietary amino acids which are metabolized in the small intestine and serve as major precursors for intestinal synthesis of L-arginine or citrulline. From the intestine, citrulline is transported to the kidney, where it is converted into L-arginine by the action of two metabolic enzymes: argininosuccinate synthase (ASS) and, argininosuccinate lyase (ASL). Approximately 60 % of net arginine synthesis in adult mammals occurs in the kidney<sup>50,51</sup> (Figure 1.5.)<sup>39</sup>.

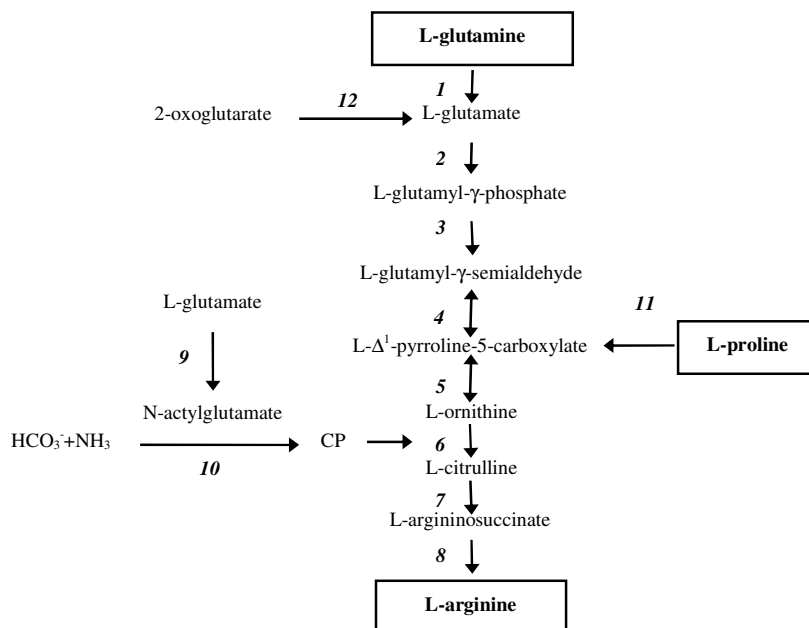


**Figure 1.5. Pathways of arginine synthesis.**

Enzymes catalyzing indicated reactions are:

1, phosphate-dependent glutaminase; 2 and 3, L- $\Delta^1$ -pyrroline-5-carboxylate (P5C) synthetase; 4, spontaneous step; 5, ornithine aminotransferase (OAT); 6, ornithine carbamoyltransferase (OCT); 7, argininosuccinate synthase (ASS); 8, argininosuccinate lyase (ASL); 9, N-acetylglutamate synthase; 10, carbamoyl-phosphate synthase I (CPS I); 11, proline oxidase; 12, aspartate aminotransferase<sup>39</sup>.

The synthesis of L-arginine also occurs within the hepatic urea cycle<sup>52</sup>, which is localized in periportal hepatocytes. This process is possible in the liver only when all the necessary intermediates of the urea cycle, including ornithine, are present. The components of the urea cycle are so closely organized within hepatocytes that intermediates generated within the pathway are immediately utilized and thus do not freely exchange with intracellular pools<sup>53</sup>.

Moreover, in non-hepatic cells, citrulline is co-produced with nitric oxide (NO), and can be recycled to L-arginine via the so-called citrulline/NO cycle or arginine/citrulline cycle. This recycling process is accomplished by the action of ASS and ASL, which are expressed in nearly all cell types (Figure 1.6.)<sup>39</sup>.

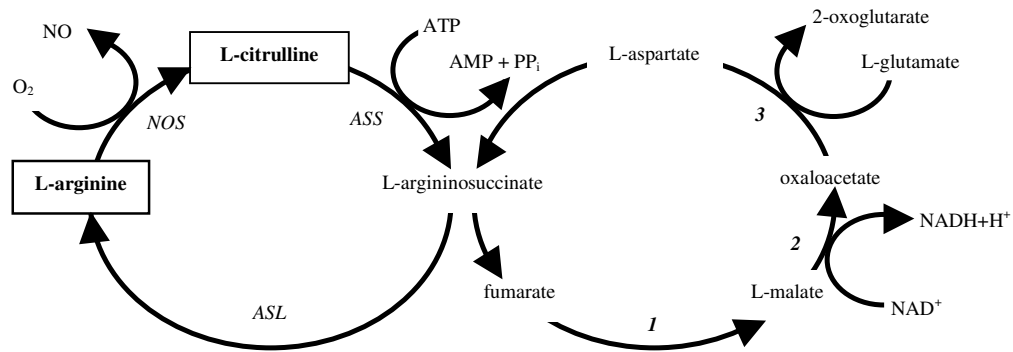


**Figure 1.6. The citrulline/NO cycle**<sup>39</sup>.

Co-production of L-citrulline and NO can be coupled to the citric acid cycle presented on the right. Fumarate produced in the cytosol enters the citric acid cycle in the mitochondrion, where it is converted into oxaloacetate. Oxaloacetate by transamination is converted to aspartate, which is transported into the cytosol. Enzymes catalyzing indicated reactions are: 1, fumarase; 2, malate dehydrogenase; 3, aspartate aminotransferase. Reactions 1-3 are reversible, what is not depicted on the diagram for the sake of simplicity. Argininosuccinate lyase (ASL), argininosuccinate synthase (ASS), nitric oxide synthase (NOS)<sup>39</sup>.

Substrate availability for arginine-requiring enzymes is not only regulated by the level of this amino acid, but also by the arginine transport system. In the majority of mammalian cells, L-arginine requirements are primarily met by the uptake of extracellular L-arginine via specific transporter systems including the  $y^+$ ,  $b^{0,+}$ ,  $B^{0,+}$ , and transporters  $y^{+L}$ <sup>54</sup>. Not every cell type expresses all of these transporters, but their expression and activity can be induced and dynamically regulated by diverse stimuli, such as bacterial endotoxins or inflammatory cytokines<sup>55,56</sup>. System  $y^+$  is considered to be the most important in the uptake of L-arginine in most cell types. It is a high-affinity,  $Na^+$ -independent transporter of not only arginine, but also for ornithine and lysine<sup>57</sup>. However, other cationic amino acids and positively-charged analogs can effectively inhibit L-arginine uptake by this system. The  $y^+$  system, as with the other arginine transport systems, displays diverse expression levels among different cell types and can be dynamically regulated at the pretranslational level<sup>39</sup>. For instance, this system is

present in many cell types, although is absent from hepatocytes. Nevertheless, its expression can be efficiently induced in these cells by inflammatory cytokines<sup>58</sup>. Additionally, expression of this system is reported to be co-induced by inducible nitric oxide synthase (iNOS) in wide variety of cell types, which suggests that an increase in L-arginine transport capacity supports the elevated NO synthesis.

### 1.2.3. L-arginine catabolism

L-arginine can be catabolized via multiple pathways. In contrast to a single enzyme that produces L-arginine, four sets of enzymes use this amino acid as a substrate in mammalian cells: nitric oxide synthase (NOS), arginase (ARG), arginine:glycine amidinotransferase (AGAT), and arginine decarboxylase (ADC). With the exception of ADC, all of these enzymes act on the guanidine group of L-arginine. Some of these enzymes have multiple isoforms, which leads to a high complexity of L-arginine metabolism. There are three distinct isoforms of NOS: neuronal (nNOS), inducible (iNOS), endothelial (eNOS); and two isoforms of ARG (type 1 and 2).

The metabolic complexity extends further as the product of one enzyme may inhibit the activity of another. Moreover, the cellular distribution of enzyme expression varies widely. Some of these enzymes can be coexpressed within the same cell, whereas others are highly restricted to a specific subcellular compartment. For instance, almost all cells can express iNOS upon appropriate stimuli<sup>59</sup>, whereas expression of AGAT is limited to kidney, pancreas, and liver<sup>60</sup>. The activity of ADC as well as ARG2 was reported in mitochondria of many different cell types, in contrast to ARG1 which is a cytosolic enzyme localized to the liver. The overview of the L-arginine catabolic pathway is presented in a simplified scheme in (Figure 1.7.)<sup>38</sup>.



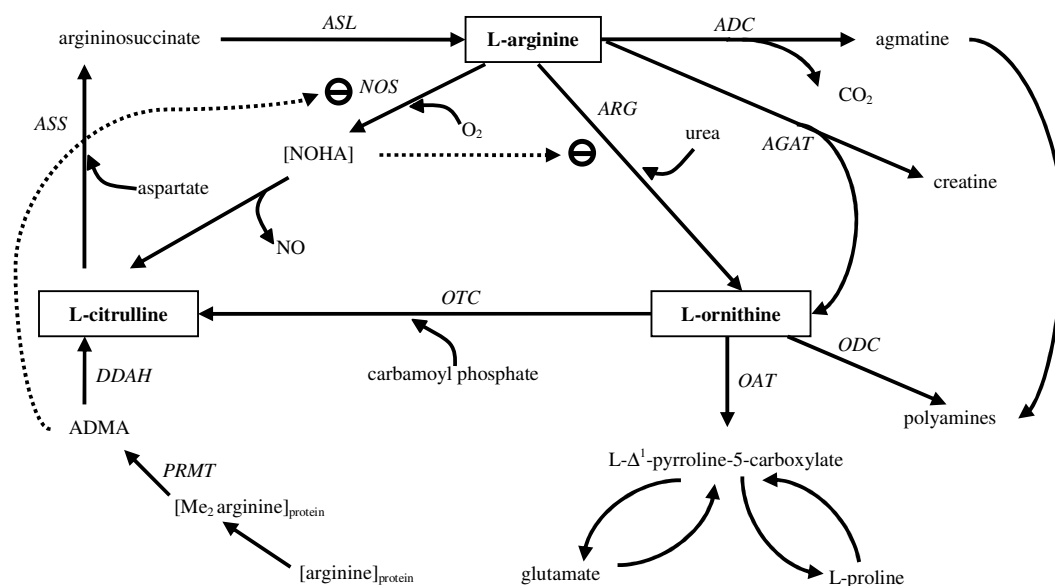


**Figure 1.7. Arginine metabolic pathways.**

For the sake of clarity, only enzymes that directly use or produce arginine, ornithine or citrulline are indicated, and not all reactants and products are depicted. Inhibition of nitric oxide synthase (NOS) and arginase (ARG) by asymmetric dimethylarginine (ADMA) and N<sup>G</sup>-hydroxy-L-arginine (NOHA), respectively, are illustrated by the dashed lines and dash within a circle. Amino acid residues within proteins are indicated by brackets. Arginine decarboxylase (ADC), arginine:glycine amidinotransferase (AGAT), arginase (ARG), argininosuccinate lyase (ASL), argininosuccinate synthase (ASS), dimethylarginine dimethylaminohydrolase (DDAH), dimethyl (Me<sub>2</sub>), nitric oxide (NO), ornithine aminotransferase (OAT), ornithine transcarbamylase (OTC), protein arginine methyltransferase (PRMT) <sup>38</sup>.

Arginine:glycine amidinotransferase is a mitochondrial enzyme that takes part in a well-known pathway, where it initiates the synthesis of creatine. This enzyme transfers the guanidino group from L-arginine to glycine, to form guanidineacetate and ornithine <sup>61</sup>. It is present mainly in renal tubules and pancreas but also to a lesser extent in the liver and other organs. The catabolism of L-arginine through AGAT is determined by dietary levels of creatine, which acts as a feedback repressor of this enzyme <sup>62</sup>.

The existence of ADC in mammalian cells was for a long time controversial. It was reported to be present in plants and bacteria, but it was thought to be absent in mammalian cells. Its activity was subsequently identified in the brain, liver, kidney, adrenal gland, macrophages, and the small intestine <sup>63-65</sup>. However, the presence and

activity of this enzyme remains somewhat unclear since recent reports have challenged previous conclusions. Nevertheless, this enzyme was shown to convert L-arginine to CO<sub>2</sub> and agmatine, and it was demonstrated to be localized in the mitochondrial fraction of cell homogenates<sup>66</sup>.

Arginase is a central enzyme in L-arginine metabolism as it facilitates downstream conversion of this amino acid to urea, ornithine, proline, polyamines, glutamate, or glutamine. There are two distinct types of mammalian ARG: ARG1 (type 1) and ARG2 (type 2), which are encoded by independent genes. Both enzymes are similar with respect to their enzymatic activity, but different with regard to subcellular and tissue localization, and regulation of expression<sup>67</sup>. Arginase-1 is a cytosolic enzyme mainly expressed in the liver as a component of urea cycle, where it converts arginine to ornithine and urea. In limited amounts it is also expressed in other organs. Arginase-2, on the contrary, is a mitochondrial enzyme, expressed in many organs including the kidney, brain, small intestine, mammary gland, and in endothelium and macrophages<sup>67-70</sup>. Differential isoenzymes expression patterns could be explained by the fate of synthesized ornithine, preferentially directed either to proline or glutamate synthesis via ornithine aminotransferase (OAT), or to polyamine synthesis via ornithine decarboxylase (ODC)<sup>39</sup>.

The family of NOS isoenzymes is the best characterized group of L-arginine metabolizing enzymes. It comprises nNOS (neuronal or type 1), iNOS (inducible or type 2), and eNOS (endothelial or type 3). The nNOS and eNOS are constitutively expressed in many different cell types, whereas iNOS displays induced expression and activity after stimulation by bacterial endotoxin or inflammatory cytokines. With the exception of iNOS, both nNOS and eNOS demonstrate activity that is dynamically regulated by Ca<sup>2+</sup>/calmodulin. Moreover, L-arginine can also play a structural role by promoting the dimerization of NOS, which is crucial in order to activate the enzymes<sup>71</sup>. Additionally, NOS isoenzymes display distinct patterns of subcellular localization, which may be a consequence of the diverse regulation of NOS activity. For instance, nNOS is mainly associated with the rough endoplasmic reticulum and postsynaptic membranes in the brain and with the sarcolemma of skeletal muscle<sup>72</sup>, whereas eNOS is associated with caveolae in the plasma membrane<sup>73</sup>. In contrast to these two isoenzymes, iNOS is primarily cytosolic<sup>59</sup>.

#### 1.2.4. Arginase and nitric oxide synthase balance

The NOS and ARG isoenzymes are reported to be expressed simultaneously under wide variety of conditions, which results in cross-reactions with consequences that are not simple to study. As both enzymes utilize L-arginine as a substrate, they can influence each other by limiting the substrate availability<sup>39,74</sup>. The interplay between these enzymes can also be explained by their kinetics. The mammalian ARG display  $K_m$  values for L-arginine that are in the 2–20 mM range, whereas the NOS  $K_m$  is in the 2-20  $\mu$ M range. Nevertheless, the  $V_{max}$  for ARG at physiological pH is more than 1000-fold higher than the NOS  $V_{max}$ , which in the rat liver are approximately 1400  $\mu$ mol/min per mg, and 1  $\mu$ mol/min per mg, respectively. This suggests that ARG activity is able to limit L-arginine for NO synthesis in these cells<sup>67,75</sup>. Thus, several investigations have shown that ARG limits NO production by NOS, under some circumstances<sup>76-78</sup>. The converse situation has not been demonstrated yet, what is connected with the fact that synthesis of NO is accompanied by production of N<sup>G</sup>-hydroxy-L-arginine (NOHA). This intermediate of NO synthesis behaves as an endogenous inhibitor of ARG, therefore, it is speculated that the inhibitory effects of NOS on ARG activity reflect rather the inhibitory potential of NOHA<sup>79</sup>, which leads to the conclusion that the interplay between both enzymatic systems is more complex than the fact that they use the same substrate.

Finally, turnover of the proteins containing methylated arginine residues can also have an affect on NOS activity. By the action of enzymes called protein arginine methyltransferases (PRMT) the arginine residues incorporated into proteins can be methylated. Further degradation of such proteins leads to the release of monomethylated (NMMA), asymmetrically dimethylated (ADMA), and symmetrically dimethylated (SDMA) arginine. The first two of these modified L-arginine types behave as NOS inhibitors<sup>80</sup>, and especially ADMA represents a risk factor for cardiovascular diseases<sup>81-84</sup>.

Thus, the balance and the crosstalk between ARG and NOS isoenzymes seem to be crucial under a vast number of circumstances or disease states. Nitric oxide, produced by the action of NOS, is a putative neurotransmitter and cytotoxic effector molecule, which causes vasodilatation of blood vessels. These characteristics make NOS and NO pivotal factors in various cardiovascular diseases, congestive heart failure, and coronary

artery disease. In turn, elevated expression of ARG during inflammation or infection may not only decrease levels of NO, but also stimulate the synthesis of proline and polyamines via increased production of ornithine<sup>85</sup>. This ARG-mediated increase of polyamine and proline production<sup>86</sup> subsequently promotes cell proliferation<sup>87</sup> and a collagen synthesis. These processes play important roles in infections, chronic inflammatory diseases, and particularly in wound healing and fibrotic disorders.

Thus, several studies suggest that L-arginine is a crucial player in many disease states, and its supplementation may have an effect on the recovery process of the organism<sup>41,88-90</sup>. Moreover, the complexity of multiple metabolic pathway of L-arginine indicates the importance of the crosstalk between single enzymes, but also suggests that the imbalance between them may be critical in the development of several diseases in which processes including abnormal wound healing connected with cell overproliferation are involved.

#### **1.2.4.1. Functional consequences of arginase and nitric oxide synthase regulation**

It is well characterized that L-arginine metabolism is mainly determined by the activity of ARG and NOS isoenzymes. It is also known that these two enzymes may be differentially regulated within diverse cell types as well as under variety of conditions. For instance, activity of iNOS and both ARG isoenzymes was reported to be increased in mouse macrophages upon LPS exposure<sup>91,92</sup>. In several other studies, it was demonstrated that wound and peritoneal macrophages convert L-arginine to citrulline and ornithine at comparable rates, which can indicate that both NOS and ARG pathways are functional<sup>93</sup>. However, other reports demonstrated differential regulation of iNOS and ARG isoenzymes in RAW 264.7 macrophages and mouse peritoneal macrophages upon 8-bromo-cAMP and Interferon- $\gamma$  stimulation<sup>68</sup>. Experiments performed on cardiac myocytes demonstrated that ARG2 is predominant in these cells, and can negatively regulate nNOS activity<sup>76</sup>. The upregulation of ARG isoforms was also shown in disease processes in which NO signaling is dysregulated, for example, endothelial dysfunction of aging<sup>94</sup>, hypertension<sup>95</sup>, atherosclerosis<sup>96</sup>, and erectile dysfunction of diabetes<sup>97,98</sup>. Uncontrolled upregulation of ARG expression was also reported in the myeloid suppressor cells in renal cell carcinoma patients<sup>99</sup>. The high activity of these enzymes

originated from tumor cells, in which the metabolism of L-arginine to ornithine is required to maintain rapid cell proliferation. Depletion of L-arginine may lead to the limited production of NO and difficulties in immune response to the disease state. In contrast to the negative influence of ARG overexpression on homeostasis and the development of several diseases, there are data pointing to protective roles of ARG in mouse model of colitis <sup>100</sup>. As iNOS activity worsen the state of colitis patient, upregulation of ARG with its enhanced production of polyamines plays a beneficial role in recovery. The balance between NOS and ARG seems to be crucial also for the processes of wound and skin repair. Upon injury of healthy skin, the activity of ARG isoenzymes as well as iNOS was demonstrated to be elevated and localized in epithelial sites <sup>101</sup>. Diabetes-impaired skin repair was characterized by abnormally elevated ARG activity in wound tissues where iNOS expression was absent leading to decreased NO production. These lower NO levels led to impaired re-epithelialization within the wound. Both enzymes were also suggested to be important in the pathophysiology of psoriasis <sup>102</sup>. Overexpression of ARG1 in psoriatic skin lesions led to the limited iNOS-mediated synthesis of NO *in vivo*, which was beneficial, since the high output of NO, a potent regulator of proliferation and differentiation, contributes the hyperproliferative disease state in psoriasis.

#### **1.2.4.2. Arginase and nitric oxide synthase regulation in lung disorders**

Different combinations of cytokines can regulate ARG and NOS in diverse ways. The Th1-associated cytokines INF- $\gamma$  or TNF- $\alpha$  activate iNOS, whereas the Th2-type cytokines IL-4, IL-10, and IL-13 appear to induce ARG <sup>85,103</sup>. These characteristics may underlie the differential regulation of these two enzymes upon inflammatory stimulation, included in several lung disorders.

Studies performed on tissue biopsies from patients with asthma revealed that this lung disorder is characterized by chronic airway inflammation associated with lung remodeling. Further studies performed in a mouse asthma model demonstrated high induction of ARG1 and ARG2 expression during development of the disease <sup>104</sup>. Arginase-1 was shown to be localized in the active inflammatory sites around airways and blood vessels. Macrophages appeared to be the major source of these enzymes, which

potentially have a role in the recovery of the tissue from inflammation and infection. Increased expression of ARG with concomitant suppression of NO generation led to airway hyperresponsiveness and increased generation of mucus and collagen, which may contribute to pathogenesis of asthma.

The balance between NOS and ARG activity was also shown to be disturbed in cystic fibrosis (CF). Airway disease in CF is characterized by chronic inflammation, chronic bacterial infection, and infection-associated pulmonary exacerbations<sup>105</sup>. Despite the inflammatory character of this lung disease, patients exhibit lower levels of fractional exhaled NO and bioactive NO in airway fluids. This decreased NO production has a negative influence on the defense against bacterial infections, and contributes to airway obstruction. The results of several studies demonstrated increased activity of ARG in patients with CF, which as in asthma, limits substrate for NO generation and in consequence leads to decrease in iNOS activity<sup>106,107</sup>.

These findings suggested that L-arginine depletion caused by increased ARG activity may play a pivotal role in the diseases connected with increased smooth muscle contractility. In line with this indication, experiments carried out on patients with pulmonary arterial hypertension (PAH) revealed significantly higher activity of ARG in lysates of bronchial and vascular tissue of lungs from patients with PAH as well as in lung endothelial cells<sup>108</sup>. The L-ornithine originating from ARG activity contributes to vascular remodeling in PAH via conversion to polyamines and proline<sup>109</sup>.

#### **1.2.4.3. L-Arginine metabolism in idiopathic pulmonary fibrosis**

A dysregulated ARG/NOS balance in several lung disorders, as well as the activity of ARG in the production of polyamines and proline that control cell proliferation and collagen production, respectively, suggest an important role of ARG in fibrotic diseases. The role of ARG in the pathogenesis of IPF remains to be fully elucidated, since only a low number of studies have been performed up until now in this field. One report indicated higher expression of pulmonary ARG1 in a mouse model of herpes virus-induced lung fibrosis<sup>110</sup>. Additionally, the induction of both ARG isoenzymes in macrophages in bleomycin-induced lung fibrosis was demonstrated<sup>111</sup>.

---

However, no data demonstrating a functional involvement of ARG in IPF pathogenesis have been published thus far. It is well known that several interleukins, growth factors, and chemokines are involved in IPF development, however, one of them, transforming growth factor-beta (TGF- $\beta$ ) seems to play an important, if not pivotal, role in IPF pathogenesis. The presence of active TGF- $\beta$  in the lung leads to induction of altered alveolar and parenchymal structures, development of honeycomb structures, presence of fibroblasts and myofibroblasts, enhanced matrix deposition, and collagen synthesis<sup>112</sup>. Of interest are the studies demonstrating that TGF- $\beta$ 1-stimulated collagen production is dependent on proline formation. Moreover, it has been shown that TGF- $\beta$ 1 stimulates polyamine and proline generation by the induction of genes regulating the transport and metabolism of L-arginine<sup>56</sup>. These findings indicate a possible link between arginine metabolism and IPF pathogenesis, and explain the need for further investigation of L-arginine metabolizing enzymes.

## 2. Aim of the study

It is well-established that an imbalance between the L-arginine metabolic enzymes arginase and nitric oxide synthase, may contribute to the development of several lung diseases. Arginase may significantly impact collagen synthesis due to augmented L-proline bioavailability, endothelial dysfunction of the pulmonary vascular bed due to decreased NO synthesis, and increased cell proliferation induced by the enhanced bioavailability of polyamines. As these processes are reported to be involved in the pathogenesis of idiopathic pulmonary fibrosis, this project aims to functionally characterize L-arginine metabolic enzymes in experimental and idiopathic pulmonary fibrosis. In this context, the research focus was:

1. Expression analysis of L-arginine metabolic enzymes in a mouse model of bleomycin-induced lung fibrosis.
2. Elucidation of the role of these enzymes and their impact on cellular L-arginine levels.
3. Analysis of TGF- $\beta$  contribution to the regulation of L-arginine metabolic enzymes.
4. Verification of these results in lung specimens from IPF patients.



### 3. Materials and Methods

#### 3.1. Materials

##### 3.1.1. Equipment

ABI PRISM 7500 Sequence Detection System	Applied Biosystems, USA
C57BL/6N mice	Charles River, Germany
Cell Culture Incubator; Cytoperm2	Heraeus, Germany
Chroma SPIN-1000 DEPC-H <sub>2</sub> O Columns	Biosciences, Clontech, USA
Developing machine; X Omat 2000	Kodak, USA
Electrophoresis chambers	Bio-Rad, USA
Film cassette	Sigma-Aldrich, Germany
Filter Tip FT: 10, 20, 100, 200, 1000	Greiner Bio-One, Germany
Filter units 0,22 µm syringe-driven	Millipore, USA
Fluorescence microscope; LEICA AS MDW	Leica, Germany
Freezer -20 °C	Bosch, Germany
Freezer -40 °C	Kryotec, Germany
Freezer -80 °C	Heraeus, Germany
Fridge +4 °C	Bosch, Germany
Fusion A153601 Reader	Packard Bioscience, Germany
Gel blotting paper 70 × 100 mm	Bioscience, Germany
Glass bottles: 250, 500, 1000 ml	Fischer, Germany
GS-800TM Calibrated Densitometer	Bio-Rad, USA
HPLC system:	
ASI-100 auto sampler	Dionex, USA
P680 gradient pump	Dionex, USA
RF-2000 fluorescence detector	Dionex, USA
Data acquisition system Chromeleon 6.60,	Dionex, USA
Light microscope Olympus BX51	Olympus, Germany
µBondapak™ C18 guard column	Waters, USA

---

Mini spin centrifuge	Eppendorf, Germany
Multifuge centrifuge, 3 s-R	Heraeus, Germany
Oasis MCX solid-phase extraction cartridges	Waters, USA
PCR-thermocycler	MJ Research, USA
Pipetboy	Eppendorf, Germany
Pipetmans: P10, P20, P100, P200, P1000	Gilson, France
Power Supply; Power PAC 300	Bio-Rad, USA
Petri dish with vents	Greiner Bio-One, Germany
Pipette tip: 200, 1000 µl,	Sarstedt, Germany
Pipette tip 10 µl	Gilson, USA
Quantity One software	Bio-Rad, USA
Radiographic film X-Omat LS	Sigma-Aldrich, Germany
Serological pipette: 5, 10, 25, 50 ml	Falcon, USA
SunFire™ C18 column	Waters, USA
Test tubes: 15, 50 ml	Greiner Bio-One, Germany
Tissue culture chamber slides	BD Falcon, USA
Tissue culture dish 100 mm	Greiner Bio-One, Germany
Tissue culture flask 250 ml	Greiner Bio-One, Germany
Tissue culture plates: 6, 48 well	Greiner Bio-One, Germany
Trans blot transfer medium (0,2 µm)	Bio-Rad, USA
Western Blot Chambers:	
Mini Trans-Blot	Bio-Rad, USA
Mini-Protean 3 Cell	Bio-Rad, USA
Vortex machine	Eppendorf, Germany
Vacuum centrifuge	Eppendorf, Germany

### 3.1.2. Reagents

Acetonitrile	Roth, Germany
Acrylamide solution, Rotiphorese Gel 30	Roth, Germany
Agarose	Invitrogen, UK
Albumine, bovine serum	Sigma-Aldrich, Germany
Ammonium persulphate	Promega, Germany
Ammonium sulphate	Sigma-Aldrich, Germany
$\beta$ -glycerophosphate	Sigma-Aldrich, Germany
$\beta$ -mercaptoethanol	Sigma-Aldrich, Germany
Bleomycin sulphate	Almirall Prodesfarme, Spain
Bromophenol blue	Sigma-Aldrich, Germany
Calcium chloride	Sigma-Aldrich, Germany
Complete <sup>TM</sup> Protease inhibitor	Roche, Germany
D-(+)-Glucose	Sigma-Aldrich, Germany
D-MEM medium	Gibco BRL, Germany
D-MEM medium	Sigma-Aldrich, Germany
Dimethyl sulfoxide	Sigma-Aldrich, Germany
DNA Ladder (100 bp, 1kb)	Promega, USA
Ethylendinitrilo-N, N, N', N', -tetra-acetic-acid (EDTA)	Promega, USA
Ethylene glycol-bis (2-amino-ethylether)-N,N,N',N' -tetraacetic-acid (EGTA)	Sigma-Aldrich, Germany
Dulbecco's phosphate buffered saline 10 $\times$	PAA Laboratories, Austria
Dulbecco's phosphate buffered saline 1 $\times$	PAA Laboratories, Austria
Ethanol absolute	Riedel-de Haën, Germany
ECL Plus Western Blotting Detection System	Amersham Biosciences, UK
Ethidium bromide	Roth, Germany
Fetal calf serum (FCS)	Gibco BRL, Germany
Glycine	Roth, Germany
GoTaq® Flexi DNA polymerase	Promega, USA
Hydrochloric acid	Sigma-Aldrich, Germany

---

2-(-4-2-hydroxyethyl)-piperazinyl-1-ethansulfonate (HEPES)	Sigma-Aldrich, Germany
Igepal CA-630	Sigma-Aldrich, Germany
ImProm-II <sup>TM</sup> Reverse Transcriptase	Promega, USA
L-arginine	Sigma-Aldrich, Germany
Lipofectamine <sup>TM</sup> 2000	Invitrogene, UK
Luciferase Assay Reagent 10-Pack	Promega, USA
Luciferase Cell Culture Lysis 5× Reagent	Promega, USA
Magnesium chloride	Sigma-Aldrich, Germany
Magnesium sulfate	Sigma-Aldrich, Germany
Methanol	Fluka, Germany
N <sup>G</sup> -hydroxy-L-arginine, monoacetate salt (NOHA)	Calbiochem, Germany
N,N,N',N'-tetramethyl-ethane-1,2-diamine (TEMED)	Bio-Rad, USA
Oligo(dT)15 Primer	Promega, USA
Opti-MEM medium	Gibco BRL, Germany
<i>Ortho</i> -phthaldialdehyde (OPA)	Grom-chromatography, Germany
PCR Nucleotide Mix	Promega, USA
Penicillin-streptomycin	PAA Laboratories, Austria
Potassium acetate	Sigma-Aldrich, Germany
Potassium borate	Grom-chromatography, Germany
Potassium chloride	Merck, Germany
Potassium phosphate	Sigma-Aldrich, Germany
Precision Plus Protein <sup>TM</sup> Standards	Bio-Rad, USA
2-Propanol	Merck, Germany
QIAprep Spin Miniprep Kit	Qiagen, Germany
QuantiChrom <sup>TM</sup> Arginase Assay Kit	BioAssay Systems, USA
Quick Start <sup>TM</sup> Bradford Dye Reagent	Bio-Rad, USA
RNasin inhibitor	Promega, Germany
RNeasy Midi Kit	Qiagen, Germany

---

Roti®-Quick-Kit	Roth, Germany
Sircol™, Soluble Collagen Assay	Biocolor, UK
Sodium acetate	Sigma-Aldrich, Germany
Sodium chloride	Merck, Germany
Sodium dodecyl sulfate (SDS)	Promega, USA
Sodium ortho vanadate	Sigma-Aldrich, Germany
Sodium phosphate	Sigma-Aldrich, Germany
Sodium sulfate	Merck, Germany
SuperSignal® West Pico Chemiluminescent Substrate	Pierce, USA
SYBER® Green PCR Kit	Qiagen, Germany
Transforming growth factor $\beta$ 1 (TGF- $\beta$ 1)	R&D Systems, USA
Tween 20	Sigma-Aldrich, Germany
Tris	Roth, Germany
Triton X-100	Promega, USA
Trypsin/EDTA	Gibco BRL, Germany

### **3.1.3. Mammalian cells**

#### **3.1.3.1. Cell lines**

NIH-3T3 (Swiss mouse embryo), fibroblasts, DSMZ, Germany

#### **3.1.3.2. Primary cells**

Mouse primary lung fibroblasts were isolated from bleomycin-treated and saline-treated animals. Human primary lung fibroblasts were isolated from tissues obtained from healthy transplant donors, as described in 3.2.12.2.

### **3.1.4. Animal model of pulmonary fibrosis**

#### **3.1.4.1. Bleomycin-induced lung fibrosis in mice**

Bleomycin is an effective antineoplastic drug, nevertheless its repeated systemic administration may result in lung inflammation that can progress to fibrosis. Because bleomycin-induced lung fibrosis is easily reproduced in many different mammalian species, an experimental model using this drug was adopted with a goal of investigating the cellular and molecular basis of interstitial lung fibrosis.

All animal studies in the project were performed according to the guidelines of the University of Giessen and approved by the local authorities (Regierungsprasidium Giessen, no. II25.3–19c20–15; GI20/10-Nr.22/2000). Specific pathogen-free female C57BL/6N mice weighing 18–20 g (supplied by Charles River, Sulzfeld, Germany), were used. Bleomycin was dissolved in 0,9 % PBS and administered as a single dose of 0,08 mg in 200 µl saline solution per animal via microsyringe application on day 0. Control animals received only PBS. Pathological changes were already observed seven days after treatment. Mice were sacrificed for analysis at 3, 5, 7, 14, 21 days after exposure to bleomycin, and animal lungs were collected and processed for embedding and sectioning, reserved for primary fibroblasts isolation, or immediately snap-frozen in liquid nitrogen.

## 3.2. Methods

### 3.2.1. RNA isolation

Isolation of RNA from lung tissue and cultured cells material was performed according to the manufacturer's instructions provided with a RNeasy Midi Kit and Roti®-Quick-Kit, respectively.

### 3.2.2. Reverse transcription reaction

Reverse transcription polymerase chain reaction (RT-PCR) is an enzymatic process performed by an enzyme called reverse transcriptase. This enzyme synthesizes complementary DNA (cDNA) using RNA as a template.

In order to perform RT-PCR, 500 ng of mouse or human total RNA was added to 1  $\mu$ l of oligo-(dT)15 (100  $\mu$ g/ml). The reaction mixture was heated to 70 °C for 5 min, chilled on ice, and the following RT reagents were added:

RT reaction component	Volume	Final concentration
5× RT Buffer (free MgCl <sub>2</sub> )	4 $\mu$ l	1×
25 mM MgCl <sub>2</sub>	4,8 $\mu$ l	6 mM
10 mM dNTP mix	1 $\mu$ l	0,5 mM
RNasin inhibitor (1 U/ $\mu$ l)	1 $\mu$ l	1 U
Reverse transcriptase (1 U/ $\mu$ l)	1 $\mu$ l	1 U
H <sub>2</sub> O (RNase free)	to 20 $\mu$ l	not applicable

To synthesize cDNA, the reaction mixture was incubated at 25 °C for 5 min and at 42 °C for 1 h. Synthesized cDNA was either stored at -20 °C or used for other experiments directly.

### 3.2.3. Polymerase chain reaction

The polymerase chain reaction (PCR) is an enzymatic technique that facilitates the production of millions of copies of specific DNA. The amplification of cDNA, previously reverse-transcribed from RNA, is carried out by an enzyme called DNA polymerase. Principally, each PCR cycle consists of three steps:

- Denaturation - separation of double-stranded DNA to single strands.
- Annealing - primers binding to the appropriate sequence of single DNA strands.
- Elongation - synthesis of a new DNA strand by DNA polymerase.

#### 3.2.3.1. Semi-quantitative polymerase chain reaction

Semi-quantitative PCR reaction in principal proceeds as described in 3.2.3. Amplification of cDNA was performed according to the manufacturer's instructions provided with the GoTaq® Flex DNA Polymerase. The PCR reaction mix was prepared as follows:

PCR reaction component	Volume	Final concentration
5× PCR Buffer (free MgCl <sub>2</sub> )	10 µl	1×
25 mM MgCl <sub>2</sub>	5 µl	2,5 mM
10 mM dNTP mix	1 µl	0,2 mM
10 µM forward primer*	1 µl	0,2 µM
10 µM reverse primer*	1 µl	0,2 µM
Taq DNA Polymerase (5 U/µl)	0,25 µl	1,25 U
cDNA template	1 µl	not applicable
H <sub>2</sub> O (autoclaved)	to 50 µl	not applicable

\* All primer sequences are listed in Table 6.1.2.



The PCR reaction components were mixed on ice and transferred to a PCR machine. To perform effective amplification of cDNA, the following program was performed:

Step	Time	Temperature
Denaturation	1 min	94 °C
Annealing	1 min	57-60 °C*
Elongation	30 s	72 °C

\* Annealing temperatures varied depending on the primers used in the experiment.

The steps were repeated in 22-28 cycles depending on the amplified sequence. Amplicons were immediately separated by the agarose gel electrophoresis and visualized by staining with ethidium bromide.

### 3.2.3.2. Real-time polymerase chain reaction

Quantitative Real Time PCR is used to simultaneously quantify and amplify specific sequence of DNA. The procedure follows the PCR strategy but after each amplification round, the DNA is quantified. Quantification is performed by means of fluorescent dye – SYBR® Green I – which directly binds to double-stranded DNA. The bound dye generates a signal that is proportional to the DNA concentration.

Reactions were performed according to the manufacturer's instructions provided with a SYBER® Green PCR Kit. PCR reaction mix was prepared as follows:

PCR reaction component	Volume	Final concentration
Platinum® Syber® Green qPCR SuperMix-UDG	13 µl	1×
50 mM MgCl <sub>2</sub>	1 µl	2 mM
10 µM forward primer*	0,5 µl	0,2 µM
10 µM reverse primer*	0,5 µl	0,2 µM
cDNA template	1 µl	not applicable
H <sub>2</sub> O (autoclaved)	to 25 µl	not applicable

\* All primers sequences are listed in Table 6.1.1.

The amplification and quantification of cDNA was carried out by means of following program:

Step	Timee	Temperature
Denaturation	5 s	95 °C
Annealing	5 s	59-60 °C*
Elongation	30 s	72 °C

\*Annealing temperatures varied depending on the primers used in the experiment.

The steps were repeated in 45 cycles.

A ubiquitously- and equally-expressed gene that is free of pseudogenes was used as the reference gene in all quantitative real time PCR reactions. The relative transcript abundance of a gene was presented as  $\Delta C_t$  values ( $\Delta C_t = C_{t\text{reference}} - C_{t\text{target}}$ ). Relative changes in transcript levels compared to controls were displayed as  $\Delta\Delta C_t$  values ( $\Delta\Delta C_t = \Delta C_{t\text{treated}} - \Delta C_{t\text{control}}$ ). All  $\Delta\Delta C_t$  values corresponded approximately to the binary logarithm of the fold change.

### 3.2.4. DNA agarose gel electrophoresis

Agarose gel electrophoresis was performed in order to separate and analyze DNA products obtained by PCR. Percentage of the gels varied 1–2,5 % depending on the size of the DNA amplicon. Agarose was mixed with 1× TAE buffer and 0,5 µg/ml ethidium bormide – a DNA intercalating dye – that enables visualization of the DNA fragments under ultraviolet light. The DNA samples were mixed with 6× DNA loading buffer and loaded onto the gel. Electrophoresis was performed at 100 V/cm in 1× TAE buffer.

#### 1× TAE:

40 mM Tris-acetate, pH = 8,0

1 mM EDTA, pH = 8,0

6× DNA loading buffer:

0,025 % (w/v) bromophenol blue

40 % (w/v) sucrose

**3.2.5. Protein isolation**

Proteins were extracted either from total lung tissue or mammalian cells. Depending on the biological material, two different extraction methods were performed.

**3.2.5.1. Protein isolation from tissues**

Lung tissue preserved in liquid nitrogen was homogenized by addition of ice-cold tissue lysis buffer. Tissue lysate was then passed 5–8 times through a 0,9 mm gauge needle fitted to a Rnase-free syringe. Homogenized tissue was then incubated for 30 min on ice and centrifuged  $15\ 000 \times g$  for 15 min at 4 °C. Resulting supernatant was used as a tissue extract and stored at -20 °C for further experiments.

Tissue lysis buffer:

20 mM Tris-HCl, pH = 7,5

150 mM NaCl

1 mM EDTA

1 mM EGTA

1 % Triton X-100

2,5 mM Na<sub>3</sub>PO<sub>4</sub>

1 mM β-glycerophosphate

1 mM Na<sub>3</sub>VO<sub>4</sub>, phosphates inhibitor – added immediately prior homogenization

Complete™, protease inhibitor mix – added immediately prior homogenization

### 3.2.5.2. Protein isolation from cells

Cells were harvested at indicated time points by scraping in the cell lysis buffer with a rubber policeman. Collected cells were passed 5–8 times through a 0,9 mm gauge needle until a homogenous lysate was obtained. Lysates were then incubated for 30 min on ice and centrifuged  $15\,000 \times g$  for 15 min at 4 °C. Resulting supernatants were used as cell extracts and stored at -20 °C for further experiments.

#### Cell lysis buffer:

20 mM Tris-HCl, pH = 7,5

150 mM NaCl

1 mM EDTA

1 mM EGTA

0,5 % Igepal CA-630

1 mM  $\text{Na}_3\text{VO}_4$ , phosphates inhibitor – added immediately prior homogenization

Complete™, protease inhibitor mix – added immediately prior homogenization

### 3.2.5.3. Protein quantification

Protein concentrations in tissue and cell extracts were spectrophotometrically determined using Quick Start™ Bradford Dye Reagent and a Fusion A153601 Reader according to the manufacturer's instructions. The protein assay is based on the color change of Coomassie Brilliant Blue G-250 dye in response to various protein concentrations. The dye binds primarily to basic and aromatic amino acids residues. Ten microliters of sample was mixed with 200 µl of Bradford Dye Reagent and transferred to a 96-well plate. Six dilutions of protein standard, bovine serum albumin, 0,05–0,5 µg/µl were prepared and mixed with Bradford Dye Reagent in the same ratio as the sample of unknown concentration. Reaction mixtures were incubated for 15 min at room temperature. The absorbance of the samples was measured at 570 nm. The unknown amount of protein in the sample was determined by interpolation, reading the concentration of protein on the standard curve that corresponded to its absorbance.

### 3.2.6. SDS polyacrylamide gel electrophoresis

Protein extracts were separated by means of SDS polyacrylamide gel electrophoresis (SDS-PAGE). Before loading onto the gel, 30 µg of protein was combined with 10× SDS-loading buffer, and denaturated by heating for 5 min at 100 °C. Separation of proteins was performed in the gel consisting of 5 % stacking gel and 10 % resolving gel. Electrophoresis was carried out in SDS-running buffer at 120 V.

#### 10× SDS-loading buffer:

625 mM Tris-HCl, pH = 6,8

50 % (v/v) glycerol

20 % (w/v) SDS

9 % (v/v) β-mercaptoethanol

0,3 % (w/v) bromophenol blue

#### Stacking gel:

5 % acrylamide:bisacrylamide

125 mM Tris-HCl, pH = 6,8

0,1 % (w/v) SDS

0,1 % (w/v) APS

0,1 % (v/v) TEMED

#### Resolving gel:

10 % acrylamide:bisacrylamide

375 mM Tris-HCl, pH = 8,8

0,1 % (w/v) SDS

0,1 % (w/v) APS

0,1 % (v/v) TEMED

SDS-running buffer:

25 mM Tris

250 mM glycine

0,1 % (w/v) SDS

**3.2.7. Immunoblotting**

Immunoblotting was performed in order to visualize and detect specific proteins separated previously by means of SDS-PAGE.

**3.2.7.1. Protein blotting**

Proteins separated by SDS-PAGE were transferred to 0,25 µm pure nitrocellulose membrane or polyvinylidene difluoride (PVDF) membrane depending on the experiment. Activation of the PVDF membrane was carried out in 100 % methanol directly prior to protein blotting. Transfer was performed in transfer buffer at 120 V for 1 h.

Transfer buffer:

25 mM Tris

192 mM glycine

20% (v/v) methanol

**3.2.7.2. Protein detection**

Membranes were blocked in blocking solution for 1 h at room temperature. The PVDF membranes were dried prior to blocking and soaked with 100% methanol. After blocking, membranes were incubated with the appropriate primary antibodies either for 1 h at room temperature or overnight at 4 °C \*. Afterwards membranes were washed three times for 10 min with 1× PBST buffer, incubated with horse radish peroxidase-labeled secondary antibody for 1 h at room temperature, and then washed five times for 10 min with 1× PBST. Specific bands were visualized by chemiluminescence using an

Enhanced Chemiluminescence Immunoblotting system. In order to re-probe membranes with another antibody, membranes were stripped with stripping buffer for 15 min at 52 °C and subsequent protein detection was performed as described above.

Blocking solution:

5 % (w/v) non-fat dry milk

1× PBS

0,1 % (v/v) Tween-20

1× PBST:

1× PBS

0,1 % (v/v) Tween-20

Stripping buffer:

62,5 mM Tris-HCl, pH = 6,8

2 % (w/v) SDS

100 mM  $\beta$ -mercaptoethanol

\* Primary antibody concentrations varied depending on the antibodies used in the experiment, and are presented in Tables 6.2.1. and 6.2.2.

### **3.2.8. Densitometry**

Densitometric analysis of autoradiography was performed using a GS-800TM Calibrated Densitometer and the 1-D analysis software Quantity One. Protein expression was normalized to  $\beta$ -actin levels detected by an anti- $\beta$ -actin antibody.

### 3.2.9. Immunohistochemistry

In order to localize and detect expression of indicated proteins in the lung tissue, immunohistochemical analysis was performed using a Histostain-SP Kit. Whole lung sections were deparaffinized in xylene three times for 10 min, and rehydrated in 100 % ethanol twice for 5 min, 95 % ethanol twice for 5 min, 70 % ethanol twice for 5 min, and 1× PBS twice for 5 min. Antigen retrieval was performed by incubation of the slides in 1× citrate buffer for 20 min at 100 °C, followed by cooling the slides for next 10 min. Endogenous peroxidase activity was quenched by incubating the sections with 3 % (v/v) H<sub>2</sub>O<sub>2</sub> for 10 min. Sections were blocked with blocking solution provided in the kit for 10 min at room temperature, followed by incubation with the primary antibody overnight at 4 °C \*. Afterwards, sections were washed twice with 1× PBS for 5 min, and incubated with biotinylated secondary antibodies for 10 min, followed by the streptavidin-conjugated enzyme for 10 min, and chromogenic substrate for 10 min. Slides were developed for 5 min with diaminobenzidine (DAB) and counterstained with Mayers hematoxylin. Sections were mounted using mounting medium and examined for staining using an Olympus BX51 microscope.

\* Primary antibody concentrations varied depending on the antibodies used in the experiment, and are presented in Tables 6.2.1. and 6.2.2.

### 3.2.10. Immunocytochemistry

Immunocytochemistry was performed to visualize the localization of particular proteins inside the cells. Cells were seeded in 8-well chamber slides. After 24 h, culture medium was removed and cells were washed twice for 5 min with ice-cold 1× PBS. Cells were fixed in 100 % methanol for 5 min at -20 °C, washed twice for 5 min with 1× PBS and then incubated in blocking solution for 1 h at room temperature. Afterwards, cells were incubated with the appropriate primary antibody overnight at 4 °C \*, then washed 3 times for 5 min with 1× PBS. Subsequently, incubation with fluorescein-5-isothiocyanate -labeled secondary antibodies (1:200 dilution) was performed for 1 h at



room temperature. After five washing rounds for 5 min each, performed with 1× PBS, chamber slides were covered with mounting medium containing 4',6-diamidino-2-phenylindole (1:1000 dilution) to visualize the nucleus of the cells. The localization of the proteins was analyzed by means of fluorescent microscopy.

Blocking solution:

5 % (v/v) FCS

1× PBS

\* Primary antibody concentrations varied depending on the antibodies used in the experiment, and are presented in Tables 6.2.1. and 6.2.2.

### **3.2.11. Amino acid analysis**

#### **3.2.11.1. Isolation of basic amino acids**

All procedures were performed as previously described<sup>113</sup>. Tissue extracts were subjected to crude fractionation on Oasis MCX solid-phase extraction cartridges (30 mg, 1 ml). One-hundred microliters of each sample was then adjusted to a final volume of 1 ml with PBS. All conditioning, washing, and elution steps were performed on a vacuum-manifold with a capacity for 20 columns at a flow rate of 0,5 ml/min. The SPE cartridges were conditioned with 2 ml of methanol/water/ammonia (50:45:5, v/v/v), followed by 2 ml PBS prior to sample application. Samples were passed through SPE cartridges and contaminating components were removed with 2 ml of 0,1 M HCl, followed by 2 ml methanol. Basic compounds were eluted with 1 ml of methanol/water/ammonia (50:45:5, v/v/v). Samples were dried in a vacuum centrifuge and used immediately or stored at -20 °C until analysis. Eluates were redissolved in 230 µl of distilled water and centrifuged at 14 000 × g for 2 min to remove particulates prior to derivatization for high performance liquid chromatography.

### 3.2.11.2. Derivatization and chromatographic separation

All procedures were performed as previously described<sup>114</sup>. The *ortho*-phthaldialdehyde reagent (OPA) was freshly prepared in potassium borate buffer, according to the manufacturer's instructions. Thirty microliters of each sample was combined with 62,5 µl of OPA, immediately transferred to the auto sampler, and injected exactly after 2 min. Quantification of amino acids was performed on a HPLC system consisting of an ASI-100 auto sampler, a model P680 gradient pump, a model RF-2000 fluorescence detector, and a data acquisition system Chromeleon 6.60. Separation was performed according to a method previously described<sup>113</sup>. Fluorescent amino acid derivatives were separated on a SunFire™ C18 column (4,6 × 150 mm; 3,5 µm particle size; 100 Å pore size) with a µBondapak™ C18 guard column at 30 °C and a flow rate of 1,1 ml/min. After injecting 125 µl of the sample, separation was performed under isocratic conditions with 8,8 % (v/v) acetonitrile in 25 mM potassium phosphate buffer (pH = 6,8) as solvent. The isocratic conditions were maintained for 12 min. In order to elute strongly bound compounds, the column was flushed with acetonitrile/water (50:50, v/v) for 15 min and reequilibrated under isocratic conditions for 25 min prior to the next injection. Fluorescent derivatives were detected at excitation and emission wavelengths of 330 and 450 nm, respectively. Calibration was performed by external calibration with L-arginine standard.

### 3.2.12. Culture of mammalian cells

#### 3.2.12.1. Cell culture condition

The mouse fibroblast NIH-3T3 cell line and primary mouse and human lung fibroblasts were grown in plate culture dishes in D-MEM medium containing 10 % (v/v) fetal calf serum (FCS) at 37 °C, 5 % CO<sub>2</sub> and 95–100 % humidity. Cells were passaged after achieving 80–90 % confluence. Cells were washed with 1× PBS and then incubated with 3 ml trypsin/EDTA solution for 2–3 min in order to detach the cells. Seven milliliters of D-MEM containing FCS was added to cells to further block the enzymatic

reaction. The cell suspension was transferred to the new culture dishes in dilution 1:5 or 1:10.

PBS (phosphate-buffered saline):

0,08 % (w/v) NaCl

0,02 % (w/v) KCl

0,115 % (w/v) Na<sub>2</sub>HPO<sub>4</sub> · 2H<sub>2</sub>O

0,02 % (w/v) KH<sub>2</sub>PO<sub>4</sub> · 2H<sub>2</sub>O

pH = 7,4 adjusted with NaOH; sterilized for 20 min at 121 °C, 15 psi

Trypsin/EDTA solution:

0,25 % (w/v) trypsin

1,23 g/l EDTA

### **3.2.12.2. Isolation of primary lung fibroblasts**

Mouse lung primary fibroblasts were isolated from bleomycin- and saline-treated animals, while human lung primary fibroblasts were derived from healthy transplant donors. In order to isolate primary lung fibroblasts, human and mouse tissues were processed in the same way. Lungs were perfused free of blood, and individual lung lobes were removed to a petri dish. Using sterile technique, lung lobes were finely minced with scissors, and lung mince was cultured for 10–14 days in D-MEM containing 10 % FCS and antibiotics (100 U/ml penicillin, 100 µg/ml streptomycin). After 10 days, fibroblasts had grown out from the tissue and were passaged by standard trypsinization. To insure the purity of the culture, cells were morphologically characterized by light microscopy, additionally specific staining for  $\alpha$ -smooth muscle actin and vimentin was performed. For experiments described here, cells from early passages were used. Cells were plated at 30 000 cells/cm<sup>2</sup> either in 6-well plates or in 100-mm plates, depending on the experiment.

### 3.2.12.3. Transient transfection using lipofectamine

In principal, transient transfection consists on transfer of foreign DNA into the eukaryotic cell. As introduced DNA is not inserted into the genome, it is lost by the cell in the later stages of the cell cycle.

The NIH-3T3 cells were seeded onto culture plates dishes at a density 20 000 cells/cm<sup>2</sup>, and were cultured in D-MEM containing 10 % FCS for 24 h to achieve 80–90 % confluency. The transfection was performed using Lipofectamine™ 2000 transfection reagent. Lipofectamine (2,5 µl per 1 µg of transfected DNA) was mixed with Opti-MEM medium. After 5 min incubation at room temperature the appropriate amount of DNA was added to the mixture. In order to let DNA and lipofectamine create complexes, incubation for a further 20 min at room temperature was performed. Metabolized medium was aspirated from the cells, and the cells were covered with 100 µl of transfection mixture. After 4–6 h, the transfection mixture was removed and starvation medium consisting of D-MEM containing 0,1 % FCS was added to the cells.

### 3.2.13. Luciferase assay

An appropriate amount of NIH-3T3 cells was plated in a 48-well plate and the transfection procedure was conducted as described above. Luciferase reporter plasmids pCAGA<sub>12</sub>-luc, or pGL3-control, at 0,2 µg/well, were used for transfection with lipofectamine. Twenty-four hours after transfection, cells were stimulated with TGF-β1 (2 ng/ml) alone or TGF-β1 (2 ng/ml) in combination with the ARG inhibitor NOHA, at the following concentrations: 20 µM, 100 µM and 500 µM. Twenty-four hours after the stimulation, medium was aspirated and 100 µl luciferase lysis buffer was added to each well. The cells were incubated with shaking for 30–40 min at room temperature. Subsequently, 40 µl of cell lysate was combined with 50 µl of luciferase assay reagent and transferred into a 96-well plate. The luminescence of the sample was analyzed in a Fusion A153601 Reader.

### 3.2.14. Sircol collagen assay

Total collagen content in cell lysates was determined using the Sircol Collagen Assay Kit according to the manufacturer's instructions. This is a quantitative dye-binding method designed to analyze the amount of collagen produced in mammalian tissues or cells during *in vitro* culture. The dye reagent contains the Sirius Red anion with sulphonic acid side chain groups, which react with the side chain groups of the basic amino acids present in collagen.

Equal amounts of cell lysates containing 50 µg of protein were added to 1 ml of Sircol dye reagent followed by 30 min of mixing at room temperature. After centrifugation at 10 000 × g for 10 min, the supernatant was carefully removed and 1 ml of alkali reagent was added, and the pellet was dissolved by vortexing. Samples and collagen standards were analyzed at 540 nm in a Fusion A153601 Reader. Collagen concentrations were calculated using standard curve with acid-soluble type I collagen.

### 3.2.15. Arginase activity assay

Arginase activity in human lung homogenates was monitored using QuantiChrom™ Arginase Assay Kit according to the manufacturer's instructions. The method utilizes a chromogen that forms a colored complex specifically with urea produced in the arginase reaction.

Equal amounts of lung tissue extracts containing 50 µg of proteins were combined with 10 µl of 5× substrate buffer and the reaction mixture was incubated for 2 h at 37 °C. Subsequently, 200 µl of urea reagent was added to each reaction mixture, followed by incubation for 15 min at room temperature. Samples and urea standard were analyzed at 520 nm in the Fusion A153601 Reader. Arginase activity, displayed in units per liter of sample, was calculated from the following formula:

$$\text{Activity} = \frac{(\text{OD}_{\text{sample}} - \text{OD}_{\text{blank}})}{(\text{OD}_{\text{standard}} - \text{OD}_{\text{water}})} \times [\text{Urea standard}] \times 50 \times 10^3 : (40 \times t)$$

Urea standard            - 1 mM

t (reaction time)        - 120 min

## 4. Results

### 4.1. Analysis of L-arginine metabolism during bleomycin-induced lung fibrosis

#### 4.1.1. Expression analysis of L-arginine transporters

To investigate potential changes in the levels of L-arginine transporters during the development of lung fibrosis, mRNA expression of solute carriers family (SLC) in the mouse lung fibrosis model was analyzed. The mRNA was isolated from lung homogenates of mice subjected to bleomycin treatment for 7, 14 and 21 days, whereas animals treated with saline served as controls. The mRNA levels of transporters were determined by semi-quantitative RT-PCR (Figure 4.1.). No significant changes in the expression were observed during the development of lung fibrosis in the bleomycin mouse model.

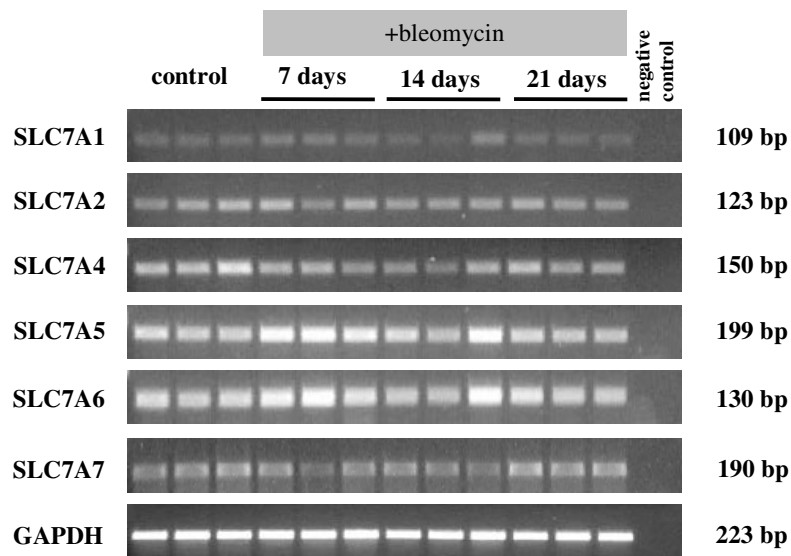


**Figure 4.1. Expression analysis of SLC during bleomycin-induced lung fibrosis.** Expression levels of mRNA from control and bleomycin-treated mice for 7, 14 and 21 days assessed by semi-quantitative PCR. GAPDH served as a control gene. Gels are representative for three independent experiments.

#### 4.1.2. Analysis of protein arginine methyltransferase expression

Protein arginine methyltransferases (PRMT) methylate L-arginine residues in proteins resulting in the generation of mono- and dimethylated forms of L-arginine. As previously mentioned, asymmetrically dimethylated (ADMA) and monomethylated (NMMA) L-arginine analogs behave as NOS inhibitors. In order to assess the potential role of PRMT isoenzymes in the pathogenesis of lung fibrosis, their expression levels were investigated during bleomycin-induced lung fibrosis. Both mRNA and proteins were isolated from mice treated with bleomycin for 7, 14 and 21 days. The analysis of expression on the mRNA level was performed by means of semi-quantitative RT-PCR (Figure 4.2.) and the results were verified by the analysis of protein levels by immunoblotting (Figure 4.3.). Both methods did not reveal significant changes in PRMT expression levels during bleomycin-induced lung fibrosis. Interestingly, PRMT5 protein levels were decreased three weeks after drug administration, which is during the period of animal recovery.

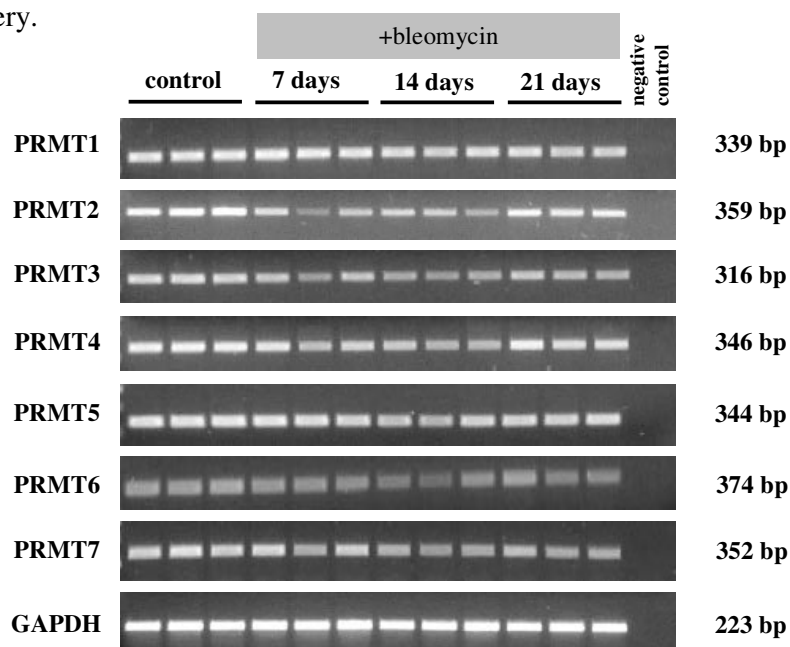


**Figure 4.2. Analysis of PRMT mRNA expression during bleomycin-induced lung fibrosis.**

The mRNA levels of control and bleomycin-treated mice for 7, 14 and 21 days assessed by semi-quantitative RT-PCR. The GAPDH gene served as a control gene. Gels are representative for three independent experiments.

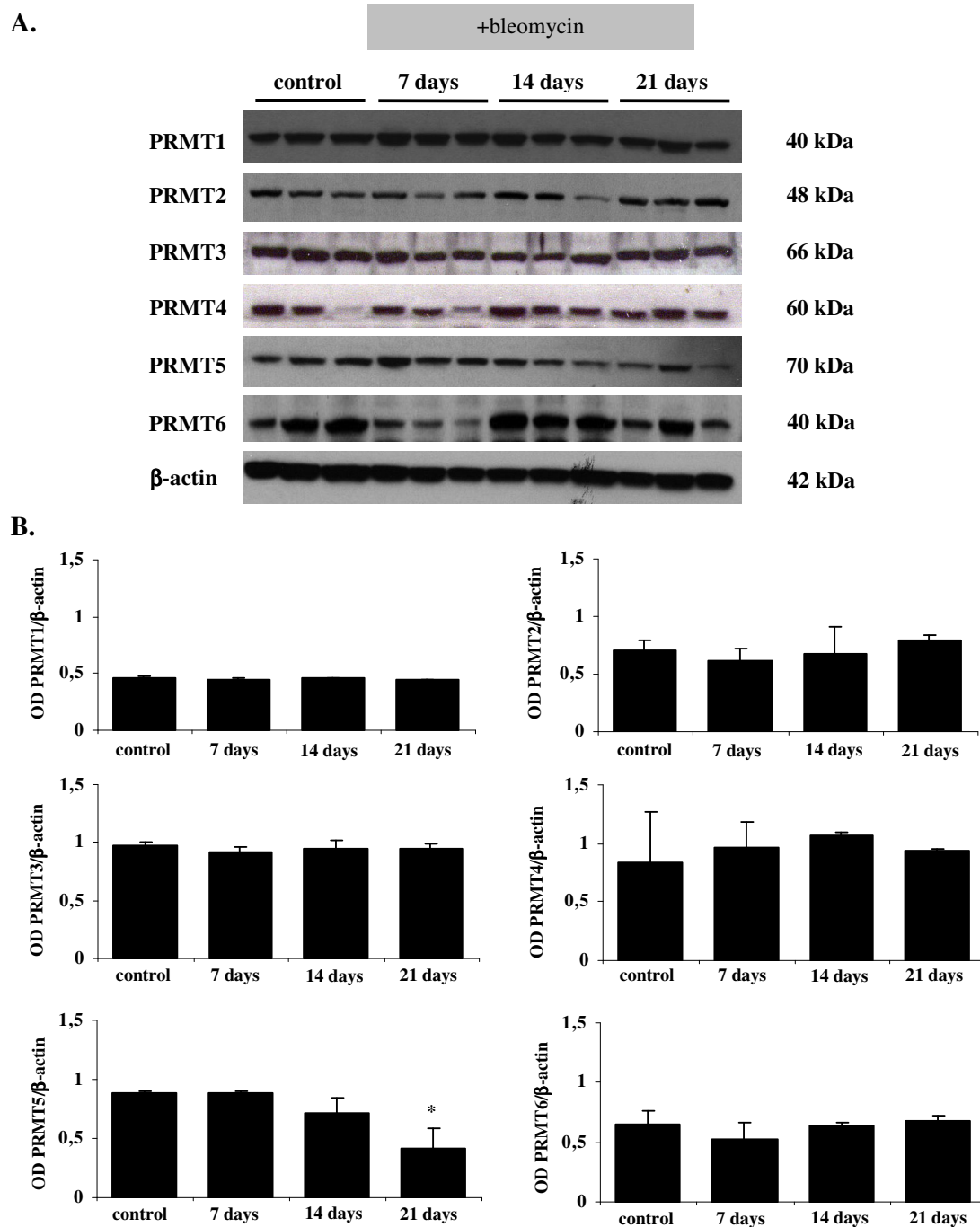


**Figure 4.3. Analysis of PRMT protein expression during bleomycin-induced lung fibrosis.**

(A) Protein expression levels of control and bleomycin-treated mice for 7, 14 and 21 days assessed by IB.  $\beta$ -actin served as a protein loading control. (B) The results obtained by IB were densitometrically analyzed ( $n=3$ , \*  $p < 0,05$ ), statistical analysis included two-tailed t-test.



### 4.1.3. Analysis of L-arginine catabolic enzymes expression

In order to further study L-arginine metabolism in the mouse lung fibrosis model, semi-quantitative RT-PCR was performed to examine the mRNA levels of L-arginine catabolic enzymes. The expression of the following enzymes was analyzed: ARG1, ARG2, eNOS, iNOS, OAT, ODC. Three of the enzymes: eNOS, OAT, ODC did not exhibit any expression changes during bleomycin-induced lung fibrosis. In contrast, significant expression differences were observed for ARG1 and ARG2, and to a lesser extent, for iNOS (Figure 4.4.). While the expression of ARG1 and ARG2 was significantly increased seven days after bleomycin administration, iNOS expression gradually increased up to 21 days after treatment.

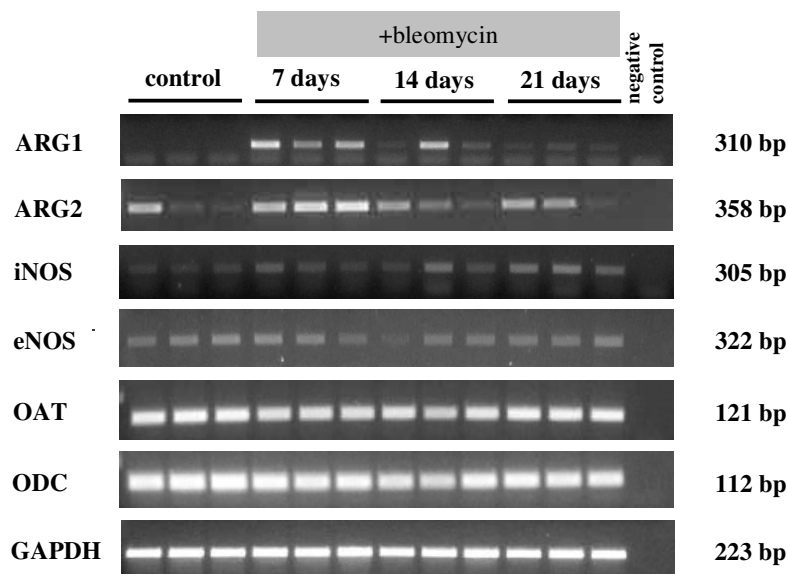


**Figure 4.4. Expression of L-arginine catabolic enzymes during bleomycin-induced lung fibrosis.**

Expression levels of mRNA from control and bleomycin-treated mice for 7, 14 and 21 days assessed by semi-quantitative RT-PCR. The GAPDH gene served as a control gene. Gels are representative for three independent experiments.

#### 4.1.4. Expression of arginase-1, -2 during development of lung fibrosis

The mRNA expression of ARG1 and ARG2 in lung tissue was found to be enhanced at early stages (7 days) of bleomycin-induced lung fibrosis. To further verify the expression of ARG1 and ARG2 in lung tissue and their involvement in the process of fibrogenesis, expression analysis of both enzymes was performed in animals treated with bleomycin for 3, 5, 7, 14, 21 days using quantitative RT-PCR (Figure 4.5.). Results obtained demonstrated that both enzymes exhibited increased expression five days after bleomycin administration, reaching the highest expression seven days after bleomycin treatment. In detail, ARG1 exhibited a 5,7 fold induction at day 7, whereas ARG2 exhibited only 1,5 fold induction. The expression of both ARG remained elevated until 21 days after treatment.

Additionally, analysis of ARG protein levels was performed by immunoblotting (Figure 4.6.). Interestingly, ARG1 was undetectable in the control mouse lungs. In line with the mRNA expression, protein levels of both enzymes revealed the highest increase seven days after bleomycin treatment compared to control animals, where ARG1 again displayed a higher fold induction than did ARG2. Also on the protein level, both enzymes demonstrated elevated expression until 21 days after bleomycin administration.

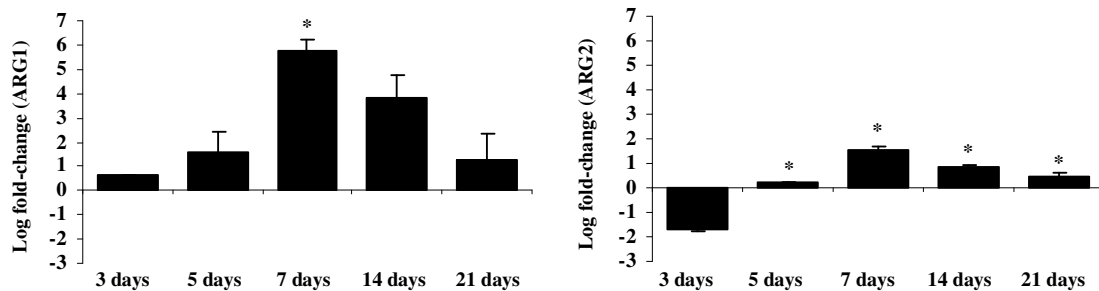


**Figure 4.5. ARG mRNA expression during bleomycin-induced lung fibrosis.**

The mRNA expression levels of control and bleomycin-treated mice for 3, 5, 7, 14 and 21 days assessed by qRT-PCR. The PBGD gene served as a control gene, (n=3, \* p< 0,05), statistical analysis included two-tailed t-test.

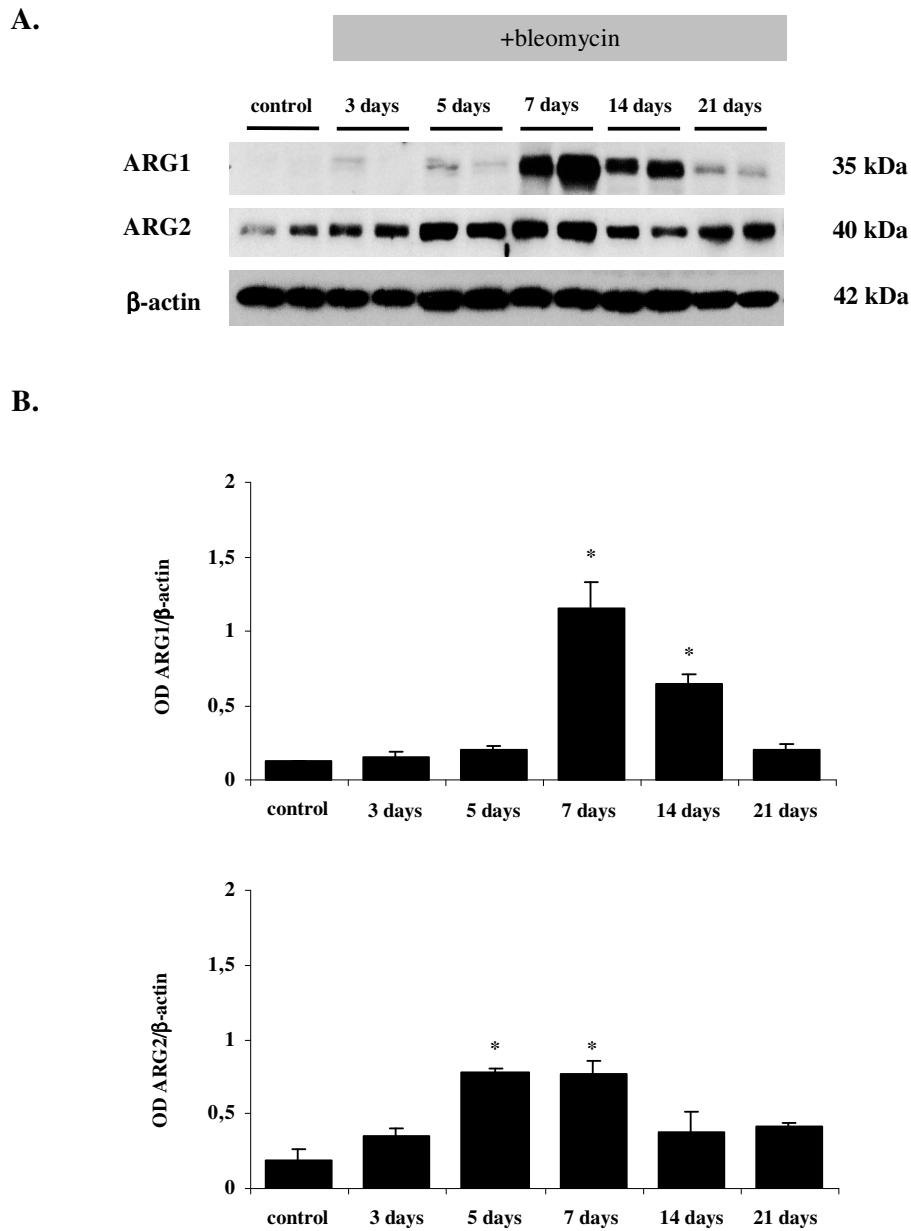


**Figure 4.6. ARG protein expression during bleomycin-induced lung fibrosis.**

(A) Protein expression levels of control and bleomycin-treated mice for 3, 5, 7, 14 and 21 days assessed by IB.  $\beta$ -actin served as a protein loading control. (B) The results obtained by IB were densitometrically analyzed ( $n=3$ , \*  $p < 0,05$ ), statistical analysis included two-tailed t-test.

#### **4.1.5. Levels of free L-arginine during lung fibrosis**

In order to investigate whether the dramatic increase in ARG isoenzymes levels in the mouse lung after bleomycin treatment resulted in altered free lung L-arginine levels, the L-arginine concentration was determined by amino acid analysis. Free cellular L-arginine was measured in lung tissue homogenates, derived from control and bleomycin-treated mice (Figure 4.7.). Results indicated decreased L-arginine levels in the lung when mice were subjected to bleomycin treatment. This decrease was most evident seven days after bleomycin treatment, at the time of the highest ARG expression in the lung:  $104,4 \pm 7,5$  pmol L-arginine/mg protein versus  $965,9 \pm 208,8$  pmol L-arginine/mg protein in lungs from mice subjected to bleomycin for 7 days and controls, respectively. L-arginine levels gradually increased after day 7, but remained decreased even 21 days after bleomycin treatment, compared with controls.

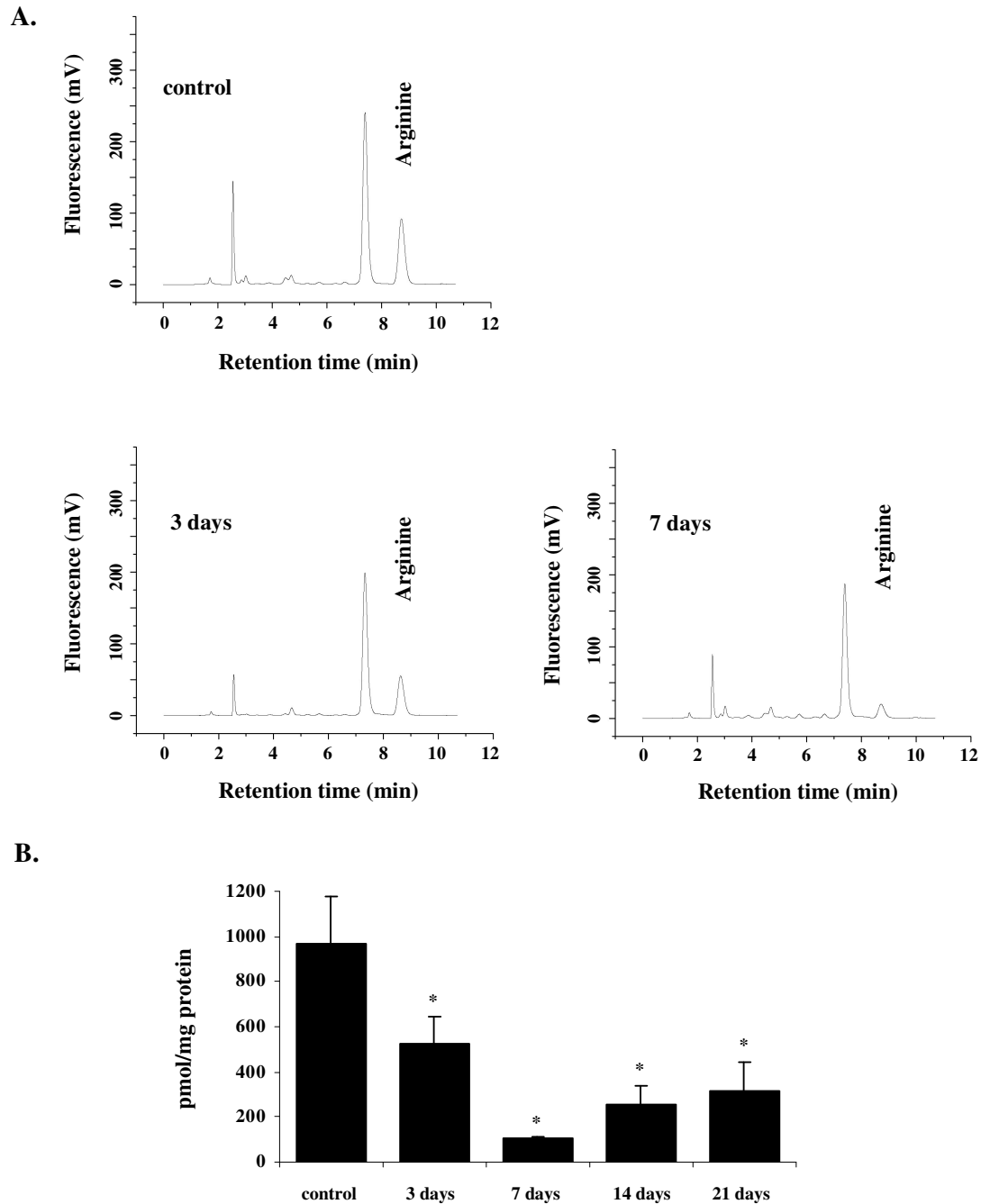


**Figure 4.7. Levels of free cellular L-arginine during bleomycin-induced lung fibrosis.**

(A) Representative HPLC chromatograms illustrating free L-arginine levels in mouse lung homogenates from control versus three and seven days after bleomycin administration. (B) Concentration of free L-arginine in lung homogenates (n=6, \*,  $p < 0,001$ ), statistical analysis included two-tailed t-test.

#### 4.1.6. Localization of arginase-1, -2 in the lung during lung fibrosis

Previous results displayed an increase in ARG isoenzyme expression in total lung homogenates from bleomycin-treated mice. In order to verify ARG expression patterns in lung tissue, immunohistochemistry was performed on the sections obtained from control and bleomycin-treated mice for seven and fourteen days (Figure 4.8.). Moreover, it was examined whether the expression is specifically localized to particular cell types in the mouse lung.

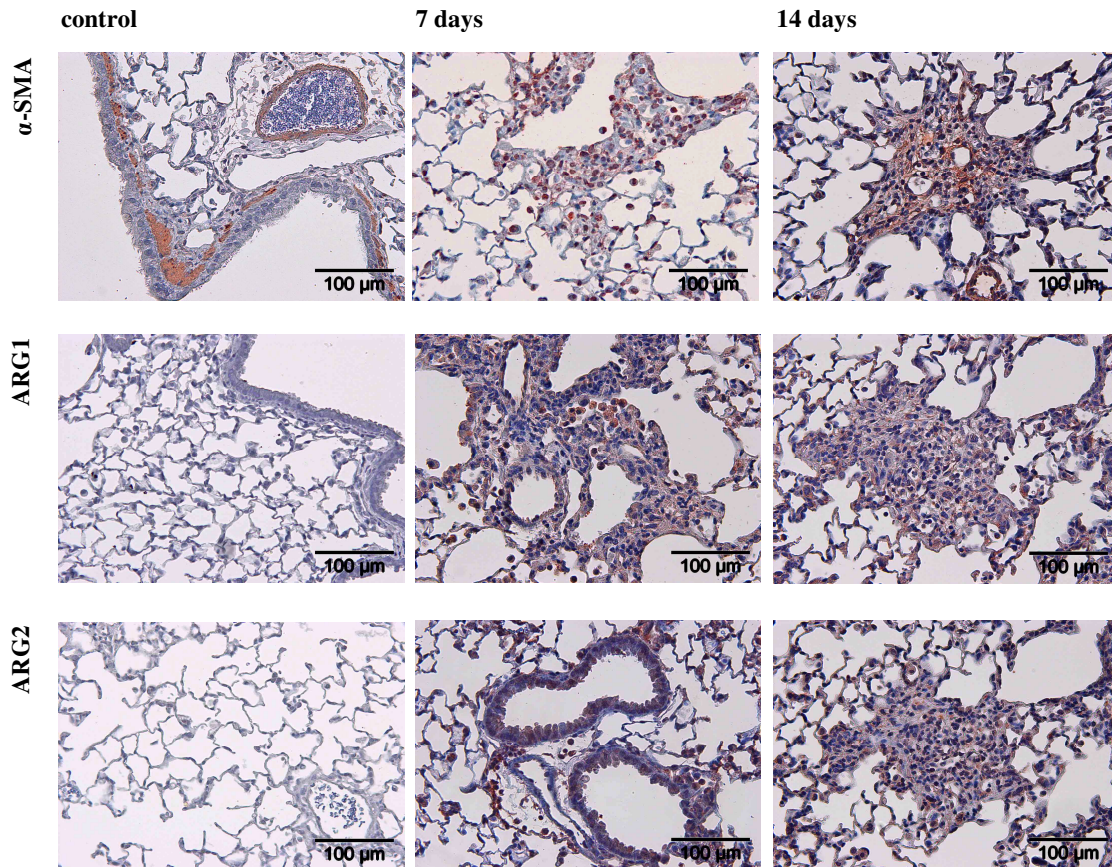


**Figure 4.8. Localization of ARG1 and ARG2 in mouse lung sections.**

Paraffin-embedded sections prepared from the lungs of control and bleomycin-treated mice for seven and fourteen days stained for ARG1, ARG2, and  $\alpha$ -smooth muscle actin (SMA).

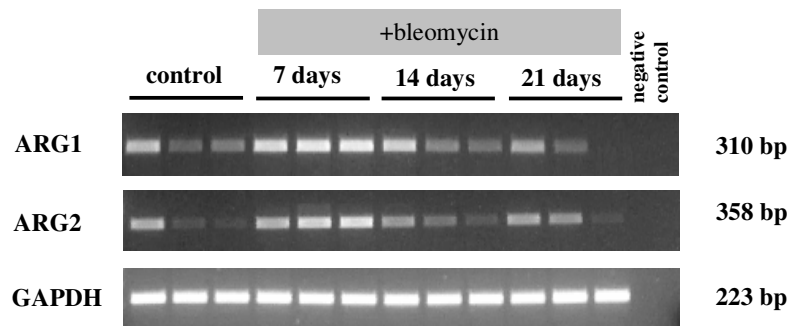
In accordance with previous reports <sup>111</sup>, ARG1 was localized to macrophages and inflammatory regions, whereas ARG2 was present in bronchial epithelial cells. This localization pattern was mostly observed in the sections obtained from animals sacrificed seven days after drug administration. These results are of importance since the first week after bleomycin administration is described to be the inflammatory phase preceding fibrogenesis. Moreover, both ARG1 and ARG2 also exhibited the expression in fibrotic foci, which was seen fourteen days after drug administration, the period where the fibrogenic processes start. No expression of either isoenzyme was observed in control animals.

## **4.2. Expression of arginase-1, -2 in fibroblasts**

### **4.2.1. Arginase-1, -2 expression in primary mouse fibroblasts**

Both ARG1 and ARG2 have been reported to be highly expressed in alveolar macrophages and immune cells during lung inflammation <sup>104,115</sup>. As immunohistochemical results indicated the localization of ARG isoenzymes in lung fibrotic foci, further investigations were performed in order to examine expression of these enzymes in mouse primary lung fibroblasts - the key cell type responsible for increased collagen deposition during lung fibrosis. Therefore, isolation of mRNA as well as proteins was carried out using primary fibroblasts derived from the lungs of control and bleomycin-treated mice for 7, 14 and 21 days. The mRNA expression analysis was performed by means of semi-quantitative and quantitative RT-PCR (Figure 4.9.). The results were verified by analysis of protein expression levels by immunoblotting (Figure 4.10.). Both ARG1 and ARG2 expression was detectable in normal lung fibroblasts, and in accordance with previous results, both enzymes were significantly upregulated at the mRNA and protein levels in fibroblasts isolated from bleomycin-treated mice. Interestingly, ARG1 expression was significantly enriched in fibroblasts, compared with lung homogenates. This was evident at the mRNA level, as well as at the protein level, suggesting an important role of ARG1 in this cell type.

A.



B.

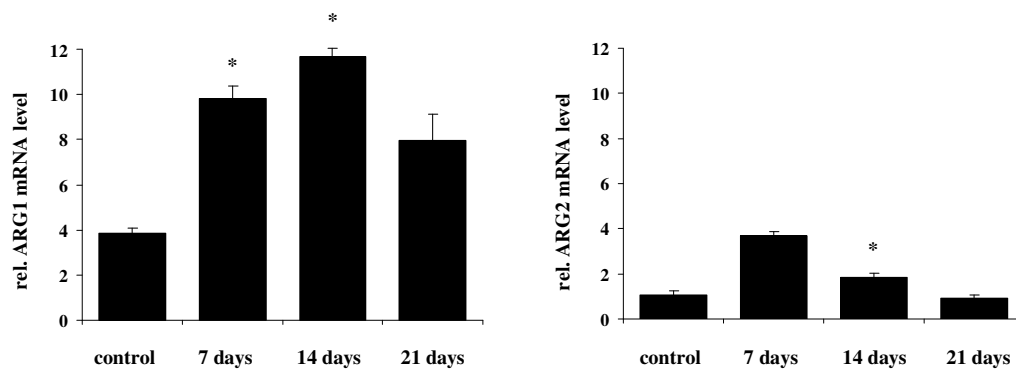
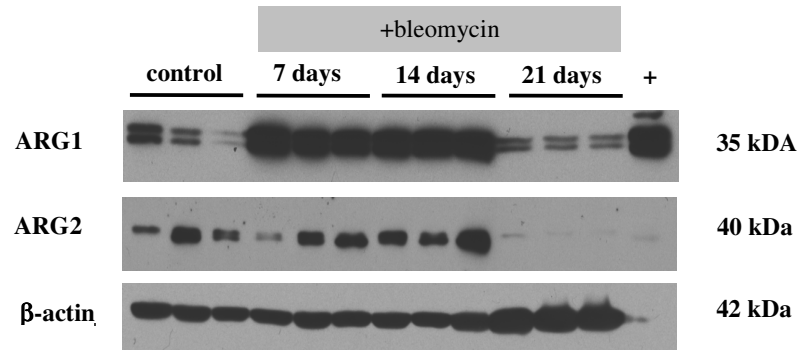


**Figure 4.9. ARG mRNA expression in primary mouse lung fibroblasts.**

ARG1 and ARG2 expression in lung primary fibroblasts isolated from control and bleomycin-treated mice for 7, 14 and 21 days analyzed by (A) semi-quantitative RT-PCR, (B) qRT-PCR. The GAPDH and PBGD genes served as control genes. Gels are representative for three independent experiments, ( $n=3$ , \*  $p < 0,05$ ), statistical analysis included two-tailed t-test.



A.



B.

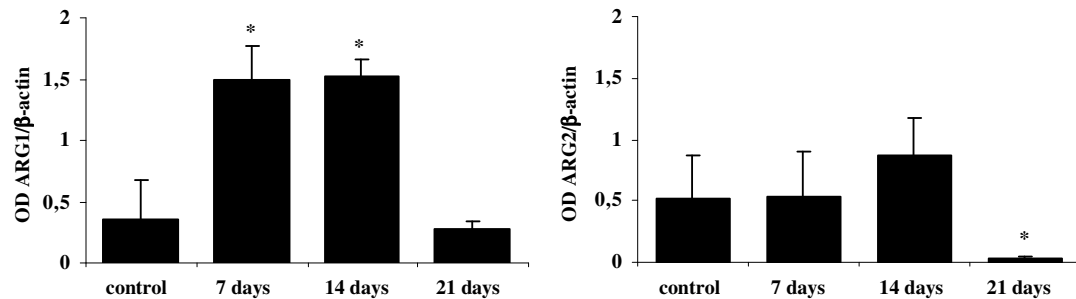


**Figure 4.10. ARG protein expression in primary mouse lung fibroblasts.**

ARG1 and ARG2 expression in lung primary fibroblasts isolated from control and bleomycin-treated mice for 7, 14 and 21 days analyzed by (A) IB.  $\beta$ -actin served as a protein loading control. (B) The results obtained by IB were densitometrically analyzed (n=3, \* p< 0,05), statistical analysis included two-tailed t-test.

#### 4.2.2. Arginase-1, -2 immunolocalization in primary mouse fibroblasts

To support previous observations, immunocytochemical staining was performed in mouse lung primary fibroblasts. Staining of ARG1 and ARG2 was performed by indirect immunofluorescence with rabbit anti-ARG1 and rabbit anti-ARG2 antibodies (Figure 4.11.). Both ARG isoenzymes displayed diffuse staining throughout the cytoplasm. Similar localization patterns of ARG isoenzymes were also observed in NIH-3T3 mice fibroblasts.

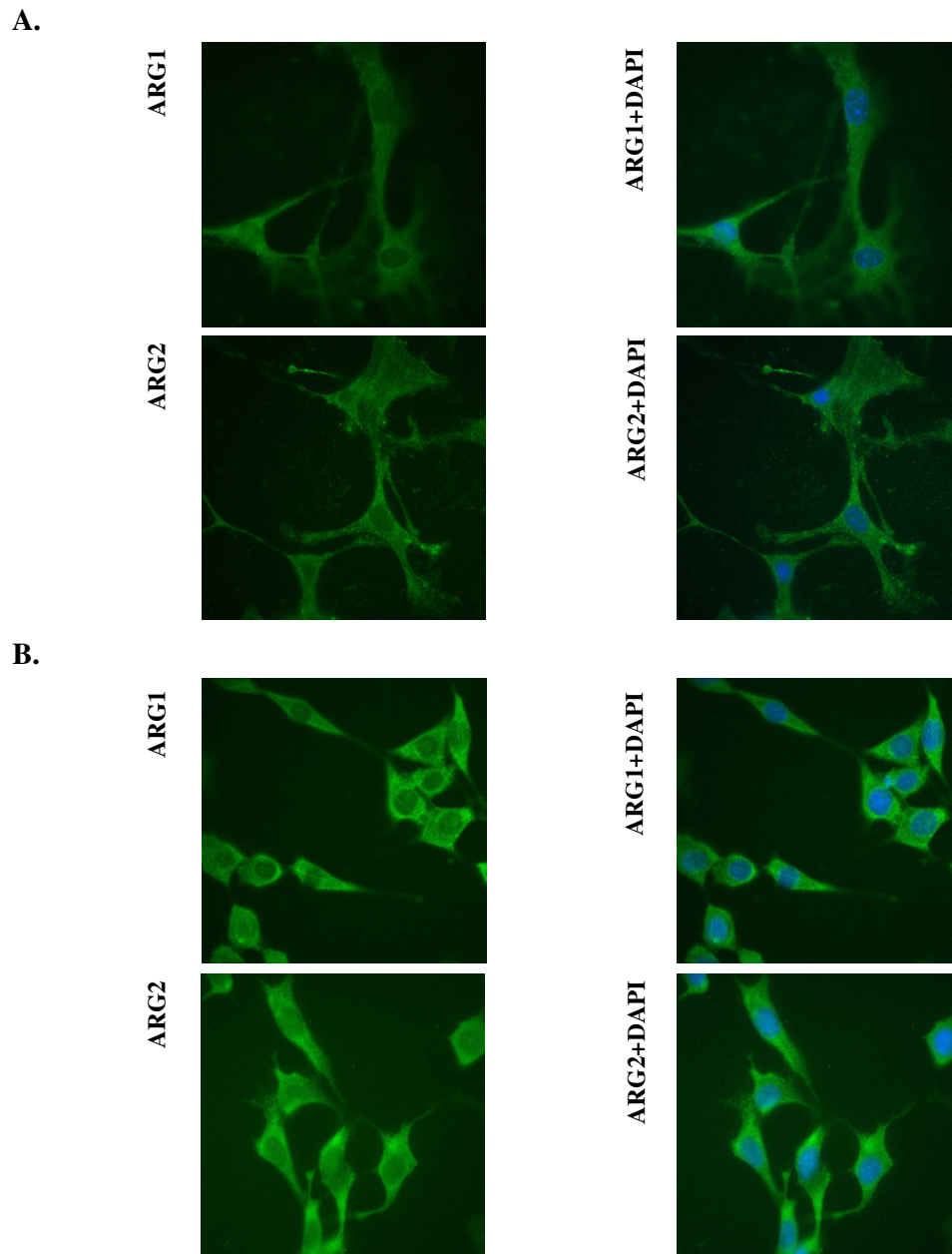


**Figure 4.11. ARG localization in primary mouse lung fibroblasts.**

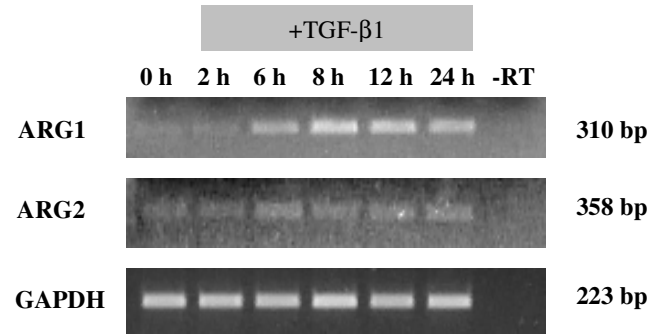
ARG1 and ARG2 localization visualized with secondary FITC-labelled antibody (green). Cell nuclei were visualized with DAPI (blue) in **(A)** mouse primary lung fibroblasts and **(B)** NIH-3T3 fibroblasts.

### **4.2.3. Induction of arginase-1, -2 expression by profibrotic agents**

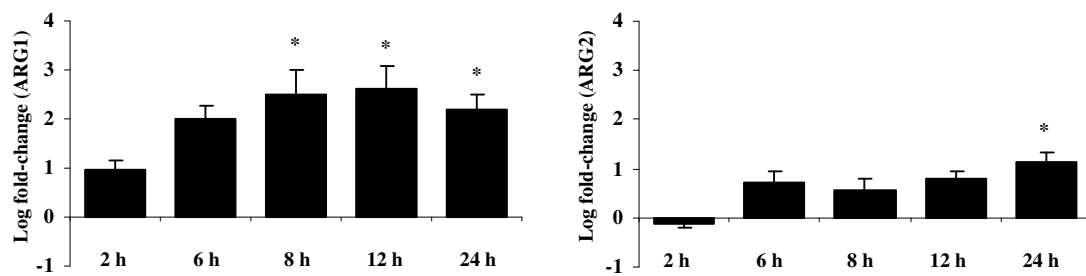
Transforming growth factor-beta1 (TGF- $\beta$ 1) is the key profibrotic growth factor operative in lung fibrosis. Its presence leads to induction or altered expression of many genes in various diseases including lung fibrosis. In order to elucidate the regulatory mechanisms of ARG expression in lung fibrosis, an investigation was performed to examine whether TGF- $\beta$ 1 can alter ARG expression in a bleomycin-induced lung fibrosis model. Primary lung fibroblasts, derived from control mice, were stimulated with TGF- $\beta$ 1 (2 ng/ml) for up to 24 h, and mRNA expression was analyzed by semi-quantitative and quantitative RT-PCR (Figure 4.12.). The TGF- $\beta$ 1 rapidly increased ARG1 mRNA expression, as early as 2 h after treatment. Both ARG1 and ARG2 expression was increased by up to eight-fold and two-fold, respectively, in response to TGF- $\beta$ 1, in primary mouse fibroblasts.

A similar experiment was carried out in NIH-3T3 mice fibroblasts. Cells were stimulated with TGF- $\beta$ 1 (2 ng/ml) for up to 24 h, and mRNA isolation was performed in order to analyze the influence of this profibrotic agent on ARG expression by quantitative RT-PCR. In the line with results for primary cells, similar differences in TGF- $\beta$ 1-dependent ARG1 expression were observed in NIH-3T3 fibroblasts, while ARG2 decreased in this cell type.

A.



B.



C.

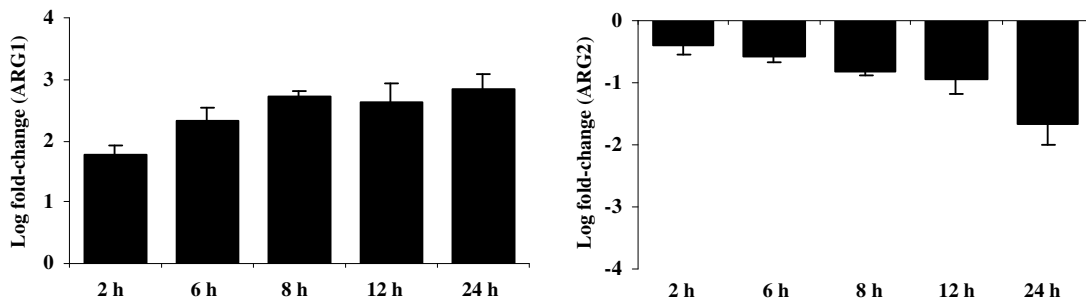


**Figure 4.12. TGF- $\beta$ 1-induced ARG expression in fibroblasts.**

ARG1 and ARG2 expression in mouse primary fibroblasts, stimulated with TGF- $\beta$ 1 for 2, 6, 8, 12 and 24 h, analyzed by (A) semi-quantitative RT-PCR and (B) qRT-PCR. (C) Expression of both ARG in NIH-3T3 fibroblasts, stimulated with TGF- $\beta$ 1 for 2, 6, 8, 12 and 24 h assessed by qRT-PCR. The GAPDH and PBGD genes served as control genes, (n=3, \*p< 0,05), statistical analysis included two-tailed t-test. Gels are representative for three independent experiments.

### 4.3. Effect of arginase inhibitor on TGF- $\beta$ 1 signaling and extracellular matrix formation

#### 4.3.1. Arginase inhibition in NIH-3T3 fibroblasts

##### 4.3.1.1. Effect of arginase inhibition on TGF- $\beta$ 1-induced collagen deposition

Increased collagen deposition, largely mediated by enhanced TGF- $\beta$ 1 signaling, represents the pathological hallmark of fibrosis<sup>14</sup>. Previous results indicated that elevated activity of TGF- $\beta$ 1 in lung fibrosis leads to increased expression of ARG isoenzymes which may suggest the involvement of these enzymes in collagen production. Therefore, an investigation was performed to determine collagen deposition in the presence of the ARG inhibitor N<sup>G</sup>-hydroxy-L-arginine (NOHA) in NIH-3T3 fibroblasts. Cells were stimulated with TGF- $\beta$ 1 (2 ng/ml) for up to 24 h, and cellular collagen content was analyzed by Sircol assay (Figure 4.13.). The TGF- $\beta$ 1-induced increase in collagen production was completely attenuated by ARG inhibition, using NOHA at concentrations from 100 to 500  $\mu$ M.

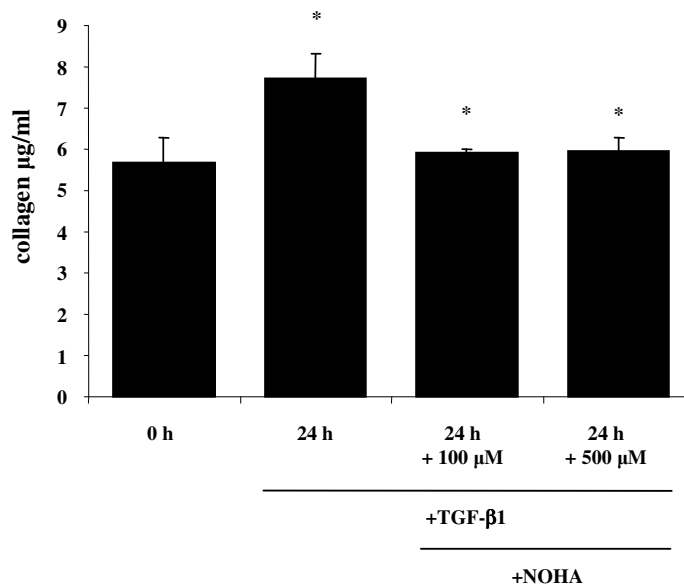
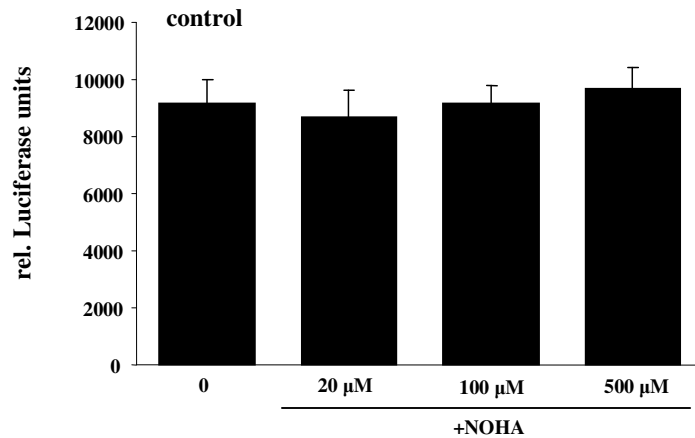


**Figure 4.13. Regulation of collagen deposition by NOHA in NIH-3T3 fibroblasts.** Alterations to collagen levels in NIH-3T3 fibroblasts upon TGF- $\beta$ 1 stimulation in the presence or absence of an arginase inhibitor, (n=3, \* p< 0,05), statistical analysis included two-tailed t-test.

#### 4.3.1.2. Effect of arginase inhibition on TGF- $\beta$ 1 signaling

In order to estimate whether the inhibitory effect of NOHA on collagen deposition was due to blocking of TGF- $\beta$ 1 signaling, a luciferase assay was performed (Figure 4.14.). The NIH-3T3 cells were transfected with a luciferase reporter plasmid pCAGA<sub>12</sub>-luc or with pGL3-control, and stimulated with TGF- $\beta$ 1 alone or TGF- $\beta$ 1 in combination with NOHA, at a concentration of: 20  $\mu$ M, 100  $\mu$ M, 500  $\mu$ M.

A.



B.

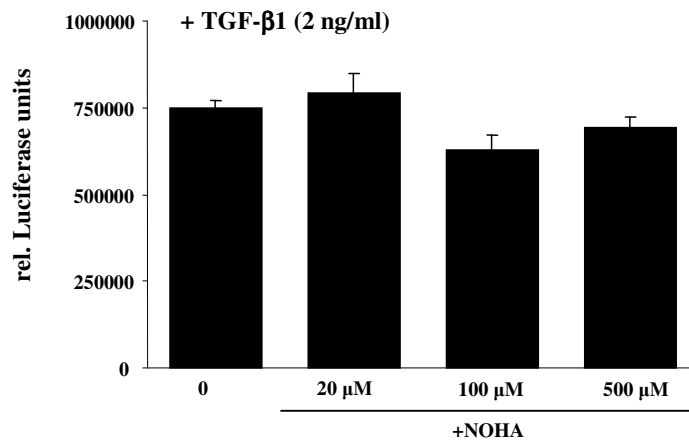


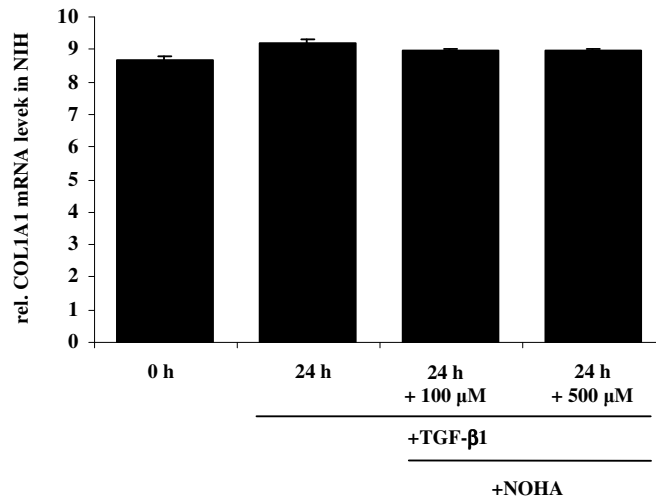
**Figure 4.14. TGF- $\beta$ 1 signaling in the presence of NOHA in NIH-3T3 fibroblasts.** The effect of NOHA on TGF- $\beta$ 1 signaling assessed on (A) baseline and (B) TGF- $\beta$ 1-induced pCAGA<sub>12</sub>-luc expression. Luciferase expression plotted in relative Luciferase units corrected for transfection efficiencies (n=6, \* p< 0,05), statistical analysis included two-tailed t-test.

The results obtained indicate that decreased collagen deposition in the presence of ARG inhibitor was not due to a general inhibitory effect of NOHA on TGF- $\beta$ 1 signaling, since the Smad-driven reporter gene expression of pCAGA<sub>12</sub>-luc remained unchanged in the presence of this inhibitor.

#### **4.3.1.3. Effect of arginase inhibition on extracellular matrix components expression**

To further investigate the effects of NOHA, it was investigated whether an ARG inhibitor can affect the expression of ECM components. The NIH-3T3 cells were stimulated with TGF- $\beta$ 1 for up to 24 h in the presence or absence of NOHA. Subsequently, mRNA was isolated and expression levels of collagen 1A1 (COL1A1) and  $\alpha$ -smooth muscle actin ( $\alpha$ -SMA) were examined using quantitative RT-PCR (Figure 4.15.). Although previous data indicated NOHA inhibitory influence on collagen deposition, interestingly, in this experiment NOHA did not display any influence on collagen and smooth muscle actin mRNA levels. This result suggests NOHA functions at a post-transcriptional level in the examined cell type.

A.



B.

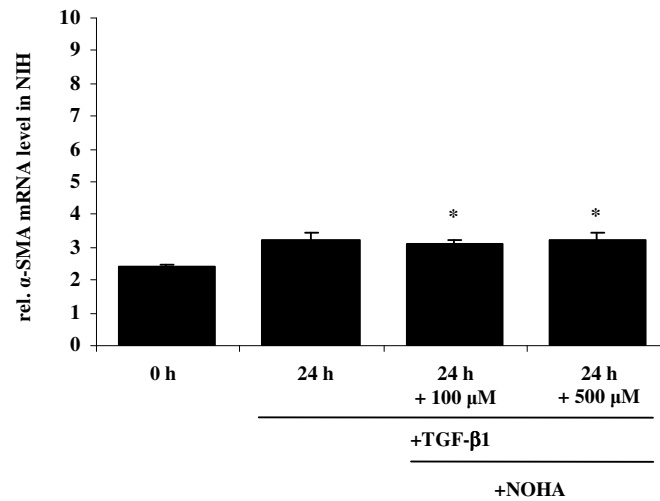


**Figure 4.15. Influence of NOHA on expression of ECM components by NIH-3T3 fibroblasts.**

The effect of NOHA on (A) COL1A1 and (B)  $\alpha$ -SMA mRNA expression in NIH-3T3 fibroblasts determined by qRT-PCR. The PBGD gene served as a control gene, (n=3, \* p< 0,05), statistical analysis included two-tailed t-test.



### 4.3.2. Arginase inhibition in human primary fibroblasts

Although the ARG inhibitor NOHA exhibited a strong effect on collagen deposition in NIH-3T3 fibroblasts, further investigation was required in order to verify whether NOHA displayed a similar influence on human primary fibroblasts.

#### 4.3.2.1. Effect of arginase inhibition on TGF- $\beta$ 1-induced collagen deposition

Human primary lung fibroblasts, derived from healthy transplant donors, were stimulated with TGF- $\beta$ 1 alone or TGF- $\beta$ 1 in combination with NOHA. Subsequently, cellular collagen content was analyzed by Sircol assay (Figure 4.16.). In agreement with the observations made for mouse NIH-3T3 fibroblasts, NOHA at concentrations 500  $\mu$ M completely abolished TGF- $\beta$ 1-induced increase in collagen production.

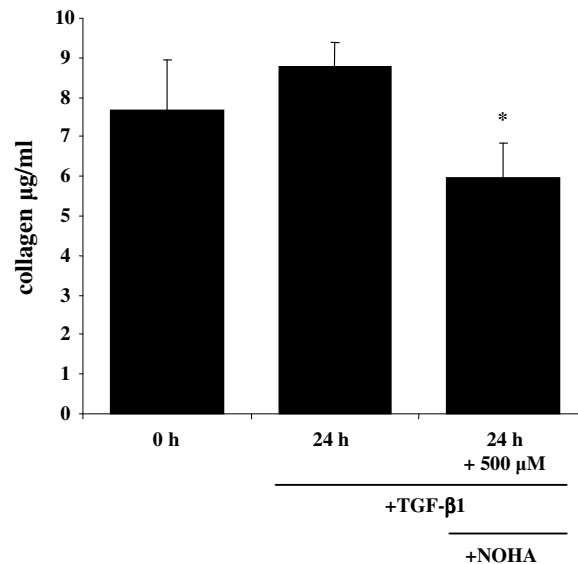


**Figure 4.16. Effect of NOHA on collagen deposition by human primary fibroblasts.** Alterations to collagen levels in human primary lung fibroblasts assessed upon TGF- $\beta$ 1 stimulation in the presence or absence of NOHA, an arginase inhibitor, (n=3, \* p< 0,05), statistical analysis included two-tailed t-test.

#### 4.3.2.2. Arginase inhibitor effect on expression of extracellular matrix components

Levels of COL1A1 and  $\alpha$ -SMA mRNA expression were examined by quantitative RT-PCR upon stimulation of human primary lung fibroblasts with TGF- $\beta$ 1 alone or TGF- $\beta$ 1 in combination with NOHA (Figure 4.17.). In line with results obtained for NIH-3T3 fibroblasts, mRNA levels of COL1A1 and  $\alpha$ -SMA in human primary lung fibroblasts were not affected in the presence of ARG inhibitor, which further supports the assertion that NOHA exhibits regulatory effects at the translational level.

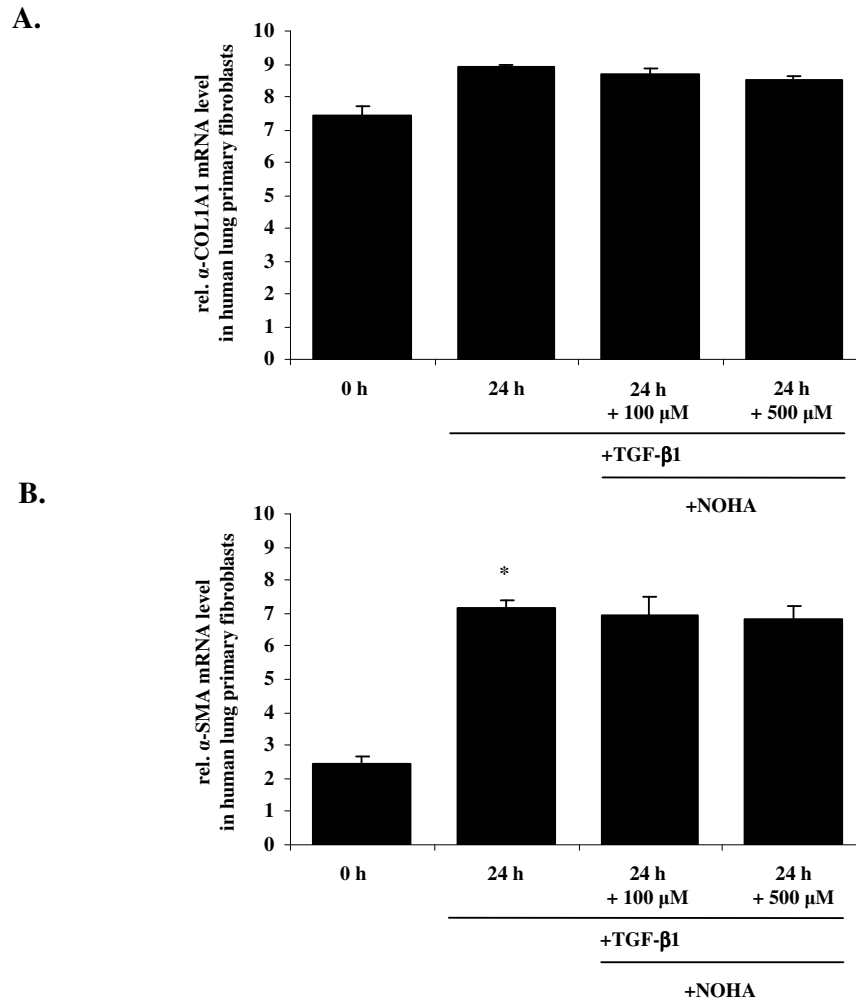


**Figure 4.17. Effect of NOHA on expression of ECM components by human primary fibroblasts.**

The effect of NOHA on (A) COL1A1 and (B)  $\alpha$ -SMA mRNA expression in human primary lung fibroblasts determined by qRT-PCR. The PBGD gene served as a control gene, (n=3, \* p<0,05), statistical analysis included two-tailed t-test.

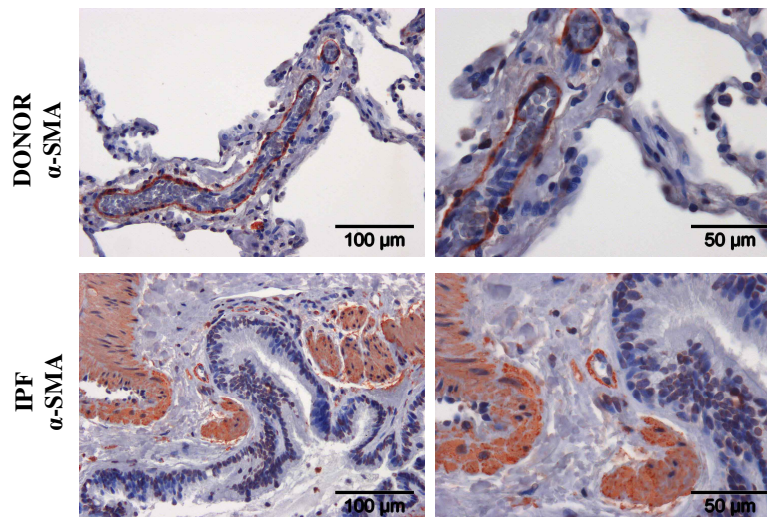
#### 4.4. Arginase-1, -2 in idiopathic pulmonary fibrosis

Since ARG1 and ARG2 were upregulated in bleomycin-induced lung fibrosis in mice, additional experiments were conducted in order to determine if the expression levels of these enzymes differ in human pathological conditions. For this purpose, the expression, localization and activity of ARG isoenzymes were assessed in human IPF and donor lungs.

##### 4.4.1. Arginase-1, -2 localization in human lungs

To examine whether ARG isoenzymes specifically localize to particular human cell types, immunohistochemistry was performed on the lung sections obtained from IPF patients and transplant donors (Figure 4.18.). Contrary to the results obtained for mice lung sections, both ARG1 and ARG2 exhibited strong staining in lungs from donors. Both enzymes were localized in bronchial epithelial cells, interestingly, strong staining for ARG1 was detected on cilia of the epithelial cells of healthy donors. In IPF patients ARG1 was observed to some extent in fibroblasts, but the signal in bronchial epithelial cells remained limited to the cilia. In contrast to bleomycin model, ARG2 exhibited clear distribution in alveolar epithelial type II cells in IPF.

A.



B.

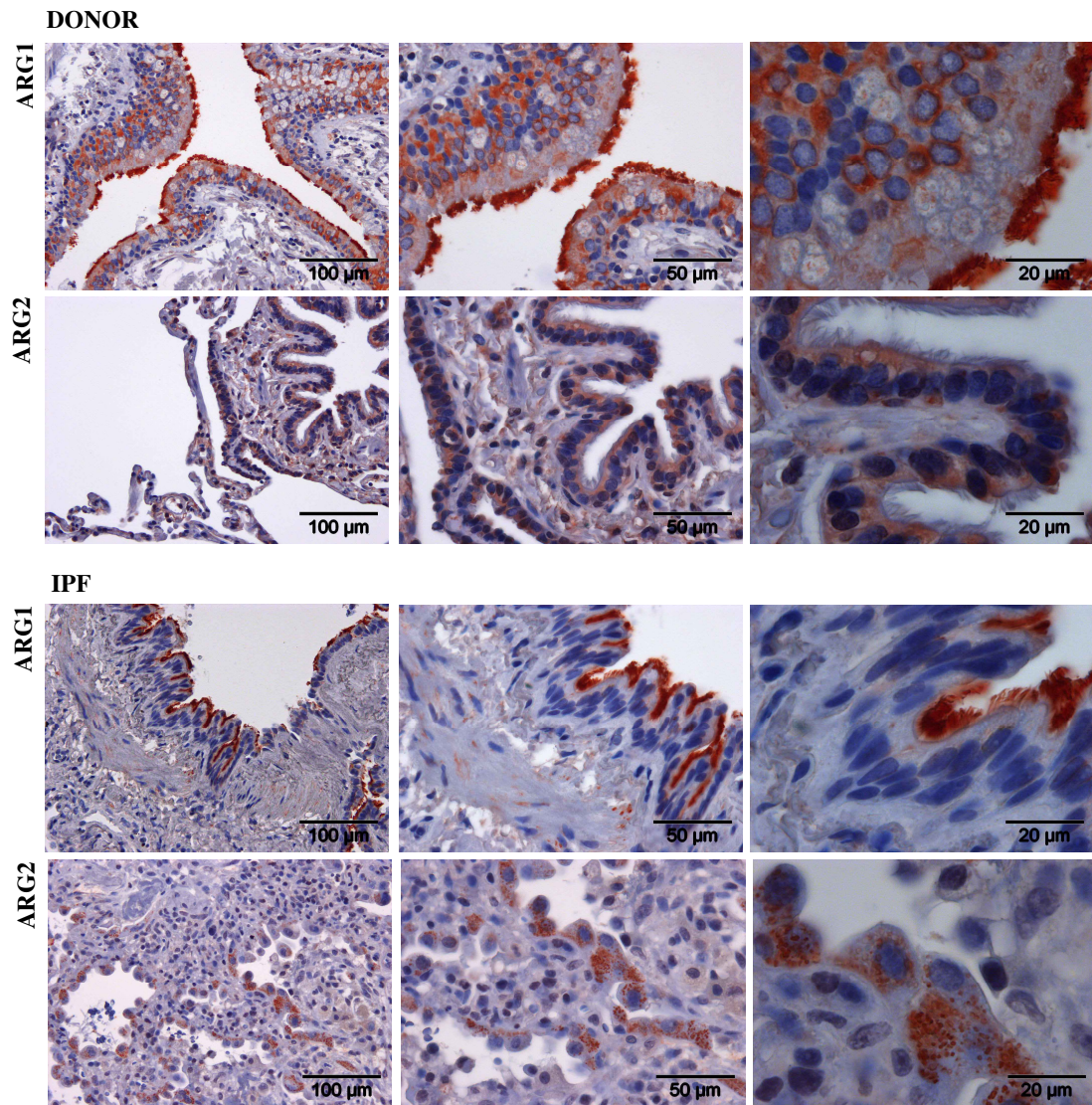


**Figure 4.18. Localization of ARG1 and ARG2 in human lung sections.**

Paraffin-embedded sections prepared from the lungs of healthy transplant donors and IPF patients stained for (A)  $\alpha$ -SMA, and (B) ARG1, ARG2.

#### 4.4.2. Arginase-1, -2 expression in human lungs

To further verify the expression of ARG1 and ARG2 in human lung tissue, mRNA isolation was performed from lung tissue of transplant donors and IPF patients. Quantification of mRNA levels was conducted by means of quantitative RT-PCR (Figure 4.19.).

Interestingly, the results obtained for human samples did not follow the pattern observed in bleomycin-induced lung fibrosis. Although in donors the enzymes exhibited low expression levels, which is in accordance with the results from unchallenged mice, no elevated ARG mRNA levels were observed in IPF patients. Moreover, ARG1 displayed decreased levels in IPF patients.

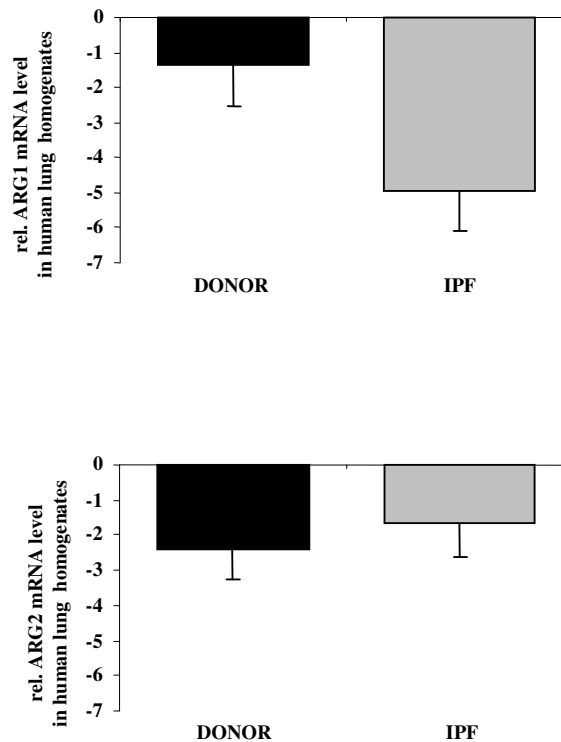


**Figure 4.19. ARG mRNA expression in human lung homogenates.**

ARG1 and ARG2 mRNA expression in human lung from transplant donor versus IPF patients analyzed by qRT-PCR. The PBGD gene served as a control gene, (n=3), statistical analysis included two-tailed t-test

#### 4.4.3. Arginase-1,-2 activity in human lungs

Since mRNA levels do not necessarily correlate with cellular protein levels and enzymatic activity, further studies were carried out in order to determine the activity of ARG isoenzymes in human lung tissue. For this purpose, lung homogenates were prepared from donors and IPF patients, and quantification of ARG activity was conducted with the QuantiChrom™ Arginase Assay Kit (Figure 4.20.). In line with previous experiments, no significant difference in ARG activity was observed in IPF patients versus donors.

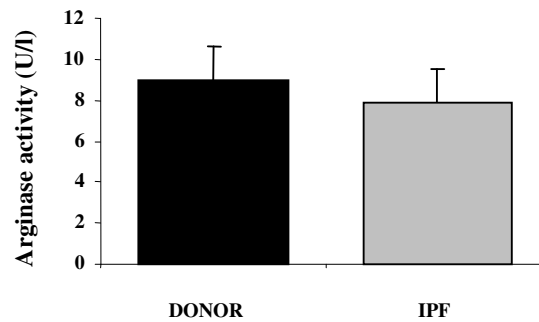


**Figure 4.20. ARG activity in human lung homogenates.**

Arginase activity in human lung from healthy donor transplant versus IPF patients analyzed by Arginase Assay Kit, (n=3), statistical analysis included two-tailed t-test

## **5. Discussion**

### **5.1. Involvement of arginase-1, -2 in lung diseases**

Recently, several reports have shown an interest in ARG expression and activity, as these enzymes affect L-arginine bioavailability for NOS <sup>116</sup>, and impact several lung diseases, such as asthma <sup>117</sup> and cystic fibrosis <sup>107</sup>. Interestingly, ARG-mediated attenuation of NO production by constitutive NOS was linked to airway hyperreactivity <sup>118</sup>, which could be reversed by pharmacological inhibition of ARG <sup>119</sup>. Apart from NO synthesis, ARG can also directly influence collagen metabolism, as its product, L-ornithine, is metabolized to polyamines and L-proline, the latter being highly enriched in collagen. Thus, ARG expression and activity may significantly impact pathophysiologic mechanisms involved in lung fibrosis, including increased collagen synthesis due to augmented L-proline bioavailability, endothelial dysfunction of the pulmonary vascular bed due to decreased NO synthesis, and higher cell proliferation induced by enhanced bioavailability of polyamines.

### **5.2. Arginase isoenzymes in an animal model of lung fibrosis**

#### **5.2.1. Arginase-1, -2 expression pattern**

In the present study, the well-established model of bleomycin-induced lung fibrosis in mice was used in order to analyze in detail the regulation of L-arginine metabolism in this lung disorder. The salient finding of this study was a significant upregulation of ARG1 and ARG2 expression in fibrotic lungs (Figure 4.4.), particularly evident seven and fourteen days after bleomycin administration. More detailed analysis of ARG isoenzyme expression revealed that, as early as three and five days after drug administration, an upregulation of ARG isoenzymes at the mRNA (Figure 4.5.) and protein levels (Figure 4.6.) was detected. These data confirmed results from an earlier study <sup>111</sup>, which indicated an upregulation of ARG and ODC mRNA, and ARG1 and ARG2 protein in lung homogenates of bleomycin-treated mice. Similar to data presented

in our project, ARG1 protein expression was also undetected in lung homogenates from control mice, but was present after seven days of bleomycin treatment. In contrast to this study, we detected ARG2 protein in lungs from control mice, while this was not the case in the cited study. Interestingly, the expression levels of cationic L-arginine transporters (Figure 4.1.) and other enzymes of arginine metabolism (Figure 4.3., and Figure 4.4.), with the exception of iNOS, remained unchanged during lung fibrosis. The iNOS expression displayed a progressive increase during the development of lung fibrosis.

Increased ARG expression during lung fibrosis was of functional relevance, as it correlated with decreased levels of free lung cellular L-arginine (Figure 4.7.). The highest depletion of the amino acid was observed seven and fourteen days after drug administration. It is well-established that IPF may be affected by Th2-mediated inflammation, which leads to progressive deposition of ECM, fibrogenesis, and destruction of the pulmonary parenchyma. Similar patterns can be observed in a bleomycin-induced lung fibrosis model, where approximately seven days after drug administration, a strong inflammatory response is evident, followed by the onset of fibrosis two weeks after treatment with bleomycin. Recently, it has been also demonstrated that iNOS and ARG activities can be differentially modulated by Th1 and Th2 cells and their cytokines<sup>103</sup>. Th1 cytokines (e.g. INF- $\gamma$ ) activate iNOS<sup>120</sup>, whereas Th2 cytokines (e.g. IL-4, IL-13) promote ARG activity<sup>121</sup>. Thus, the upregulation of the ARG expression observed during bleomycin-induced lung fibrosis may be explained by the fact that mice inflammatory response is dominated by the production of Th2-associated cytokines, including IL-4, IL-5, IL-10 and IL-13.

### **5.2.2. Cellular localization of arginase-1, -2**

Both ARG1 and ARG-2 were reported to be ubiquitously expressed in various tissue types. Despite their similarity concerning enzymatic properties, they differ with regard to subcellular localization and tissue distribution. The ARG1 is cytosolic enzyme, highly expressed in the liver, whereas ARG2 is enriched in mitochondria, and displays expression in organs such as the kidney, brain, small intestine, or mammary glands<sup>70</sup>. Immunohistochemical data presented in our project indicated the expression of both



ARG1 and ARG2 in lung sections from mice treated with bleomycin, seven and fourteen days after drug administration. The ARG was localized in areas of increased inflammation, as well as in fibrotic lesions (Figure 4.8.). These results are in accordance with *in vitro* experiments demonstrating that several Th2-associated cytokines are involved in the generation of alternatively activated macrophages, characterized by up-regulation of ARG1<sup>122,123</sup>. Further confirmation of the immunohistochemical results was obtained by the analysis of ARG expression in primary lung fibroblasts isolated from animals treated with bleomycin for different time points (Figure 4.9., and Figure 4.10.). Both ARG1 and ARG2 were highly expressed in fibroblasts, and their expression was increased in fibroblasts derived from bleomycin-treated mice compared with controls. In healthy mouse lungs, ARG1 and ARG2 mRNA were expressed at similar levels, but ARG2 protein could be detected at higher levels than ARG1 (Figure 4.6.). In contrast, in primary lung fibroblasts, ARG1 mRNA was expressed at higher levels than ARG2, and was also regulated much more potently by bleomycin treatment *in vivo*, as demonstrated by quantitative RT-PCR (Figure 4.9.), and immunoblotting analysis (Figure 4.10.).

These results are in agreement with data reporting that proinflammatory cytokines IL-4 and IL-13 appear to be important regulatory mediators for ARG in airway rat fibroblasts, since they caused significant upregulation of these enzymes<sup>124</sup>. Additionally, ARG1 expression was also detected by immunohistochemical staining in interstitial fibroblasts in Herpes virus-induced lung fibrosis<sup>110</sup>. Nevertheless, results presented in our project are of high importance, as they directly indicate upregulation of ARG isoforms and quantify expression of these enzymes in the primary lung fibroblasts derived from bleomycin- and saline-treated mice.

### **5.2.3. Regulation of arginase-1, -2 by profibrotic factors**

#### **5.2.3.1. TGF- $\beta$ 1-mediated arginase expression**

It is well established that TGF- $\beta$  plays an important role in the process of wound healing and fibrosis<sup>125</sup>. This multifunctional peptide is capable of enhancing proliferation of mesenchymal cells and synthesis of ECM. It has been also reported that TGF- $\beta$

contributes to early events that lead to bleomycin-induced pulmonary fibrosis. Mammalian TGF- $\beta$  exists in three isoforms<sup>126</sup> (TGF- $\beta$ 1, TGF- $\beta$ 2, TGF- $\beta$ 3), all of which were shown to be present in the normal lung. However, it was demonstrated that TGF- $\beta$  isoform gene expression can be differentially controlled during experimental pulmonary fibrosis, with TGF- $\beta$ 1 being the predominant isoform expressed during the pathogenesis of lung fibrosis<sup>127</sup>. In the present project, it was demonstrated that TGF- $\beta$ 1 potently induced ARG1 expression in lung fibroblasts (Figure 4.12.). This interesting result is in agreement with studies demonstrating TGF- $\beta$ -induced ARG activity in macrophages<sup>128</sup>. The TGF- $\beta$  is one of the most important cytokines in wound healing, as it leads to increased deposition of collagen by stimulated fibroblasts, moreover it was reported to induce the inhibition of NO production by macrophages through decreasing the stability and translation of mRNA for NOS and increasing its degradation<sup>129</sup>. The NO, a highly reactive free radical with pleiotropic effects, was demonstrated as a potentially important antifibrotic molecule in the regulation of wound healing<sup>130,131</sup>. Moreover, there are studies indicating NO-dependent suppression of TGF- $\beta$  expression<sup>132</sup>. Thus, the results presented in this project connected with the possible imbalance in L-arginine/NO pathway caused by overexpression of TGF- $\beta$ , suggest that ARG1 may be a key enzyme influencing collagen synthesis in fibroblasts.

### 5.2.3.2. Arginase-dependent collagen synthesis

In order to analyze whether ARG1 can affect the process of lung fibrosis and collagen synthesis, further experiments were performed. Based on the results presented in our project and published data, it can be argued that arginine depletion by increased ARG expression can affect cell and lung functions in several ways: on the one hand, the dramatic reduction of free L-arginine leads to its decreased bioavailability for NOS, thus leading to decreased NO production, as was demonstrated in detail in macrophages and epithelial cells<sup>133,134</sup>. Although ARG isoenzymes have a significantly lower  $K_m$  for L-arginine, they exhibit a 1000 $\times$  higher  $V_{max}$  compared with NOS, as such having the capacity to functionally inhibit NOS via substrate depletion<sup>74</sup>. Reduced NO levels, on the

other hand, have been shown to lead to airway and vascular smooth muscle cell proliferation, as well as enhanced susceptibility to pulmonary infections<sup>87</sup>, features occurring in pulmonary fibrosis. Next, and probably much more important, augmented generation of L-ornithine by ARG increases the bioavailability of polyamines and L-proline, essential regulators of cell proliferation and collagen synthesis, respectively<sup>49</sup>. Since fibroblast proliferation and collagen accumulation are hallmarks of lung fibrosis, this pathway could present an attractive option for therapeutic intervention. To elucidate the possible impact of ARG activity on collagen synthesis and deposition, experiments with the ARG inhibitor N<sup>G</sup>-hydroxy-L-arginine, NOHA, were performed. Inhibition of ARG activity using NOHA significantly attenuated TGF- $\beta$ 1-induced collagen deposition in NIH-3T3 cells (Figure 4.13.), as well as in primary human lung fibroblasts (Figure 4.16).

This presents strong evidence that ARG1 is the key enzyme influencing collagen synthesis in fibroblasts. These results are in agreement with recently published data indicating that ARG plays an important role in the pathophysiology of transplant-related pulmonary fibrosis. Here, it was demonstrated that downregulation of ARG protein expression and a reduction of ARG activity is a central mechanism for the protective role of pirfenidone, an antifibrotic agent with no immunosuppressive effect, in transplant-related pulmonary fibrosis<sup>135</sup>.

Additional experiments were performed in order to test whether NOHA has an effect on fibroblast ECM gene expression (Figure 4.15. and Figure 4.17.). Interestingly, these results revealed no regulation of COL1A1 and  $\alpha$ -SMA gene expression in presence of NOHA. Thus, these data strengthen the argument that ARG inhibition blocks ECM deposition by acting on its biosynthesis in a post-transcriptional manner.

### **5.2.3.3. Influence of arginase on TGF- $\beta$ 1 signaling**

As TGF- $\beta$ 1 is an important mediator in the pathogenesis of fibrosis, it is also important to examine downstream events of its activity, such as intracellular signaling. The active form of TGF- $\beta$  binds to the type II TGF- $\beta$  receptor (TGF- $\beta$ RII), which leads to the assembly of a heterotetrameric complex of TGF- $\beta$ RII and TGF- $\beta$ RI, both of

which are transmembrane serine/threonine kinase receptors. The TGF- $\beta$ RI is also known as activin-like kinase 5 (ALK5), and within this heterotrimeric complex, the kinase domain of ALK5 is phosphorylated by TGF- $\beta$ RII. Subsequently, ALK5 phosphorylates and activates the intracellular receptor-activated Smad proteins (Smad2 and Smad3). These proteins interact with Co-Smad, Smad4, to enter the nucleus and modify transcription of a series of genes involved in matrix expression, cell differentiation, and proliferation<sup>135</sup>.

In the absence of Smad3, ALK5 cannot transmit signal through to the nucleus and thus cannot upregulate expression of matrix genes in either bleomycin or TGF- $\beta$ -mediated fibrotic stimulation<sup>136,137</sup>. In other words, these data indicate that the progressive nature of fibrosis can proceed only in the presence of intact TGF- $\beta$ RI signaling mechanism and/or intact Smad3 signaling.

To further test the influence of ARG inhibition on TGF- $\beta$  signaling, fibroblasts were transfected with the pCAGA<sub>12</sub> luciferase reporter plasmid, and incubated with the ARG inhibitor NOHA. The effect of NOHA on TGF- $\beta$ 1-dependent signaling was studied (Figure 4.14.). Our results indicated that NOHA did not exert any effect on TGF- $\beta$ 1 signaling, as the Smad-driven reporter gene expression of the pCAGA<sub>12</sub>-luc remained unchanged in the presence of this inhibitor. Interestingly, although ARG inhibition was able to attenuate collagen synthesis, it did not inhibit TGF- $\beta$ 1 signaling, as such exhibiting pathway specificity, and the perspective of modulating collagen metabolism, but leaving unaffected the potent anti-inflammatory properties exerted by TGF- $\beta$ 1.

### **5.3. Limitations of the bleomycin model of lung fibrosis**

Idiopathic pulmonary fibrosis is a chronic interstitial lung disorder of unknown etiology. It is characterized by progressive parenchymal fibrosis and ventilatory restrictions. Although the pathogenesis of this disease is complex and poorly understood, it has been suggested that inflammation does not play a major role in initiating this disorder. According to a number of recently published data, IPF represents an

epithelial/fibroblastic disorder. This hypothesis suggests that epithelial injury and activation, rather than alveolitis, represent a key factor in the pathogenesis of IPF. Over the last years, the bleomycin model of pulmonary fibrosis has been most commonly studied in order to elucidate the regulatory mechanisms in pulmonary fibrogenesis. Intratracheal instillation of bleomycin leads to pulmonary fibrosis, which partly resembles human fibrotic lung disease. These characteristics include patchy parenchymal inflammation of variable intensity, epithelial cell injury with reactive hyperplasia, basement membrane damage, and interstitial as well as intraalveolar fibrosis. Despite these similarities, several issues have been raised regarding the validity of the bleomycin model. The main concerns relate to the speed of disease onset, as lung remodeling is much accelerated in this model, and to the durability<sup>138</sup>. Generally, bleomycin-induced pulmonary fibrosis in mice is almost complete within the fourth week after administration of the drug. During the acute stage of the disease, approximately two weeks after drug instillation, acute lung injury is a predominant feature of this model. As a result of this lung injury, remodeling of normal alveolar structure occurs during the chronic stage of the disease. Moreover, animals treated with bleomycin exhibit inflammation at early stages, from three days post-instillation to late stages such as 14–21 days after drug administration, where it coincides with lung fibrosis. In addition, bleomycin-induced fibrosis is reversible, and as such, is difficult to compare with IPF.

Thus, all traditional models of IPF start with inflammation, and with unknown etiology, there is no appropriate experimental model available. Nevertheless, it has to be considered that the main discrepancies between the bleomycin model and human IPF relate to the chronic stages of the disease, as such bleomycin model still represents an important tool to test molecular mechanisms involved in IPF pathogenesis.

## **5.4. Arginase-1, -2 in idiopathic pulmonary fibrosis**

### **5.4.1. Arginase-1, 2 localization in human lung tissues**

To investigate whether ARG isoenzymes displayed a pattern of localization in human lung tissue similar to the mouse model, immunohistochemical staining was performed on human lung sections from control transplant donors and IPF patients (Figure 4.18.). Interestingly, both ARG isoforms were detected in IPF patients as well as in healthy controls, in contrast to the bleomycin model, where ARG signal was undetected in control animals. The ARG1 was detected in epithelial cells in donors tissues, whereas in IPF patients, localization of this enzyme was strong in bronchial epithelial cells where it was confined to cilia of these cells. Additionally, inflammatory cells like macrophages exhibited positive staining for ARG1, which confirms the function of this enzyme in inflammatory reactions in the airways<sup>117</sup>. Similar to ARG1, ARG2 exhibited localization in bronchial epithelial cells in donor lung tissue, but unlike ARG1, it was undetected within the cilia of these cells. Interestingly, lung sections from IPF patients, ARG2 was detectable in alveolar epithelial type II cells. Moreover, both enzymes exhibited to some extent, localization within fibrotic lesions, in agreement with previously reported results indicating ARG localization in areas with pleural thickening, interstitial fibrosis, and epithelial cells<sup>110</sup>.

### **5.4.2. Expression of arginase-1, -2 in human lung tissues**

Interestingly, differences in ARG localization between donors and IPF patients were not as prominent as in the bleomycin-induced fibrosis model. It has to be considered, however, that immunohistochemistry is not a quantitative method of protein expression. Therefore, further analysis of ARG expression in the lungs of donors and IPF patients was performed using quantitative RT-PCR (Figure 4.19.). In line with results obtained for control animals, mRNA levels of ARG isoforms were low in healthy donors, but, no increased expression was observed in the lungs of IPF patients. Conversely, ARG1 demonstrated even lower mRNA levels in the lungs of IPF patients. These results

contrast with data indicating an upregulation of ARG1 expression in IPF patients at the protein level <sup>110</sup>. To confirm these expression results, analysis of ARG activity in donors and in IPF patients was performed (Figure 4.20.). In agreement with mRNA expression data presented in our project, there was no significant induction of ARG activity in lungs of IPF patients in comparison to lungs from healthy transplant donors. Since very little is known about ARG regulation in human lung tissue, and published data remain contradictory, it would be of benefit to further investigate this issue in future studies.

## 5.5. Conclusions and future perspectives

L-arginine serves as a substrate for both ARG and NOS. The pathways of these two enzymes can therefore interfere with one another through substrate competition <sup>52</sup>. The NO can regulate a number of aspects of human airway biology, including airway and vascular smooth muscle tone <sup>139</sup>, whereas elevations of ARG levels accompany a variety of pathological states, including pulmonary diseases such as asthma, silicosis, or pulmonary hypertension. Interestingly, it became apparent that cytokines, for instance IL-4 or IL-13, which are implicated in various lung disorders, also behave as inducers of ARG, and contribute to the increase in enzyme levels observed in these diseases.

In this investigation, we hypothesized that L-arginine metabolizing enzymes are altered in pulmonary fibrosis. In order to explore this idea, an initial characterization of enzyme expression was performed in the mouse model of bleomycin-induced lung fibrosis. The upregulation of ARG1 and ARG2 in fibrotic lungs was demonstrated, which correlated with decreased levels of L-arginine in the lung. Both ARG isoforms were localized to fibrotic lesions, and highly expressed in primary lung fibroblasts derived from bleomycin-treated mice. It was also reported that TGF- $\beta$ 1, a key profibrotic mediator, potently induced ARG expression in lung fibroblasts. Additionally, it was demonstrated that the ARG inhibitor has a potent inhibitory effect on TGF- $\beta$ 1-induced collagen deposition by mouse and human fibroblasts.

Experiments performed on human lung tissues from control transplant donors and IPF patients, however, did not fully support the results obtained from the animal model of

lung fibrosis. The discrepancy between these results for human disease and animal model, however, can be explained. First, significant changes in ARG expression, as well as in free L-arginine levels in the animal model of fibrosis were observed during the inflammatory and early fibroproliferative phase of the disease, which corresponds to the first and second week after bleomycin instillation. This may suggest the involvement of ARG isoenzymes in the early stages of the disease, which until now are difficult to recognize in IPF, as early detection of this disease remains difficult. It cannot be excluded that the levels of ARG are connected with progression of pulmonary fibrosis. Second, it remains difficult to compare gene expression results for humans and mice, as tissues from IPF are often difficult to obtain. Moreover, the animal model of lung fibrosis allows the generation of material of high reproducibility, whereas incomplete patients history often contributes to a high level of heterogeneity of human material. In order to elucidate this issue, and to minimize ambiguous results, further investigations should be performed in the future, possibly entailing more diseases such as COPD (chronic obstructive pulmonary disease) and asthma.

Since inhibition of ARG activity significantly attenuated TGF- $\beta$ 1-induced collagen deposition in primary human lung fibroblasts, it would be of benefit to investigate ARG expression in other cell types isolated from IPF patients or healthy donors. Methods such as microdissection would be a useful tool to collect material not only from lung fibroblasts, but also from epithelial cells, as they expressed ARG in lungs from IPF patients. Furthermore, this would clarify whether manipulation of ARG activity in pulmonary fibrosis offers the intriguing possibility of interfering with the development of the disease. It also has to be considered that unrestricted pharmacological inhibition of ARG with the usage of compounds like NOHA can alter the liver urea cycle function and can cause hepatotoxicity. Therefore, reliable methods should be developed to induce the loss of ARG function specifically in the lung, such as localized delivery of short-lived, reversible inhibitors of arginase.



## 6. Appendix

### 6.1. List of primers used for PCR amplification

#### 6.1.1. Quantitative RT-PCR

<b>Quantitative RT-PCR</b>				
<b>GeneBank™ Accession number</b>	<b>Forward Primer (5'-3')</b>	<b>Reverse Primer (5'-3')</b>	<b>Annealing temperature (°C)</b>	<b>Amplicon size (bp)</b>
ARG1 mouse NM_007482.2	GGAACCCAGAGAGAG CATGA	TTTTTCCAGCAGACCA GCTT	60	132
ARG1 human NM_000045.2	CTACAAAACAGGGCTA CTCTCAGGAT	GTTTCGAGTFACTTCTTC TGGTGTCTTC	60	83
ARG2 mouse NM_009705.1	ACCAGGAAGTGGCTGA AGTG	TGAGCATCAACCCAGA TGAC	60	141
ARG2 human NM_001172.3	AGAAAAGGAGTGGAG CATGG	GATCATCTTTGGGGAC TGGA	60	126
COL1A1 mouse NM_007742.2	ACGTCCTGGTGAAGTT GGTC	TCCAGCAATACCCTGA GGTC	59	117
COL1A1 human NM_000088.2	CCAGAAGAAGTGGTAC ATCAGC	CGCCATACTCGAAGT GAAT	59	94
PBGD mouse NM_013551.1	ATGTCCGGTAACGGCG GC	GGTACAAGGCTTTCAG CATCG	60	138
PBGD human NM_000190.3	CCCACGCGAATCACTC TCAT	TGTCTGGTAACGGCAA TGCG	60	69
α-SMA mouse NM_007392.2	CTGACAGAGGCACCAC TGAA	CATCTCCAGAGTCCAG CACA	59	159
α-SMA human NM_001613.1	GAGAAGAGTTACGAGT TGCCTG	TGTTAGCATAGAGGTC CTTCCTG	59	180

### 6.1.2. Semi-quantitative RT-PCR

<b>Semi-quantitative RT-PCR</b>				
<b>GeneBank™ Accession number</b>	<b>Forward Primer (5'-3')</b>	<b>Reverse Primer (5'-3')</b>	<b>Annealing temperature (°C)</b>	<b>Amplicon size (bp)</b>
ADC mouse NM_172875.1	GAC TTTGTGATGGTGG AGGAG	GAGGCAGGTGCTTCAG AAAG	58	148
ARG1 mouse NM_007482.2	AAGCTGGTCTGCTGGA AAAA	CTGGTTGTCAGGGGAG TGTT	60	310
ARG2 mouse NM_009705.1	TGGGATGCCACCTAAA AGAC	CCTGGCAGTTGTGGTA CCTT	60	358
DDAH1 mouse NM_026993.1	CAAATCAACGAGGTGC TGAA	TGCGCTTCTGGGTAC TCTT	58	302
DDAH2 mouse NM_016765.1	ACTTGGACTCCGAAT TGTG	CATCTGGGAGGGTCAG AGAG	58	318
GAPDH mouse XR_001547.1	AAC TTTGGCATTGTGG AAGG	ACACATTGGGGGTAGG AACA	59	223
OAT mouse NM_016978.1	GGTGACACAATTACC ATCCT	CTTGGCTGACAGCACC ATAA	58	121
ODC mouse NM_013614.1	TTTACTGCCACATCC TTGA	CGAGGTCCGCAACATA GAAC	58	112
PRMT1 mouse NM_019830.1	CACCCTCACATACCGC AACTCC	CAGCCACTTGTCCTCGA GCGT	60	339
PRMT2 mouse NM_133182.1	CGACAAGCAACTGGA GGAATAC	ACCTTCTCGGGCAGCA CCAC	60	359
PRMT3 mouse NM_1133740	TGCACCATCAGCCTT GTAT	GACCCTGTGTGGCAA TTCT	60	316
PRMT4 mouse NM_021531.2	CACCCCACGATTTCTG TTCT	CTTTCACCAGGACCT CTGC	60	346
PRMT5 mouse NM_013768.1	CAGGCTGTATGCTGTG GAGA	GCATCTCAAAGTGTGC CTCA	60	344
PRMT6 mouse NM_178891.3	TATGGCGTGGATATGA GCTG	CCGGAATGTCCGTAT CTTG	60	374
PRMT7 mouse NM_145404.1	ATTGCCAGGTCATCCT ATGC	CAAACAGCTCCGTGAT CAGA	60	352
NOS2 mouse NM_010927.1	AGACCTCAACAGAGCC CTCA	GCAGCCTTGTCTTT GACC	58	305
NOS3 mouse NM_008713.2	ATGTGCGCCCCTGTTA CTC	CACAGGGATGAGGTTG TCCT	58	322
SLC7A1 mouse NM_007513.2	TGGCTGGAAGTGTGATT CTCT	ACGTGAGAACTCTCCG ATGG	59	109
SLC7A2 mouse NM_007514.2	TTGCCGTGTGCCTTGT ATTA	CAGCCACCATGACAAA GAGA	59	123
SLC7A4 mouse NM_144852.2	TTCTACAGGCGGGTT ACAG	GGCAAACACCTGGAA GAAGA	59	150
SLC7A5 mouse NM_011404.2	TGGTCTTCGCCACCTA CTTG	AAGCCGAGCAAAATG ATGAG	59	199
SLC7A6 mouse NM_178798.2	CCCACCTGTGATCCTC CATA	CCTTGGCATACTGAA TGTG	59	130

<b>Semi-quantitative RT-PCR</b>				
<b>GeneBank™ Accession number</b>	<b>Forward Primer (5'-3')</b>	<b>Reverse Primer (5'-3')</b>	<b>Annealing temperature (°C)</b>	<b>Amplicon size (bp)</b>
SLC7A7 mouse NM_011405.1	ATCCGCCTCTGGACTT CTCT	GTTCCCCACTTGACAT AGGC	59	190
SLC7A9 mouse NM_021291.1	GAGACAAGCCTGAGG AGACG	ATGGTGCCCAATGA TACA	59	121
SLC6A14 mouse NM_020049.2	TCCAGTGAACCATGGA CAGA	AATCCCACTGCATAGC CAAC	59	177

## 6.2. List of antibodies

### 6.2.1. Primary antibodies

<b>Antibody</b>					
<b>Primary</b>	<b>Host</b>	<b>Dilution</b>			<b>Company</b>
		<b>IB</b>	<b>IHCH</b>	<b>ICCH</b>	
anti - $\alpha$ -SMC	mouse			1:500	Sigma-Aldrich
anti - ARG1	mouse	1:1000			BD Transduction Laboratories
anti - ARG1	rabbit		1:100	1:100	Santa-Cruz Biotech
anti - ARG2	rabbit	1:1000	1:100	1:100	Santa-Cruz Biotech
anti - $\beta$ -actin	rabbit	1:1000			Cell Signaling
anti - PRMT1	rabbit	1:2000			Upstate
anti - PRMT2	rabbit	1:1000			Abcam
anti - PRMT3	rabbit	1:2000			Upstate
anti - PRMT4	rabbit	1:1000			Upstate
anti - PRMT5	rabbit	1:2000			Upstate
anti - PRMT6	rabbit	1:500			Imgenex
anti - PRMT7	rabbit	1:500			Upstate

**6.2.2. Secondary antibodies**

<b>Antibody</b>					
<b>Secondary</b>	<b>Host</b>	<b>Dilution</b>			<b>Company</b>
		<b>IB</b>	<b>IHCH</b>	<b>ICCH</b>	
FITC-conjugated anti-mouse IgG	goat			1:300	ZyMax
FITC-conjugated anti-rabbit IgG	goat			1:300	ZyMax
HRP-conjugated anti-mouse IgG	goat	1:3000			Pierce
HRP-conjugated anti-rabbit IgG	goat	1:3000			Pierce

## 7. References

1. Homolka, J. Idiopathic pulmonary fibrosis: a historical review. *Cmaj* **137**, 1003-5 (1987).
2. Selman, M. & Pardo, A. Idiopathic pulmonary fibrosis: an epithelial/fibroblastic cross-talk disorder. *Respir Res* **3**, 3 (2002).
3. Raghu, G., Johnson, W. C., Lockhart, D. & Mageto, Y. Treatment of idiopathic pulmonary fibrosis with a new antifibrotic agent, pirfenidone: results of a prospective, open-label Phase II study. *Am J Respir Crit Care Med* **159**, 1061-9 (1999).
4. White, E. S., Lazar, M. H. & Thannickal, V. J. Pathogenetic mechanisms in usual interstitial pneumonia/idiopathic pulmonary fibrosis. *J Pathol* **201**, 343-54 (2003).
5. King, T. E., Jr. et al. Idiopathic pulmonary fibrosis: relationship between histopathologic features and mortality. *Am J Respir Crit Care Med* **164**, 1025-32 (2001).
6. Taskar, V. S. & Coultas, D. B. Is idiopathic pulmonary fibrosis an environmental disease? *Proc Am Thorac Soc* **3**, 293-8 (2006).
7. Tang, Y. W. et al. Herpesvirus DNA is consistently detected in lungs of patients with idiopathic pulmonary fibrosis. *J Clin Microbiol* **41**, 2633-40 (2003).
8. Stewart, J. P. et al. The detection of Epstein-Barr virus DNA in lung tissue from patients with idiopathic pulmonary fibrosis. *Am J Respir Crit Care Med* **159**, 1336-41 (1999).
9. Geist, L. J. & Hunninghake, G. W. Potential role of viruses in the pathogenesis of pulmonary fibrosis. *Chest* **103**, 119S-120S (1993).
10. Johnston, I. D., Prescott, R. J., Chalmers, J. C. & Rudd, R. M. British Thoracic Society study of cryptogenic fibrosing alveolitis: current presentation and initial management. Fibrosing Alveolitis Subcommittee of the Research Committee of the British Thoracic Society. *Thorax* **52**, 38-44 (1997).
11. Hubbard, R., Lewis, S., Richards, K., Johnston, I. & Britton, J. Occupational exposure to metal or wood dust and aetiology of cryptogenic fibrosing alveolitis. *Lancet* **347**, 284-9 (1996).
12. Grutters, J. C. & du Bois, R. M. Genetics of fibrosing lung diseases. *Eur Respir J* **25**, 915-27 (2005).
13. Marshall, R. P., Puddicombe, A., Cookson, W. O. & Laurent, G. J. Adult familial cryptogenic fibrosing alveolitis in the United Kingdom. *Thorax* **55**, 143-6 (2000).
14. Selman, M., King, T. E. & Pardo, A. Idiopathic pulmonary fibrosis: prevailing and evolving hypotheses about its pathogenesis and implications for therapy. *Ann Intern Med* **134**, 136-51 (2001).
15. Geiser, T. Idiopathic pulmonary fibrosis--a disorder of alveolar wound repair? *Swiss Med Wkly* **133**, 405-11 (2003).
16. Gauldie, J., Kolb, M. & Sime, P. J. A new direction in the pathogenesis of idiopathic pulmonary fibrosis? *Respir Res* **3**, 1 (2002).

17. Katzenstein, A. L. & Myers, J. L. Idiopathic pulmonary fibrosis: clinical relevance of pathologic classification. *Am J Respir Crit Care Med* **157**, 1301-15 (1998).
18. Kolb, M. et al. Differences in the fibrogenic response after transfer of active transforming growth factor-beta1 gene to lungs of "fibrosis-prone" and "fibrosis-resistant" mouse strains. *Am J Respir Cell Mol Biol* **27**, 141-50 (2002).
19. Agostini, C. & Gurrieri, C. Chemokine/cytokine cocktail in idiopathic pulmonary fibrosis. *Proc Am Thorac Soc* **3**, 357-63 (2006).
20. Khalil, N. & O'Connor, R. Idiopathic pulmonary fibrosis: current understanding of the pathogenesis and the status of treatment. *Cmaj* **171**, 153-60 (2004).
21. Chua, F., Gauldie, J. & Laurent, G. J. Pulmonary fibrosis: searching for model answers. *Am J Respir Cell Mol Biol* **33**, 9-13 (2005).
22. Sleijfer, S. Bleomycin-induced pneumonitis. *Chest* **120**, 617-24 (2001).
23. Burger, R. M., Peisach, J. & Horwitz, S. B. Activated bleomycin. A transient complex of drug, iron, and oxygen that degrades DNA. *J Biol Chem* **256**, 11636-44 (1981).
24. Umezawa, H., Takeuchi, T., Hori, S., Sawa, T. & Ishizuka, M. Studies on the mechanism of antitumor effect of bleomycin of squamous cell carcinoma. *J Antibiot (Tokyo)* **25**, 409-20 (1972).
25. Martin, P. Wound healing--aiming for perfect skin regeneration. *Science* **276**, 75-81 (1997).
26. Lorena, D., Uchio, K., Costa, A. M. & Desmouliere, A. Normal scarring: importance of myofibroblasts. *Wound Repair Regen* **10**, 86-92 (2002).
27. Plataki, M. et al. Expression of apoptotic and antiapoptotic markers in epithelial cells in idiopathic pulmonary fibrosis. *Chest* **127**, 266-74 (2005).
28. Thannickal, V. J., Aldweib, K. D., Rajan, T. & Fanburg, B. L. Upregulated expression of fibroblast growth factor (FGF) receptors by transforming growth factor-beta1 (TGF-beta1) mediates enhanced mitogenic responses to FGFs in cultured human lung fibroblasts. *Biochem Biophys Res Commun* **251**, 437-41 (1998).
29. Ignatz, R. A. & Massague, J. Transforming growth factor-beta stimulates the expression of fibronectin and collagen and their incorporation into the extracellular matrix. *J Biol Chem* **261**, 4337-45 (1986).
30. Uhal, B. D. et al. Alveolar epithelial cell death adjacent to underlying myofibroblasts in advanced fibrotic human lung. *Am J Physiol* **275**, L1192-9 (1998).
31. Yurchenco, P. D. & Schittny, J. C. Molecular architecture of basement membranes. *Faseb J* **4**, 1577-90 (1990).
32. Lagente, V. et al. Role of matrix metalloproteinases in the development of airway inflammation and remodeling. *Braz J Med Biol Res* **38**, 1521-30 (2005).
33. Pardo, A. et al. Gelatinases A and B are up-regulated in rat lungs by subacute hyperoxia: pathogenetic implications. *Am J Pathol* **153**, 833-44 (1998).
34. Moore, B. B. et al. CCR2-mediated recruitment of fibrocytes to the alveolar space after fibrotic injury. *Am J Pathol* **166**, 675-84 (2005).
35. Kjaer, M. et al. Metabolic activity and collagen turnover in human tendon in response to physical activity. *J Musculoskelet Neuronal Interact* **5**, 41-52 (2005).

36. Bella, J., Liu, J., Kramer, R., Brodsky, B. & Berman, H. M. Conformational effects of Gly-X-Gly interruptions in the collagen triple helix. *J Mol Biol* **362**, 298-311 (2006).
37. Canty, E. G. & Kadler, K. E. Procollagen trafficking, processing and fibrillogenesis. *J Cell Sci* **118**, 1341-53 (2005).
38. Morris, S. M., Jr. Arginine: beyond protein. *Am J Clin Nutr* **83**, 508S-512S (2006).
39. Wu, G. & Morris, S. M., Jr. Arginine metabolism: nitric oxide and beyond. *Biochem J* **336** ( Pt 1), 1-17 (1998).
40. Junbao, D. et al. Effect of L-arginine on collagen of high flow-induced pulmonary arterial remodeling. *Circ J* **69**, 603-8 (2005).
41. Shi, H. P., Most, D., Efron, D. T., Witte, M. B. & Barbul, A. Supplemental L-arginine enhances wound healing in diabetic rats. *Wound Repair Regen* **11**, 198-203 (2003).
42. Tong, B. C. & Barbul, A. Cellular and physiological effects of arginine. *Mini Rev Med Chem* **4**, 823-32 (2004).
43. Evoy, D., Lieberman, M. D., Fahey, T. J., 3rd & Daly, J. M. Immunonutrition: the role of arginine. *Nutrition* **14**, 611-7 (1998).
44. Barbul, A., Rettura, G., Levenson, S. M. & Seifter, E. Wound healing and thymotropic effects of arginine: a pituitary mechanism of action. *Am J Clin Nutr* **37**, 786-94 (1983).
45. Smith, P. A. et al. Electrogenic arginine transport mediates stimulus-secretion coupling in mouse pancreatic beta-cells. *J Physiol* **499** ( Pt 3), 625-35 (1997).
46. Papapetropoulos, A., Rudic, R. D. & Sessa, W. C. Molecular control of nitric oxide synthases in the cardiovascular system. *Cardiovasc Res* **43**, 509-20 (1999).
47. Calbet, J. A. & MacLean, D. A. Plasma glucagon and insulin responses depend on the rate of appearance of amino acids after ingestion of different protein solutions in humans. *J Nutr* **132**, 2174-82 (2002).
48. Tarry, W. C. & Makhoul, R. G. L-arginine improves endothelium-dependent vasorelaxation and reduces intimal hyperplasia after balloon angioplasty. *Arterioscler Thromb* **14**, 938-43 (1994).
49. Morris, S. M., Jr. Enzymes of arginine metabolism. *J Nutr* **134**, 2743S-2747S; discussion 2765S-2767S (2004).
50. Dhanakoti, S. N., Brosnan, M. E., Herzberg, G. R. & Brosnan, J. T. Cellular and subcellular localization of enzymes of arginine metabolism in rat kidney. *Biochem J* **282** ( Pt 2), 369-75 (1992).
51. Yu, J. G., Ishine, T., Kimura, T., O'Brien, W. E. & Lee, T. J. L-citrulline conversion to L-arginine in sphenopalatine ganglia and cerebral perivascular nerves in the pig. *Am J Physiol* **273**, H2192-9 (1997).
52. Morris, S. M., Jr. Regulation of enzymes of the urea cycle and arginine metabolism. *Annu Rev Nutr* **22**, 87-105 (2002).
53. Cheung, C. W., Cohen, N. S. & Rajzman, L. Channeling of urea cycle intermediates in situ in permeabilized hepatocytes. *J Biol Chem* **264**, 4038-44 (1989).

54. Closs, E. I., Simon, A., Vekony, N. & Rotmann, A. Plasma membrane transporters for arginine. *J Nutr* **134**, 2752S-2759S; discussion 2765S-2767S (2004).
55. Yeramian, A. et al. Arginine transport via cationic amino acid transporter 2 plays a critical regulatory role in classical or alternative activation of macrophages. *J Immunol* **176**, 5918-24 (2006).
56. Durante, W., Liao, L., Reyna, S. V., Peyton, K. J. & Schafer, A. I. Transforming growth factor-beta(1) stimulates L-arginine transport and metabolism in vascular smooth muscle cells: role in polyamine and collagen synthesis. *Circulation* **103**, 1121-7 (2001).
57. Verrey, F. et al. CATs and HATs: the SLC7 family of amino acid transporters. *Pflugers Arch* **447**, 532-42 (2004).
58. O'Sullivan, D., Brosnan, J. T. & Brosnan, M. E. Hepatic zonation of the catabolism of arginine and ornithine in the perfused rat liver. *Biochem J* **330** ( Pt 2), 627-32 (1998).
59. Knowles, R. G. & Moncada, S. Nitric oxide synthases in mammals. *Biochem J* **298** ( Pt 2), 249-58 (1994).
60. McGuire, D. M., Gross, M. D., Elde, R. P. & van Pilsum, J. F. Localization of L-arginine-glycine amidinotransferase protein in rat tissues by immunofluorescence microscopy. *J Histochem Cytochem* **34**, 429-35 (1986).
61. Humm, A., Fritsche, E., Steinbacher, S. & Huber, R. Crystal structure and mechanism of human L-arginine:glycine amidinotransferase: a mitochondrial enzyme involved in creatine biosynthesis. *Embo J* **16**, 3373-85 (1997).
62. Wyss, M. & Kaddurah-Daouk, R. Creatine and creatinine metabolism. *Physiol Rev* **80**, 1107-213 (2000).
63. Morrissey, J., McCracken, R., Ishidoya, S. & Klahr, S. Partial cloning and characterization of an arginine decarboxylase in the kidney. *Kidney Int* **47**, 1458-61 (1995).
64. Lortie, M. J. et al. Agmatine, a bioactive metabolite of arginine. Production, degradation, and functional effects in the kidney of the rat. *J Clin Invest* **97**, 413-20 (1996).
65. Sastre, M., Galea, E., Feinstein, D., Reis, D. J. & Regunathan, S. Metabolism of agmatine in macrophages: modulation by lipopolysaccharide and inhibitory cytokines. *Biochem J* **330** ( Pt 3), 1405-9 (1998).
66. Horyn, O. et al. Biosynthesis of agmatine in isolated mitochondria and perfused rat liver: studies with <sup>15</sup>N-labelled arginine. *Biochem J* **388**, 419-25 (2005).
67. Ash, D. E. Structure and function of arginases. *J Nutr* **134**, 2760S-2764S; discussion 2765S-2767S (2004).
68. Morris, S. M., Jr., Kepka-Lenhart, D. & Chen, L. C. Differential regulation of arginases and inducible nitric oxide synthase in murine macrophage cells. *Am J Physiol* **275**, E740-7 (1998).
69. Morris, S. M., Jr., Bhamidipati, D. & Kepka-Lenhart, D. Human type II arginase: sequence analysis and tissue-specific expression. *Gene* **193**, 157-61 (1997).
70. Jenkinson, C. P., Grody, W. W. & Cederbaum, S. D. Comparative properties of arginases. *Comp Biochem Physiol B Biochem Mol Biol* **114**, 107-32 (1996).



71. Stuehr, D. J. Structure-function aspects in the nitric oxide synthases. *Annu Rev Pharmacol Toxicol* **37**, 339-59 (1997).
72. Christopherson, K. S. & Bredt, D. S. Nitric oxide in excitable tissues: physiological roles and disease. *J Clin Invest* **100**, 2424-9 (1997).
73. Michel, T. & Feron, O. Nitric oxide synthases: which, where, how, and why? *J Clin Invest* **100**, 2146-52 (1997).
74. Boucher, J. L., Moali, C. & Tenu, J. P. Nitric oxide biosynthesis, nitric oxide synthase inhibitors and arginase competition for L-arginine utilization. *Cell Mol Life Sci* **55**, 1015-28 (1999).
75. Reczkowski, R. S. & Ash, D. E. Rat liver arginase: kinetic mechanism, alternate substrates, and inhibitors. *Arch Biochem Biophys* **312**, 31-7 (1994).
76. Steppan, J. et al. Arginase modulates myocardial contractility by a nitric oxide synthase 1-dependent mechanism. *Proc Natl Acad Sci U S A* **103**, 4759-64 (2006).
77. Gotoh, T. & Mori, M. Arginase II downregulates nitric oxide (NO) production and prevents NO-mediated apoptosis in murine macrophage-derived RAW 264.7 cells. *J Cell Biol* **144**, 427-34 (1999).
78. Tenu, J. P. et al. Effects of the new arginase inhibitor N(omega)-hydroxy-nor-L-arginine on NO synthase activity in murine macrophages. *Nitric Oxide* **3**, 427-38 (1999).
79. Boucher, J. L. et al. N omega-hydroxyl-L-arginine, an intermediate in the L-arginine to nitric oxide pathway, is a strong inhibitor of liver and macrophage arginase. *Biochem Biophys Res Commun* **203**, 1614-21 (1994).
80. Boger, R. H., Vallance, P. & Cooke, J. P. Asymmetric dimethylarginine (ADMA): a key regulator of nitric oxide synthase. *Atheroscler Suppl* **4**, 1-3 (2003).
81. Boger, R. H., Cooke, J. P. & Vallance, P. ADMA: an emerging cardiovascular risk factor. *Vasc Med* **10 Suppl 1**, S1-2 (2005).
82. Boger, R. H. Asymmetric dimethylarginine (ADMA) and cardiovascular disease: insights from prospective clinical trials. *Vasc Med* **10 Suppl 1**, S19-25 (2005).
83. Perticone, F. et al. Asymmetric dimethylarginine, L-arginine, and endothelial dysfunction in essential hypertension. *J Am Coll Cardiol* **46**, 518-23 (2005).
84. Mugge, A., Hanefeld, C. & Boger, R. H. Plasma concentration of asymmetric dimethylarginine and the risk of coronary heart disease: rationale and design of the multicenter CARDIAC study. *Atheroscler Suppl* **4**, 29-32 (2003).
85. Kepka-Lenhart, D., Mistry, S. K., Wu, G. & Morris, S. M., Jr. Arginase I: a limiting factor for nitric oxide and polyamine synthesis by activated macrophages? *Am J Physiol Regul Integr Comp Physiol* **279**, R2237-42 (2000).
86. Li, H. et al. Regulatory role of arginase I and II in nitric oxide, polyamine, and proline syntheses in endothelial cells. *Am J Physiol Endocrinol Metab* **280**, E75-82 (2001).
87. Wei, L. H., Wu, G., Morris, S. M., Jr. & Ignarro, L. J. Elevated arginase I expression in rat aortic smooth muscle cells increases cell proliferation. *Proc Natl Acad Sci U S A* **98**, 9260-4 (2001).
88. Grimble, G. Can daily dietary arginine supplement affect the function and subpopulation of lymphocytes in patients with advanced gastric cancer? Wu C-W,

- Chi C-W, Chiu C-C, Liu W-Y, P'eng F-K and Wang S-R. Digestion 1993; 54: 118-124. *Clin Nutr* **13**, 127-8 (1994).
89. Dhawan, V., Handu, S. S., Nain, C. K. & Ganguly, N. K. Chronic L-arginine supplementation improves endothelial cell vasoactive functions in hypercholesterolemic and atherosclerotic monkeys. *Mol Cell Biochem* **269**, 1-11 (2005).
90. Kurus, M., Esrefoglu, M., Bay, A. & Ozturk, F. Protective effect of oral L-arginine supplementation on cyclosporine induced nephropathy in rats. *Int Urol Nephrol* **37**, 587-94 (2005).
91. Mori, M. & Gotoh, T. Regulation of nitric oxide production by arginine metabolic enzymes. *Biochem Biophys Res Commun* **275**, 715-9 (2000).
92. Wang, W. W. et al. Co-induction of arginase and nitric oxide synthase in murine macrophages activated by lipopolysaccharide. *Biochem Biophys Res Commun* **210**, 1009-16 (1995).
93. Granger, D. L., Hibbs, J. B., Jr., Perfect, J. R. & Durack, D. T. Metabolic fate of L-arginine in relation to microbistatic capability of murine macrophages. *J Clin Invest* **85**, 264-73 (1990).
94. Berkowitz, D. E. et al. Arginase reciprocally regulates nitric oxide synthase activity and contributes to endothelial dysfunction in aging blood vessels. *Circulation* **108**, 2000-6 (2003).
95. Demougeot, C., Prigent-Tessier, A., Marie, C. & Berthelot, A. Arginase inhibition reduces endothelial dysfunction and blood pressure rising in spontaneously hypertensive rats. *J Hypertens* **23**, 971-8 (2005).
96. Ming, X. F. et al. Thrombin stimulates human endothelial arginase enzymatic activity via RhoA/ROCK pathway: implications for atherosclerotic endothelial dysfunction. *Circulation* **110**, 3708-14 (2004).
97. Bivalacqua, T. J. et al. Evaluation of nitric oxide synthase and arginase in the induction of a Peyronie's-like condition in the rat. *J Androl* **22**, 497-506 (2001).
98. Bivalacqua, T. J., Hellstrom, W. J., Kadowitz, P. J. & Champion, H. C. Increased expression of arginase II in human diabetic corpus cavernosum: in diabetic-associated erectile dysfunction. *Biochem Biophys Res Commun* **283**, 923-7 (2001).
99. Zea, A. H. et al. Arginase-producing myeloid suppressor cells in renal cell carcinoma patients: a mechanism of tumor evasion. *Cancer Res* **65**, 3044-8 (2005).
100. Gobert, A. P. et al. Protective role of arginase in a mouse model of colitis. *J Immunol* **173**, 2109-17 (2004).
101. Kampfer, H., Pfeilschifter, J. & Frank, S. Expression and activity of arginase isoenzymes during normal and diabetes-impaired skin repair. *J Invest Dermatol* **121**, 1544-51 (2003).
102. Schnorr, O. et al. Arginase-1 overexpression induces cationic amino acid transporter-1 in psoriasis. *Free Radic Biol Med* **38**, 1073-9 (2005).
103. Hesse, M. et al. Differential regulation of nitric oxide synthase-2 and arginase-1 by type 1/type 2 cytokines in vivo: granulomatous pathology is shaped by the pattern of L-arginine metabolism. *J Immunol* **167**, 6533-44 (2001).

104. Zimmermann, N. & Rothenberg, M. E. The arginine-arginase balance in asthma and lung inflammation. *Eur J Pharmacol* **533**, 253-62 (2006).
105. Ratjen, F. & Doring, G. Cystic fibrosis. *Lancet* **361**, 681-9 (2003).
106. Grasemann, H. et al. Decreased systemic bioavailability of L-arginine in patients with cystic fibrosis. *Respir Res* **7**, 87 (2006).
107. Grasemann, H., Schwartz, R., Matthiesen, S., Racke, K. & Ratjen, F. Increased arginase activity in cystic fibrosis airways. *Am J Respir Crit Care Med* **172**, 1523-8 (2005).
108. Xu, W. et al. Increased arginase II and decreased NO synthesis in endothelial cells of patients with pulmonary arterial hypertension. *Faseb J* **18**, 1746-8 (2004).
109. Nelin, L. D. et al. Cytokine-induced endothelial arginase expression is dependent on epidermal growth factor receptor. *Am J Respir Cell Mol Biol* **33**, 394-401 (2005).
110. Mora, A. L. et al. Activation of alveolar macrophages via the alternative pathway in herpesvirus-induced lung fibrosis. *Am J Respir Cell Mol Biol* **35**, 466-73 (2006).
111. Endo, M. et al. Induction of arginase I and II in bleomycin-induced fibrosis of mouse lung. *Am J Physiol Lung Cell Mol Physiol* **285**, L313-21 (2003).
112. Kelly, M., Kolb, M., Bonniaud, P. & Gauldie, J. Re-evaluation of fibrogenic cytokines in lung fibrosis. *Curr Pharm Des* **9**, 39-49 (2003).
113. Bulau, P. et al. Quantitative assessment of arginine methylation in free versus protein-incorporated amino acids in vitro and in vivo using protein hydrolysis and high-performance liquid chromatography. *Biotechniques* **40**, 305-10 (2006).
114. Bulau, P. et al. Analysis of methylarginine metabolism in the cardiovascular system identifies the lung as a major source of ADMA. *Am J Physiol Lung Cell Mol Physiol* **292**, L18-24 (2007).
115. Carraway, M. S., Piantadosi, C. A., Jenkinson, C. P. & Huang, Y. C. Differential expression of arginase and iNOS in the lung in sepsis. *Exp Lung Res* **24**, 253-68 (1998).
116. Ricciardolo, F. L. Multiple roles of nitric oxide in the airways. *Thorax* **58**, 175-82 (2003).
117. Zimmermann, N. et al. Dissection of experimental asthma with DNA microarray analysis identifies arginase in asthma pathogenesis. *J Clin Invest* **111**, 1863-74 (2003).
118. Meurs, H. et al. Increased arginase activity underlies allergen-induced deficiency of cNOS-derived nitric oxide and airway hyperresponsiveness. *Br J Pharmacol* **136**, 391-8 (2002).
119. Yang, M. et al. Inhibition of arginase I activity by RNA interference attenuates IL-13-induced airways hyperresponsiveness. *J Immunol* **177**, 5595-603 (2006).
120. Suschek, C. V., Schnorr, O. & Kolb-Bachofen, V. The role of iNOS in chronic inflammatory processes in vivo: is it damage-promoting, protective, or active at all? *Curr Mol Med* **4**, 763-75 (2004).
121. Munder, M. et al. Th1/Th2-regulated expression of arginase isoforms in murine macrophages and dendritic cells. *J Immunol* **163**, 3771-7 (1999).
122. Munder, M., Eichmann, K. & Modolell, M. Alternative metabolic states in murine macrophages reflected by the nitric oxide synthase/arginase balance: competitive

- regulation by CD4+ T cells correlates with Th1/Th2 phenotype. *J Immunol* **160**, 5347-54 (1998).
123. Pauleau, A. L. et al. Enhancer-mediated control of macrophage-specific arginase I expression. *J Immunol* **172**, 7565-73 (2004).
  124. Lindemann, D. & Racke, K. Glucocorticoid inhibition of interleukin-4 (IL-4) and interleukin-13 (IL-13) induced up-regulation of arginase in rat airway fibroblasts. *Naunyn Schmiedebergs Arch Pharmacol* **368**, 546-50 (2003).
  125. Border, W. A. & Noble, N. A. Transforming growth factor beta in tissue fibrosis. *N Engl J Med* **331**, 1286-92 (1994).
  126. Shi, Y. & Massague, J. Mechanisms of TGF-beta signaling from cell membrane to the nucleus. *Cell* **113**, 685-700 (2003).
  127. Leask, A. & Abraham, D. J. TGF-beta signaling and the fibrotic response. *Faseb J* **18**, 816-27 (2004).
  128. Boutard, V. et al. Transforming growth factor-beta stimulates arginase activity in macrophages. Implications for the regulation of macrophage cytotoxicity. *J Immunol* **155**, 2077-84 (1995).
  129. Gilbert, R. S. & Herschman, H. R. Transforming growth factor beta differentially modulates the inducible nitric oxide synthase gene in distinct cell types. *Biochem Biophys Res Commun* **195**, 380-4 (1993).
  130. Schaffer, M. R., Tantry, U., Thornton, F. J. & Barbul, A. Inhibition of nitric oxide synthesis in wounds: pharmacology and effect on accumulation of collagen in wounds in mice. *Eur J Surg* **165**, 262-7 (1999).
  131. Schaffer, M. R., Tantry, U., Gross, S. S., Wasserburg, H. L. & Barbul, A. Nitric oxide regulates wound healing. *J Surg Res* **63**, 237-40 (1996).
  132. Craven, P. A., Studer, R. K., Felder, J., Phillips, S. & DeRubertis, F. R. Nitric oxide inhibition of transforming growth factor-beta and collagen synthesis in mesangial cells. *Diabetes* **46**, 671-81 (1997).
  133. Morris, S. M., Jr. Arginine metabolism: boundaries of our knowledge. *J Nutr* **137**, 1602S-1609S (2007).
  134. Meurs, H. et al. Modulation of cholinergic airway reactivity and nitric oxide production by endogenous arginase activity. *Br J Pharmacol* **130**, 1793-8 (2000).
  135. Liu, H., Drew, P., Gaugler, A. C., Cheng, Y. & Visner, G. A. Pirfenidone inhibits lung allograft fibrosis through L-arginine-arginase pathway. *Am J Transplant* **5**, 1256-63 (2005).
  136. Bonniaud, P. et al. TGF-beta and Smad3 signaling link inflammation to chronic fibrogenesis. *J Immunol* **175**, 5390-5 (2005).
  137. Bonniaud, P. et al. Smad3 null mice develop airspace enlargement and are resistant to TGF-beta-mediated pulmonary fibrosis. *J Immunol* **173**, 2099-108 (2004).
  138. Borzone, G. et al. Bleomycin-induced chronic lung damage does not resemble human idiopathic pulmonary fibrosis. *Am J Respir Crit Care Med* **163**, 1648-53 (2001).
  139. Fischer, A., Folkerts, G., Geppetti, P. & Groneberg, D. A. Mediators of asthma: nitric oxide. *Pulm Pharmacol Ther* **15**, 73-81 (2002).

## **8. Declaration**

I declare that I have completed this dissertation single-handedly without the unauthorized help of a second party and only with the assistance acknowledged therein. I have appropriately acknowledged and referenced all text passages that are derived literally from or are based on the content of published or unpublished work of others, and all information that relates to verbal communications. I have abided by the principles of good scientific conduct laid down in the charter of the Justus Liebig University of Giessen in carrying out the investigations described in the dissertation.

## 9. Curriculum vitae

<b>PERSONAL DETAILS:</b>	
<b>First Name:</b>	Kamila Ewa
<b>Surname:</b>	Kitowska
<b>Date of Birth:</b>	24 <sup>th</sup> December 1979
<b>Place of Birth:</b>	Gdansk, Poland
<b>Nationality:</b>	Polish
<b>Sex:</b>	Female
<b>Marital Status:</b>	single, no children
<b>Address:</b>	Georg-Büchner Strasse 23 35392 Giessen Germany
<b>Telephone:</b>	+(49) 1621512884
<b>E-mail:</b>	Kamila.Kitowska@uglc.de kamilaki@wp.pl
<b>Present position:</b>	PhD Student (Supervisor: Dr. O. Eickelberg) Zentrum für Innere Medizin Medizinische Klinik und Poliklinik II Justus Liebig University Giessen
<b>Institute's address:</b>	University of Giessen School of Medicine Department of Medicine II Aulweg 123, Room 6-11 35392 Giessen, Germany
<b>Telephone:</b>	+(49) 641 9942303

<b>EDUCATION:</b>	
<b>2004 - present</b>	PhD Student (Supervisor: Dr. O. Eickelberg), PhD programme of the Faculties of Veterinary Medicine and Medicine, Justus Liebig University Giessen
<b>2004 - 2006</b>	PhD Student (Supervisor: Dr. O. Eickelberg), International Graduate Program “Molecular Biology and Medicine of the Lung (MBML)”, University of Giessen School of Medicine
<b>1998 - 2003</b>	MSc Studies, Department of Biotechnology, Intercollegiate Faculty of Biotechnology University of Gdansk and Medical University of Gdansk, Poland  MSc degree project: “Influence of the physical and chemical factors on the cellular uptake of diamino acid derivatives of porphyrins into HeLa cells” (Supervisor: Anna J. Podhajska MD, Ph.D, Prof)

<b>ADDITIONAL QUALIFICATIONS:</b>	
<b>2003</b>	SOCRATES/ERASMUS scholarship, University of Perugia, Italy. Six-month laboratory training in the subject: “The study of the novel gene 9/2 involved in liver regeneration”
<b>2002</b>	Participation in the Spring School “New Techniques in Monoclonal Antibodies Production and their Applications”, Institute of Molecular Biology and Biotechnology, Cracow, Poland

<b>2000, 2001</b>	Participation in the 7 <sup>th</sup> and 8 <sup>th</sup> Biotechnology Summer School organized by the Intercollegiate Faculty of Biotechnology, University of Gdansk and Medical University of Gdansk
<b>1999</b>	Chromatography course, University of Bremen

### PUBLICATIONS:

1. Patrick Bulau, Dariusz Zakrzewicz, **Kamila Kitowska**, Birgit Wardega, Joachim Kreuder, and Oliver Eickelberg. "Quantitative assessment of arginine methylation in free versus-incorporated amino acids in vitro and in vivo using hydrolysis and high-performance liquid chromatography." *BioTechniques*, 2006 Mar;40(3):305-10.
2. Ali O. Yildirim, Patrick Bulau, Dariusz Zakrzewicz, **Kamila E. Kitowska**, Norbert Weissmann, Friedrich Grimminger, Rory E. Morty, and Oliver Eickelberg. "Increased protein arginine methylation in chronic hypoxia: role of protein arginine methyltransferases". *Am J Respir Cell Mol Biol*. 2006 Oct;35(4):436-43.
3. Patrick Bulau, Dariusz Zakrzewicz, **Kamila Kitowska**, James Leiper, Friedrich Grimminger, and Oliver Eickelberg. "Analysis of methylarginine metabolism in the cardiovascular system identifies the lung as a major source of ADMA". *Am J Physiol Lung Cell Mol Physiol*. 2007 Jan;292(1):L18-24.
4. **Kamila Kitowska**, Dariusz Zakrzewicz, Melanie Konigshoff, Izabela Chrobak, Werner Seeger, Patrick Bulau, and Oliver Eickelberg. "Increased arginase expression and activity: A novel pathogenic mechanism in pulmonary fibrosis", *Am J Physiol Lung Cell Mol Physiol*, in revision
5. Melanie Konigshoff, Jochen Wilhelm, Andreas Jahn, Oana V. Amarie, Monika Kramer, **Kamila Kitowska**, Anke Wilhelm, Rainer Maria Bohle, Martin Obert, Horst Traupe, Werner Seeger, Frank Rose, Ludger Fink, Liliana Schaefer, Andreas Gunther, and Oliver Eickelberg. "WISP-1, a novel mediator of alveolar epithelial cell hyperplasia, is required for pulmonary fibrosis", *Nat Med*, in revision



**POSTER PRESENTATIONS:**

- Katarzyna Sikorska, Krzysztof P. Bielawski, Piotr Stalke, Elżbieta Anna Lakomy, Zofia Michalska, Krystyna Witczak-Malinowska, **Kamila Kitowska**, Julian Stolarczyk. "Initial analysis of C282Y mutation in a group of patients with symptoms of parenchymatous liver damage and haemochromatosis". IV Congress of Polish Society of Hepatology, Poland. Ożarów, 14-15 May 2004.
- Krzysztof P. Bielawski, **Kamila Kitowska**, Piotr Stalke, Katarzyna Sikorska "HFE gene polymorphism in hereditary haemochromatosis. Optimisation of the PCR-RFLP-based method for C282Y mutation detection in epidemiological research". IV Congress of Polish Society of Hepatology, Poland. Ożarów, 14-15 May 2004
- **Kamila Kitowska**, Patrick Bulau, Dariusz Zakrzewicz, Melanie Koenigshoff, Andreas Guenther, Werner Seeger and Oliver Eickelberg. "Bleomycin-induced Alterations of L-arginine/ADMA Levels in the Lung". American Thoracic Society, 19-24 May 2006 San Diego, California, USA
- Patrick Bulau, Dariusz Zakrzewicz, **Kamila Kitowska**, Werner Seeger and Oliver Eickelberg. "Quantitative assessment of protein arginine methylation in the lung: Determination of free versus incorporated methylarginines". American Thoracic Society, 19-24 May 2006 San Diego, California, USA
- Dariusz Zakrzewicz, Patrick Bulau, **Kamila Kitowska**, Walter Klepetko, Werner Seeger and Oliver Eickelberg. "Decreased Protein Arginine Methyltransferase Activity in Idiopathic Pulmonary Arterial Hypertension". American Thoracic Society, 19-24 May 2006 San Diego, California, USA
- Aparna Jayachandran, Melanie Koenigshoff, Matthias Hecker, Haying Yu, Ewa Rupniewska, **Kamila Kitowska**, Werner Seeger, Oliver Eickelberg. "Snail and Slug are Key Mediators of TGF-beta-induced Epithelial-to-Mesenchymal Transition in Lung Fibrosis". American Thoracic Society, 19-24 May 2006 San Diego, California, USA

<ul style="list-style-type: none"><li>▪ <b>Kamila Kitowska</b>, Patrick Bulau, Dariusz Zakrzewicz, Melanie Koenigshoff, Andreas Guenther, Werner Seeger and Oliver Eickelberg. "Bleomycin-induced Alterations of L-arginine metabolism in the Lung". 14<sup>th</sup> International Colloquium on Lung Fibrosis (ICLF), 7-10.09.2006 Mainz, Germany</li></ul>
<ul style="list-style-type: none"><li>▪ <b>Kamila Kitowska</b>, Patrick Bulau, Dariusz Zakrzewicz, Melanie Koenigshoff, Andreas Guenther, Werner Seeger and Oliver Eickelberg. "Bleomycin-induced Alterations of Pulmonary L-arginine metabolism". The 3<sup>rd</sup> International Meeting on ADAM, ADMA 2006, 1.12.2006 London, UK</li></ul>
<ul style="list-style-type: none"><li>▪ <b>Kamila Kitowska</b>, Dariusz Zakrzewicz, Melanie Koenigshoff, Matthias Hecker, Izabela Chrobak, Andreas Guenther, Werner Seeger, Patrick Bulau, and Oliver Eickelberg. "Increased Arginase Expression is a Novel Pathogenic Mechanism in Pulmonary Fibrosis". American Thoracic Society, 18-23 May 2007 San Francisco, California, USA</li></ul>
<ul style="list-style-type: none"><li>▪ Izabela Chrobak, Niels Banthien, Melanie Konigshoff, <b>Kamila Kitowska</b>, Werner Seeger, and Oliver Eickelberg. "Imbalanced expression of the type I TGF-beta receptors ALK-1 and ALK-5 in pulmonary fibrosis". American Thoracic Society, 18-23 May 2007 San Francisco, California, USA</li></ul>
<ul style="list-style-type: none"><li>▪ Melanie Koenigshoff, <b>Kamila Kitowska</b>, Andreas Jahn, Simone Becker, Oana Amarie, Frank Rose, Ludger Fink, Werner Seeger, Andreas Guenther and, Oliver Eickelberg. "Wnt-inducible protein (WISP)-1: A key regulator of alveolar epithelial cell-fibroblast crosstalk in idiopathic pulmonary fibrosis". American Thoracic Society, 18-23 May 2007 San Francisco, California, USA</li></ul>

## 10. Acknowledgements

And finally after a long way of struggling with scientific texts, publications, words ... the time has come to express my acknowledgements.

I would like to thank Prof. Dr. Werner Seeger not only because he is the boss of all bosses but especially for his vision of science that unites people from different countries in order to achieve one goal.

I would like to express my gratitude to Dr. Oliver Eickelberg for giving me a chance to do PhD in his lab, due to him I gained invaluable knowledge and experience not only how to deal with chemical reagents but also how to deal with people in various situations.

My deep gratitude goes to Patrick Bulau, without him and his ideas my project would not exist. Thank you for being the best PostDoc I could ever dream of. Thank you for your support and your stimulation for work, thank you for appreciating every small detail of my work, this is amazing feature that every boss should have. Thank you for helping me not only in scientific field but also in solving my problems connected with living in German-speaking country.

At this point I would like to thank Darek Zakrzewicz for being involved in my project, for stimulating discussion. Thank you for help with some parts of the project, which could not be performed without you and your support.

I would like to thank Rory Morty for the effort he made to read this thesis.

Special thanks to Dorothea Peters for helping me with "German part" of my thesis. I also would like to thank all members of Eickelberg group. You created a group, which was wonderful because of diversity, sometimes this diversity created problems, nevertheless in hard times we were able to solidarize.

I really would like to thank Polish community in Giessen, thanks to you it was easier to fight with home-sickness. No matter if you stayed in Giessen or you had to leave I will keep a memory of you.

At the end I would like to thank Michał without him my life in Giessen would not be possible. Thank you for your support although I know it required a lot of patience... I know that it was not easy to survive with me during all my exams, during preparation of hundreds of presentations, during writing my thesis ... Thank you

And finally I would like to thank my parents. Thank you for supporting me in all my decisions and for your limitless love, which I fill no matter where I am. Without you my dreams would never come true. All my work is dedicated to you.

I wreszcie chciałabym podziękować moim rodzicom. Dziękuję za to, że zawsze wspieraliście mnie w moich decyzjach, dziękuję za Waszą bezkresną miłość, którą czuję bez względu na to gdzie jestem. Bez Was moje marzenia nie mogłyby się spełniać. Całą moją pracę Wam dedykuję.